Bin Hu

Characterizing gas-lift instabilities

Department of Petroleum Engineering and Applied Geophysics
Norwegian University of Science and Technology
Trondheim, Norway, 2004

ABSTRACT

This dissertation mainly investigates the occurrence and characteristics of density-wave instability in gas-lift wells. The investigation is based on a simplified gas-lift system, in which water and air are used as producing fluid and lifting gas respectively, and heat transfer effect is neglected.

To carry out the investigation, both linear stability analysis and numerical simulation are performed. The linear stability analysis is based on a homogenous two-phase flow model and the numerical simulation is done by using a commercial available dynamic multiphase flow simulator. In this way, a crosscheck between the two methods can be made in order to gain confidence about the results. Both two methods are validated against casing heading problem before they are applied to density-wave instability study.

The results show that it is possible for density-wave instability to occur in those gas-lift wells producing from depleted reservoirs. The linear stability analysis and numerical simulation give the similar parametric trend in characterizing the instability. Within the normal gas-lift operation parameter range, increasing reservoir pressure and gas injection rate increases stability, but increasing tubing diameter, productivity index and system pressure decreases stability. The instability may occur only when the well loses its capability of natural flowing.

Dynamic simulation also shows that the average production rate could be significantly reduced due to the unstable gas-lift compared with the steady-state prediction. An attempt of using feedback control to stabilize the gas-lift system is also tested by using the simulator. Promising results are obtained from the test in both stabilization and increasing production.

The results of this dissertation add new knowledge to gas-lift instability fundamentals and can help in diagnosing and remedying unstable gas-lift problems.

PREFACE

To promote the role of active control in taming serious unstable flows occurring in petroleum production system, ABB, Norsk Hydro, and Norwegian University of Science and Technology jointly initiated a dr.ing research project. The project aims at investigating the mechanisms of different unstable flow phenomena and studying their control strategies. As part of the project, this dissertation is intended to investigate the occurrence and characteristics of gas-lift instabilities.

For many years, it has been observed that continuous gas-lift production can be seriously unstable and sometimes even behave as intermittent gas-lift due to various reasons. The fluctuating, and sometimes, chaotic unstable production behaviour affects many fields, particularly at their decline stages. The large fluctuation in flow is undesired as it can cause alternative gas and liquid surge in the first stage separator, which may result in poor separation, mechanical vibration, even flaring and shutdown. The oscillating bottomhole flowing pressure could lead to dynamic water and gas coning near the wellbore, which increase the average GOR and water-cut. Besides, the unstable gas-lift normally has a lower average production rate compared with the steady-state prediction, which means the lifting efficiency is reduced.

Due to aforementioned reasons, unstable gas-lift should be smoothed out in an effective and efficient manner whenever it occurs. For this purpose, the operators must recognize the types of gas-lift instabilities and their characteristics on hand before they can perform diagnoses or apply remediation. The research work in this dissertation therefore tries to improve the understandings of unstable gas-lift phenomena by classification, clarification and characterization. The dissertation is divided into seven chapters.

Chapter 1 provides a brief introduction to the concept of gas-lift and gas-lift optimization. Based on the introduction, it gives an overview of the origin and consequence of gas-lift instabilities. Besides, the basic terminologies that help to classify different gas-lift unstable phenomena are also defined here.

Chapter 2 reviews and discusses the previous research work on static instabilities occurring in oil wells. It is concerned with the casing heading problem. The investigation of the origin, the mechanism and the criteria of casing heading is critically reviewed. The advantageous of using dynamic simulation to study unstable gas-lift phenomena is defended. The results of literature survey on application of active control to unstable wells are summarized.

Chapter 3 addresses the new emerging dynamic gas-lift instability problem by summarizing some of the field observations. The similar phenomenon from unstable airlift pumping process is also reviewed. Based on the reviews and discussions, it is concluded that density-wave instability is in the background of newly observed unstable cases. Furthermore the chapter makes an introduction to density-wave instability in a horizontal system. The tasks and research methodology of this dissertation are also presented.

Chapter 4 studies the basic features of density-wave instability in a vertical system. The intention of this chapter is to discuss why the propagation of density wave can result in instability in a vertical system, and what kind of role for each pressure drop component to play in triggering the instability. A dynamic model is derived in term of the inlet flow perturbation. The model is solved analytically in order to explicitly show the answers.

Chapter 5 applies linear stability analysis to a simplified gas-lift system. The main concern of this chapter is to see if density-wave instability can occur in gas-lift wells, where the inlet restriction and friction along tubing is tremendously larger compared with those in airlift pumps. The instability is then characterized by applying parametric study, which shows the effects of changing different well parameters.

Chapter 6 is intended to verify the results and conclusions in Chapter 5 by numerical simulations. Simulation results from a commercial available dynamic multiphase flow simulator are presented in the chapter. Casing heading cycle, gas robbing in dual gas-lift and density-wave oscillation are all simulated. Besides, more simulation is done in order to investigate the production loss and demonstrate the function of active control.

Chapter 7 summarizes the main conclusions of the investigation in this dissertation. It also lists the work to be done in the future.

During the period of my study, I got a lot of helps from many people in many institutions. I want to thank my supervisor Professor Michael Golan for taking me as his student. I gratefully acknowledge his very many helpful advices, discussions and encouragement on my research work. Whenever I met difficulties, I could always expect good ideas from his mind and useful information from an ocean of literature collections in his office.

Dr Zheng Gang Xu (许政纲) from Scandpower Petroleum Technology AS is deeply acknowledged not only for him to introduce me to Mike, but also for his constructive advices in dealing with many research details. It was Dr Xu who first explained to me about density-wave instability after he had examined

some of my simulations. His perceptions on many gas-lift instability issues led me to finalize the research work in the right direction.

I want to thank Professor Ole Jørgen Nydal, Curtis H. Whitson, and Yehuda Taitel (Tel Aviv University) for their discussions and interesting lectures on the many multiphase topics. I got helps from Professor Gabor Stepan (Budapest University of Technology and Economics) and Professor Andrew Fowler (Oxford University) in solving retarded second-order dynamic system models. I had a very helpful discussion with Dr Hejie Wang (汪和杰) on linear stability analysis. I learned some control concepts from the cooperation with Professor Bjarne Foss and Dr.ing candidate Gisle Otto Eikrem.

Dr Egil Henrik Uv is acknowledged for presenting me the field observations of unstable gas-lift and offering me an easy access to the interesting field data.

I appreciate the many critical comments and interesting suggestions from Vidar Alstad, Petter Andreas Berthelsen, Tore Flåtten, Espen Storkås, and Sondre Vestøl.

I give my sincere thanks to Marit Valle Raaness and her colleagues in the administration of Petroleum Department. I also want to thank my fellow doctoral students Bamshad Nazarian and Nan Chen (程楠) for being my consulting sources for various issues.

Dr Morten Dalsmo made a great effort in initiating and managing the Petronics project. Norwegian Research Council financed this research work. Scandpower Petroleum Technology AS offered OLGA academic licence and free user support. These are also gratefully acknowledged.

I hope this dissertation can satisfy my parents who have been expecting this booklet from me for a long time. I am in debt to my 2-year-old boy Liangliang (亮亮) who should have got more care from me.

Finally, I am deeply grateful for the support and patience of my long-suffering wife Yan Chen (陈焰) during the seemingly endless of writing and revision of the dissertation.

Bin Hu (胡斌)
Sogn, Oslo
October 2004

TABLE OF CONTENTS

1 INTRODUCTION

1.1 Gas-lift concept

In oil production, when reservoir pressure is insufficient to sustain the flow of oil to the surface at adequate rates, natural flow must be aided by artificial lift. There are two basic forms of artificial lift: gas-lift and pump-assisted lift. Both methods supplement the natural energy of the reservoir and increase the flow by reducing backpressure at the wellbore caused by flowing fluids in the tubing.

Gas-lift is used only in wells that produce economically with relative high flowing bottomhole pressures, typically high-productivity reservoirs. It requires few moving parts downhole and thus is suitable for wells producing sand or other solids. It is also preferable when the well has a multi-inclination trajectory, in which installation and operation of bottomhole pump are mechanically difficult. Two types of gas-lift exit: intermittent gas-lift and continuous gas-lift. In this dissertation, “gas-lift” means the continuous gas-lift.

Gas-lift is accomplished by injecting gas into the lower part of production string. If the well produces from tubing, then the gas can be injected into it from tubing-casing annulus and mixed with the produced fluids. Due to increased gas proportion, the two-phase fluid mixture in the tubing thus obtains a lower average density that reduces hydrostatic pressure gradient. If the total pressure drop along the tubing attributes mainly to its gravity component, a lower wellbore flowing pressure can be achieved. Therefore, the production rate can be increased because of a larger drawdown.

Gas-lift can be applied to both dead wells and natural flowing wells. It can help the dead wells to produce and accelerate the production of the natural flowing wells. Figure 1-1 shows a typical gas-lift well, in which compressed gas is injected from the tubing-casing annulus into the tubing through a valve installed near its bottom. The valve is called injection valve or operating valve, and normally is an orifice. The well is also equipped with unloading valves along its tubing string, which are used for well kick-off operation. By doing so, one high-pressure compressor can be saved and the kick-off operation becomes smooth. The unloading valves could be production pressure operated (PPO) or injection pressure operated (IPO), whose openings are dependent on both casing and tubing pressures. Some gas-lift wells also use PPO or IPO valve as operating valve instead of orifice.

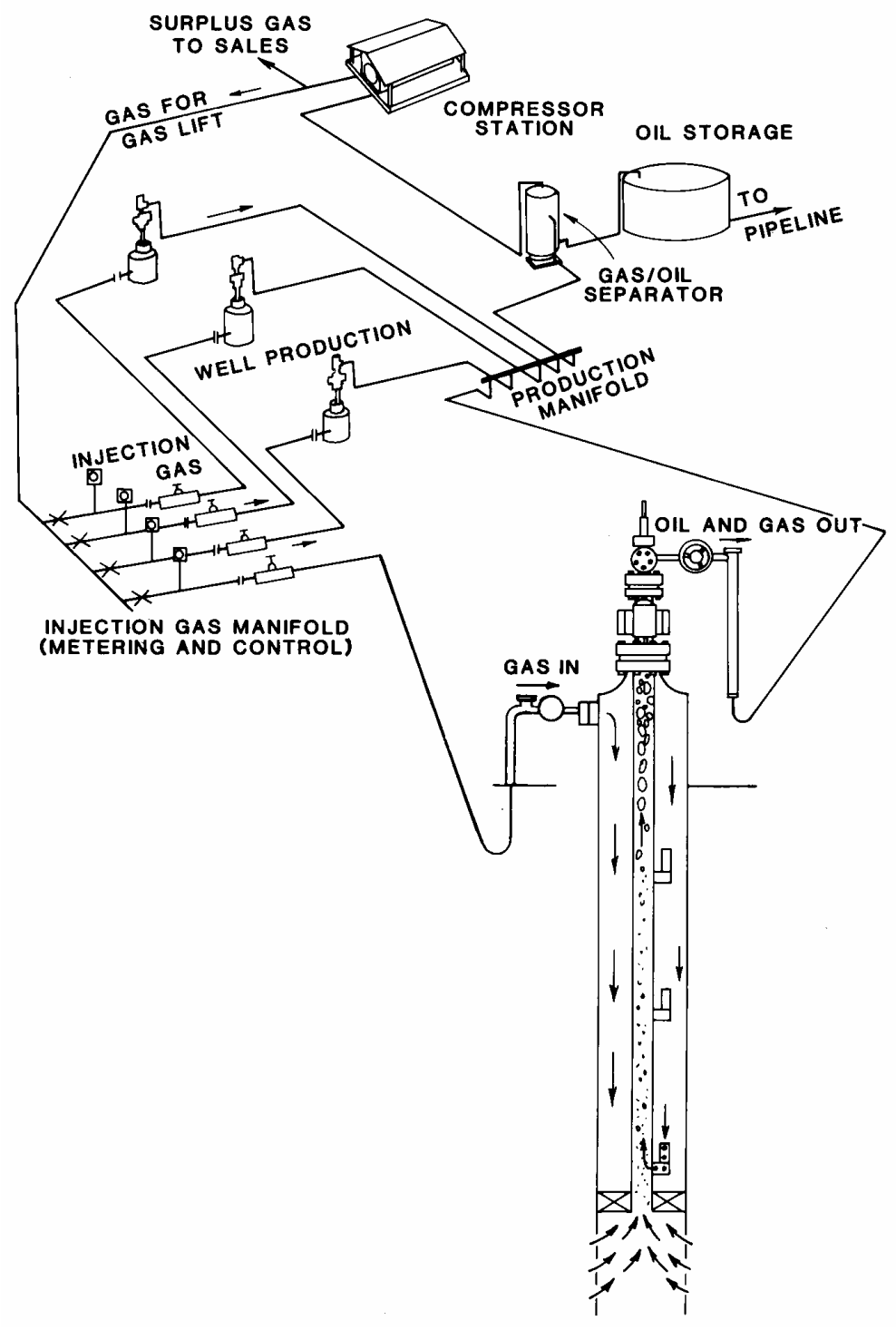

Figure 1-1 Gas-lift system. Courtesy American Petroleum Institute.

The gas-lift surface system is also sketched in Figure 1-1, which consists of a gas compression unit, a gas distribution network and flow regulation devices near the casing heads of the wells. With such a system, the lifting gas is distributed and allocated to the gas-lift wells within the field.

1.2 Gas-lift optimization

Gas allocation is determined by the gas-lift optimization procedure. A widely accepted definition of gas-lift optimization is to obtain the maximum output under specified operating conditions. In this respect it should be noted that the definition does not explicitly suggest that the maximum production be considered optimum. Instead, gas-lift optimization requires the operation offer the maximum profit.

Figure 1-2 shows the lift performance relationship curve (LPR) of a hypothetical gas-lift well. It is a typical gas-lift performance graph showing that the production rate increases rapidly with the gas injection rate at first and then tend to level off before reaching the peak. If continue increasing the gas injection, the production will gradually decrease. This is because the reduced hydrostatic pressure drop cannot compensate the increased friction loss induced by increased gas flow rate. The approximate operation points for *maximum present value profit after tax* (PVPAT), *current maximum daily operating cash increase* (OCI) and *maximum oil production rate* are all marked on the curve. Obviously, the operation point that gives the highest PVPAT should be the economic optimum for the gas-lift well even though OCI is considered the optimum in some situations.

The same principle is also applicable for a multi-well gas-lift system. Depending on the availability of total amount of lifting gas, either global or local maximum PVPAT can be achieved. If there is an enough supply of lifting gas, we can get the global maximum PVPAT, which correspondingly determines the optimum total lifting gas rate for the whole field. If the available gas supply is less than this optimum due to various reasons such as limited primary gas processing capacity, only local maximum PVPAT can be obtained. Both global and local maximum PVPAT are decided by a gas-lift optimization procedure that mainly relates on how to allocate the lifting gas to different wells within the system.

For example, given a certain amount of gas, maximum rate approach, also known as equal slope method, is often used to determine the optimized gas allocation. However, this method has its drawbacks since it does not account for the fact that the wellhead pressure and flow rates are mutually dependent due to the pressure drop in the surface gathering system. In fact, gas-lift optimization is a quite complicated issue, and in most situations the

optimization procedure relies on the practical conditions and varies from field to field.

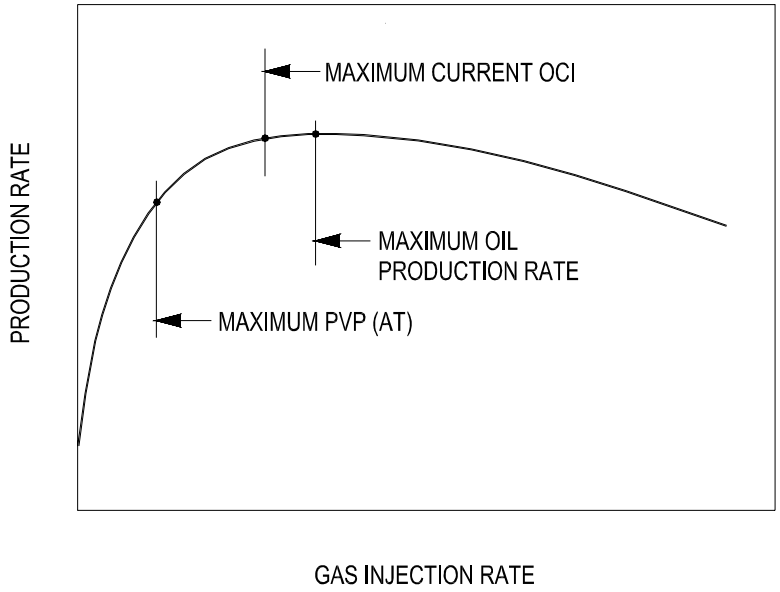

Figure 1-2 Lift performance relationship and gas-lift optimization.

But, no matter what method is used, two important points have been made clear from the practice of gas-lift optimization. First, each well should get a certain amount of gas determined by an optimized allocation procedure. This means that gas injection rate through the surface choke should be controlled constant during operation, that is, be independent on the pressure variations in both gas distribution network and tubing-casing annulus. This is called surface control in gas-lift operation.

Second, in general gas-lift wells should be operated at the upslope section of their LPR curves as required by optimization. This could also be a natural result when there is a short supply of lifting gas due to limited capacity of separation, processing and compression. Operating gas-lift wells at the upslope of their LPR curve implies that gravity becomes the dominant factor for the flow within the tubing. Gas-liquid two-phase vertical flow under gravity domination is easily to be unstable. This is particularly true for gas-lift wells.

1.3 Gas-lift instabilities

Even when an optimum can be logically defined for a field during gas-lift design, there is always an argument between the design and operation personnel on the gas-lift production. The argument relies on the discrepancies

between the planning and real production operation. To produce the oil as planned optimum is sometimes difficult to realize. Now we know, at least, some of the discrepancies are due to unstable gas-lift production.

Figure 1-3 shows two LPR curves for a same well. The solid line is predicted from steady-state simulation, and the dashed line is from dynamic simulation. The discrepancy between the two curves is due to unstable gas-lift production. This means that an unstable gas-lift could produce much less than the predicted by a steady-state simulation. The unstable region covers part of upslope section of the LPR curve and overlaps with the possible area where maximum PVPAT locates. Obviously, the traditional optimized gas-lift design based on steady-state simulation could mislead the operation personnel due to gas-lift instability.

Since gas-lift is usually applied when the reservoir pressure is depleted, particularly when the field is in its tail production, a significant production reduction due to instability implies that the field tail production must be prolonged in order to get the same recovery rate. This will tremendously increase the operation cost and would be intolerable in most situations.

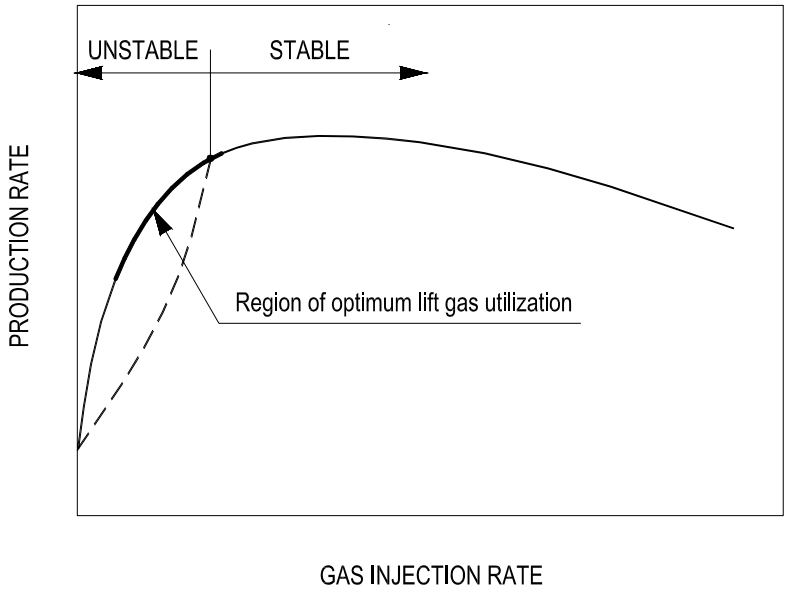

Figure 1-3 Lift performance relationship for unstable gas-lift.

Unstable gas-lift is undesired not only due to the resulted production loss, but also due to the fluctuating, and sometimes, chaotic unstable production behaviour. For many years, it has been observed that continuous gas-lift wells can be seriously unstable and sometimes even behave as an intermittent gas-

lift due to various reasons. Large fluctuation in both pressure and flow rate can result in poor separation; limit the production capacity and cause flaring and shutdown.

To handle the well flow fluctuations, the gathering and separation system is often oversized. “API recommends that, for the sizing of pipes receiving gas-lift production, a surge factor of 40 to 50% should be added to the estimated steady-state flow rate, compared with 20% for naturally flowing wells.” Asheim deduced that this was partially due to the uncertainties concerning gas-lift instabilities. The conservative design of the production system costs more investments, thus, damages the overall system optimization.

Recent reports also show that oscillating bottomhole flowing pressure could also trigger dynamic gas and water coning in the near wellbore reservoir, particularly for those wells producing from thin oil layers. This dynamic coning effect will result in a higher average water-cut and GOR.

Obviously, gas-lift instabilities need to be treated seriously for the sake of smooth and optimized production. To solve the instability problems, we need clearly understand the mechanisms and characteristics of the gas-lift instabilities, which are basically special cases for two-phase pipe flow instabilities.

The two-phase flow instabilities have long been the subject of a number of extensive reviews, which describe the various instability phenomena, and summarize the many experimental and theoretical investigations in the area. The status and achievements of researches and applications were reviewed regularly. Most of the reviewed publications are related to the operations of nuclear reactors, in which safety is a crucial issue and could be damaged by the instabilities.

The terms and definitions related to two-phase pipe flow instabilities are listed below, which are frequently used throughout this dissertation. They are not necessarily the same in the meaning as those that stand in the classical literatures. For example, the “instabilities” discussed in this dissertation may have different names and classifications compared with those appearing in the “extensive reviews” due to the differences in definitions.

Steady flow and steady state. A steady flow or a steady state, rigorously speaking, is one in which the system parameters are functions of the space variables only. Practically, however, they undergo small perturbations due to turbulence, nucleation, or slug flow etc. These perturbations play important roles in triggering several instability phenomena.

Stable and unstable. A flow is stable if its new operating condition tends asymptotically toward the initial one when it is momentarily disturbed from its steady state. The disturbances considered here are those that may occur in practice. They include the above perturbations and are often limited in amplitude. A flow is unstable if it is not stable.

Microscopic and macroscopic instabilities. Two-phase flow instabilities can be classified into two main groups termed microscopic and macroscopic instabilities, or local instability and systematic instability. Two-phase pipe flow always involves small-scale instabilities: bubbles form and collapse; a given point in the flow path may be occupied by the liquid phase and gas phase alternatively such as slug flow. These are called microscopic instabilities that occur locally at the liquid-gas interface. On the other hand, macroscopic instabilities are systematic instabilities that involve the entire two-phase flow system, which are more dependent on the boundary conditions.

Static and dynamic instabilities. For macroscopic or systematic instabilities, there is a traditional classification into static and dynamic instabilities. When an unstable steady state is perturbed, the perturbation will initially get a positive feedback from the system and lead to a departure from the steady state, this is termed a static instability. A static instability can lead to either a different steady-state condition or a periodic behavior depending on the system boundary conditions. On the other hand, a flow is subjected to a dynamic instability when the inertia and feedback effects have an essential part in the process. For dynamic instability, when the unstable steady state is disturbed, the system will have a negative feedback to the perturbation. But due to various reasons, the natural negative feedback effect is not enough for stabilization; instead it leads to a sustained flow oscillation.

The definitions of static and dynamic instability here are based on the system initial feedback response to perturbations, which are different with the traditional definitions. Since the static instability defined here could also need to take account of the system dynamic response, the static instability is then not as “static” as it was. In this dissertation, the category of static instability and dynamic instability will be based on these new definitions.

As aforementioned, the microscopic instabilities, such as the hydrodynamic slugs, always exist in our two-phase flow system. But normally, these microscopic instabilities are only considered as disturbances that would not cause too much trouble to the system stability.

On the contrary, macroscopic instabilities are rather system related behaviors, which can result in serious flow oscillations. In most situations, these oscillations are harmful to operation smoothness, safety and efficiency. The

gas-lift instabilities discussed in this dissertation are macroscopic instabilities. Depending on their origins and characteristics, the instabilities can be either static or dynamic.

2 STATIC GAS-LIFT INSTABILITY: REVIEWS AND DISCUSSIONS

2.1 Casing heading phenomenon

Both natural flowing wells and gas-lift wells can experience flow instabilities characterized by regular or irregular cyclic variations in pressure and flow rate. The unstable production phenomena were given a common name “heading” by petroleum engineers. Depending on where in the flow system the free gas of interest cyclically builds up and discharges, three classical types of heading are commonly acknowledged. They are formation heading, tubing heading and casing heading.

Gas-lift instability studies originated from casing heading. In fact, all the publications on gas-lift instabilities so far aim at solving casing heading problem. Reviews of casing heading studies show the status of gas-lift instability research.

2.1.1 Origin of casing heading

The origin of casing heading was first found in unstable natural flowing wells completed without production packer. In such wells, segregated free gas from liquid at the tubing intake can regularly accumulates in the annulus and discharges from it, thus results in periodic change of gas content in the tubing, which brings the well into oscillating or fluctuating production. During the gas accumulating and discharging cycle, liquid column level in the annulus is forced to go up and down.

Gilbert (1954) gave the first pictorial description of the casing heading process in natural flowing wells. He also summarized the main observations and characteristics of casing heading phenomenon. According to Gilbert, heading action could be eliminated by use of tubing-casing packers, and use of casing-actuated intermitters might be preferable where packers were not already installed.

Torre *et al.* (1985) gave the first quantitative hydrodynamic model for simulating casing heading. The model agreed well with laboratory data. Analysis of both observed and computed variables indicated that heading only occur if the slope of the total pressure loss as a function of gas flow rate was negative. Severity of heading increased when either the liquid or gas superficial velocity decreased. The more annulus volume available, the higher the liquid column rose, and the higher the pressure fluctuated.

Blick *et al.* (1986) performed theoretical stability analysis afterwards for natural flowing well without packer. He also investigated the theoretical possibility of applying feedback control to the unstable wells. This was followed by a root locus stability analysis of the feedback controller later (1989). The controller sensed the tubing head pressure and then activated a control that increased or decreased the tubing head choke diameter.

Today, for natural flowing wells, casing-heading problem is not a worry anymore since most of the modern wells are completed with production packer, which prevents segregated free gas from entering annulus. But for gas-lift wells, casing heading can still happen even a tubing-casing packer is set. In the following discussions and the rest of this dissertation, whenever casing heading is mentioned, we mean the case occurring in gas-lift wells completed with production packers.

2.1.2 Mechanism of gas-lift casing heading

Gas-lift casing heading has been extensively investigated since it was identified. Bertuzzi *et al.* (1953) first concisely explained the mechanism of casing heading.

As mentioned in previous section, random pressure disturbances always exist in two-phase flow system. For example, a sudden small pressure reduction could occur in the wellbore when a liquid slug flows out of the tubing. The small pressure reduction will result in a slight increase of gas injection from the annulus to the tubing due to increased pressure difference across the gas-lift valve. If the increase of gas injection causes further increased pressure difference between the annulus and the tubing, then the gas injection will increase further. This snowball effect is called positive feedback, which leads to the excursion of well operation. On the contrary, if the increase of gas injection causes reduced pressure difference between the annulus and the tubing, gas injection will decrease.

If the excursion process cannot proceed completely due to restrictions of system boundary conditions, the system will end up with a sustained oscillation. This is called gas-lift casing heading cycle. Clearly, casing heading is a static instability since its occurrence needs the system to give positive feedback response to the initial perturbations.

Xu and Golan (1989) described the gas-lift casing heading cycle step-by-step as followings.

1. Start at the gas injection point. A sudden reduction of tubing flow pressure results in more gas discharge through the downhole orifice.

2. More gas discharge will further reduce the tubing flowing pressure, promoting more gas flowing through the downhole orifice.

3. Since the gas supply through the surface choke can not meet in time the higher gas rate discharge into the production string, the casing pressure and the upstream pressure at the downhole orifice will eventually be reduced. This results in a decrease of gas flow into the tubing.

4. The tubing flowing pressure starts now to increase because of the gas injection reduction. This accelerates the reduction of gas injection into the tubing.

5. The trend now is swayed to opposite. Because of higher tubing flowing pressure and lower upstream pressure, the downhole orifice can discharge less gas than the surface now supplies. The casing pressure begins to build up.

6. As the casing pressure is built up, gas rate into tubing starts to increase. More gas injection reduces the tubing flowing pressure and thus sways the flow condition back to step 2.

Obviously, the constant or sometimes limited gas injection at the surface choke is the restriction that prevents the system from completing the excursion to a new stable steady state.

The mechanism illustrated by Bertuzzi *et al.* clearly rules out the possibility for casing heading to happen on the right side of the LPR curve after the maximum point. As discussed earlier, on the right side of LPR curve, friction is the dominant factor for the two-phase flow, thus any increased gas injection will increase the pressure on the tubing side and reduce the pressure difference across the valve.

But on the left side of the LPR curve where gravity is the dominant factor, it is very possible for the well to be unstable. This is due to that any increased gas injection will at least reduce the pressure in the tubing side, thus will possibly result in increased pressure difference across the valve, which can promote the occurrence of casing heading.

Xu and Golan tried to use graphic analysis to discuss solution stability, which located on the left side of the LPR curve. In their analysis, the gas-lift performance relationship curve (GPR) of flow within the tubing string and the discharge performance relationship curve (DPR) of flow through gas-lift valve

were generated and plotted in the same plane as shown in Figure 2-1. The two curves were based on the same node where gas-lift valve was installed. Intersections of GPR and DPR gave the steady-state solutions of flow in the gas-lift well for a certain annulus pressure. There could be more than one such solutions just like A and B in Figure 2-1.

The two solutions are different with each other in the manner how the two curves intersect. For solution A, the tangent value of GPR is less than that of DPR. For solution B, it is just opposite. Based on Figure 2-1, Xu and Golan concluded that A-type solution was unstable and B-type solution was stable. This conclusion is obviously correct under the condition that the annulus pressure is constant. Unfortunately, they did not discuss in detail about the relationship between the two types of solutions and casing heading, at which the surface gas injection rate is either restricted or even controlled constant.

Since casing heading is a static instability, we have to find out the system's response to perturbations around the two types of solutions in order to identify their relationships with casing heading. Obviously, solution B is statically stable. Assuming the tubing pressure experience a negative perturbation at solution B and cause more gas injection from the annulus, however, the increased gas injection can not promote further increased pressure difference across the valve, thus casing heading is avoided by the negative feedback effect. This concludes that the B type solution is sufficient for casing heading not to happen.

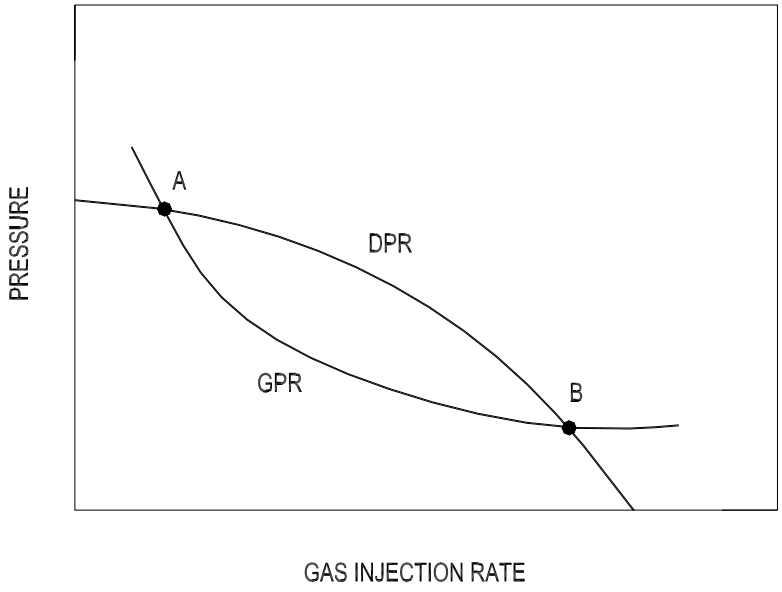

Figure 2-1 Node analysis of solution stability.

For solution A, there could be several possibilities depending on boundary conditions. First, if we assume the annulus pressure is constant instead of the surface gas injection rate, it will be very easy to derive a positive system feedback to pressure perturbations around the solution A just like Xu and Golan did. This means that the steady-state solution A will never be realized in the practical operation. The well will always one-way migrate to the right-hand stable solution B even if it can be assumed to be arbitrarily set to produce at point A by some measures at the beginning. In this situation, the static instability is called excursion. No oscillation will be observed during this excursion process.

But, if we assume the surface gas injection rate is controlled constant, two results can be derived. In this case, the annulus pressure can be changed due to the gas rate discrepancy between the surface choke and the downhole injection orifice, that is, DPR can be changed from dynamical point of view. If we consider this change in the graphic analysis, different results can be obtained.

For point A in Figure 2-2, if there is a sudden small pressure reduction in tubing, the gas injection rate will increase to q_2. Then tubing pressure goes down to p_2 corresponding to increased gas injection. But whether casing heading is promoted depends on the pressure difference across the valve instead of the pressure reduction on the tubing side only. For this reason, the pressure change in the annulus side must also be checked. Since $q_2>q_1$, the gas rate flowing into the annulus is less than that flowing out of annulus, then the annulus pressure will decrease. This results in the change of DPR. For example, it might be possible for the new DPR to be like either DPR2 or DPR2'. DPR2 still intersects with GPR, but DPR2' does not. If it is DPR2, big flow oscillation will be promoted since gas injection rate will be increased further. However, if it is DPR2', obviously it will prevent the occurrence of severe heading cycle because the new gas injection rate will be less than q_2.

The above graphic analysis is just a snapshot of the dynamical change of DPR. It is not a rigorous analysis. General speaking, it is even impossible to do so by using graphic analysis. Nevertheless, it definitely shows the possibility for casing heading not to happen under solution A. The example in the analysis is an extreme condition. In fact, it is not necessary for the new DPR to lose its contacts with GPR in order to prevent casing heading. According to Bertuzzi ***et al.***, casing heading will not happen if the pressure difference across gas-lift valve is reduced when a temporary positive gas injection rate perturbation occurs. This only requires that annulus pressure decrease faster than the tubing pressure does when the well experiences the above perturbation. Whether the annulus pressure can decrease faster than the tubing pressure, depends on the shape of GPR, the stiffness of annulus

gas and the volume capacity of annulus. A steeper of GPR curve, less stiff of annulus gas and large volume capacity of annulus decrease the stability.

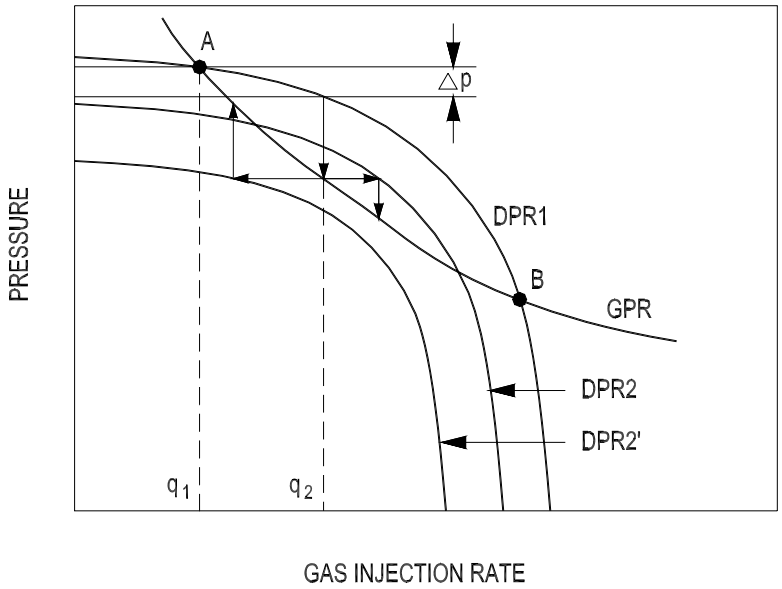

Figure 2-2 Pseudo dynamic node analysis of solution stability

From the above discussion, we can conclude that an A-type solution is only a necessary condition for casing heading instead of a sufficient condition.

Xu and Golan concluded that the stability criterion based on constant annulus pressure was insufficient to judge the occurrence of casing heading after they had studied the stability of the two solutions. But they did not address the relationship between casing heading and the two solutions properly and mistakenly deduced that casing heading could also happen for solution B.

Despite the limitations of Figure 2-1 in judging the occurrence of casing heading, it is still highly recommended to use the plots of GPR and DPR to check the solution type for gas-lift design as it at least can rule out casing heading possibility for the B-type solution. The graphic analysis is also very easy to perform in practice since both GPR and DPR are standard curves for gas-lift design.

2.1.3 Criteria of casing heading

Developing the stability criteria has significantly improved the understanding of the instability mechanism as we have seen from Xu and Golan's work despite that the simple graphic analysis by examining the tangent value of two

curves around the solutions is not sufficient for a proper casing heading judgement. However, having the casing heading mechanism in mind, it is easier for us to evaluate the performance of different stability criteria.

Predicting the threshold of casing heading is necessary during the gas-lift design and operation. A quick stability check with analytical approaches has been the basic method of serving this purpose for some years even when today some qualified dynamic gas-lift simulators are available and capable of doing the same job. There are two forms of the analytical approaches. One form is to apply linear stability analysis directly on a mathematic model of gas-lift flow system. The other is to directly develop simple mathematic criterion relationship based on the physical interpretation of the phenomenon, which involves well variables and production parameters.

Fitremann and Vedrines (1985) performed linear stability analysis for a laboratory scale gas-lift system. The system used a 4.5 m high, 28 mm ID transparent pipe as tubing and a 0.1 m^3 adjustable plenum as annulus. Lifting air was injected to the plenum through a sonic nozzle and then to the tubing by an orifice. Water was supplied from an overflow tank through a valve. The gas rate and water rate entering into the tubing could be calculated from the pressure drop measurements across the valves. The boundary conditions for the system were that separator pressure, reservoir pressure and lifting air rate were all constants, and water rate flowing into the tubing was determined by a quadratic valve flow relation.

Fitremann and Vedrines used drift-flux model with the assumption of homogeneity to describe the two-phase flow within the tubing. The model was perturbed and linearized in terms of four variables: velocity of air, velocity of water, pressure and void fraction. Then the dispersion equation of the linear equation set was obtained, which was in third order for both angular frequency and wave number. This indicated that there were three pressure waves for each frequency. By considering the boundary conditions, another linear equation set for those three pressure amplitudes was created. If written in matrix form, the determinant had to be zero as a necessary condition for the amplitude vector to have a non-zero solution. This gave another non-linear equation for angular frequency and wave number. Solving it together with the dispersion equation, the angular frequency was then obtained. It was a complex number whose real part was the natural frequency of the system and imaginary part was the logarithmic decay rate of the system. It was the sign of this logarithmic decay rate that determined the system stability. The value of zero gave the threshold between stable and unstable flow.

Fitremann and Vedrines compared their analysis with the experiments and good match was concluded. They found that increasing the volume of the

plenum decreased stability, but a high injection pressure in the plenum had a strong stabilizing effect. Fitremann and Vedrines did not apply their analysis to any actual gas-lift wells.

Blick *et al.* (1988) did theoretical stability analysis for both flowing oil wells and gas-lift wells, in which no production packer were installed. They developed a lumped parameter model that described well and reservoir variables that were affected by pressure fluctuations in the system. Those variables included tubing inertance, tubing capacitance, wellbore storage and flow perturbation from reservoir. In the model, a series of differential equations that expressed the pressure dependent variables were Laplace transformed and combined by Cramer's rule to obtain a quadratic characteristic equation with three coefficients. By using Routh's criteria, the model predicted that a well was stable when the coefficients were all positive or all negative. However, when one had a different sign with the other two, the model predicted the well was unstable.

Blick *et al.* also gave demos on how to use the criteria based on two hypothetical wells. Unfortunately, they did not give any further information on the application of their analysis on the real wells, so the accuracy of their criteria was unknown.

Besides the above two attempts of performing linear analysis, some others tried to develop simple mathematic relations as criteria for judging the occurrence of casing heading since this should be easier to use in practice.

Asheim (1988) developed two criteria expressed as algebraic inequalities. The first is related to the inflow response. It indicates that the well will be stable if the responses of reservoir inflow and gas injection to a decrease of downhole tubing pressure can result in an increase in the average density of the fluid mixture. This criterion is given by the following algebraic inequality. If it is fulfilled, then the well is stable.

$$F_1 = \frac{\rho_{gsc} B_g q_{gsc}}{q_{lsc}} \frac{J}{\left(EA_i\right)^2} > 1 \qquad \textbf{2-1}$$

Where

F_1	*Asheim stability criterion 1*
ρ_{gsc}	*Lift gas density at standard conditions, (lbm/ft^3)*
B_g	*Volume factor for gas at injection point*
q_{lsc}	*Flow rate of liquids at standard conditions, (scf/s)*
J	*Productivity index*
E	*Orifice efficiency factor*
A_i	*Injection port size, (ft^2)*

If the first criterion is not fulfilled, then the second criterion should be checked, which is related to the pressure depletion response in both tubing and gas conduit, when there is a positive perturbation for gas injection through downhole orifice. If the gas conduit pressure depletes faster than the tubing pressure does, then the pressure difference between the tubing and gas conduit will decrease, so will the gas injection rate. Thus the well is stabilized by the negative feedback effect. This criterion is given by the following algebraic inequality.

$$F_2 = \frac{V_t}{V_c}\frac{1}{gD}\frac{p_t}{(\rho_{fi}-\rho_{gi})}\frac{q_{fi}+q_{gi}}{q_{fi}(1-F_1)} > 1 \qquad \textbf{2-2}$$

where

F_2	*Asheim stability criterion 2*
V_t	*Tubing volume downstream of gas injection point, (ft^3)*
V_c	*Gas conduit volume, (ft^3)*
g	*Acceleration of gravity, (ft/s^2)*
D	*Vertical depth to injection point, (ft)*
p_t	*Tubing pressure, (psig)*
ρ_{ft}	*Reservoir fluid density at injection point, (lbm/ft^3)*
ρ_{gi}	*Lift gas density at injection point, (lbm/ft^3)*
q_{ft}	*Flow rate of reservoir fluids at injection point, (ft^3/s)*

Asheim showed that, by the above criteria, stability was promoted by a high lifting gas rate, a high productivity index, a small injection port and a small gas conduit. The criteria were tested against some reported field data and only one case was unmatched among total 5 cases. One significant advantage of the criteria is that they only need information on variables that are used in the design of the gas-lift installation.

If compare Asheim's criteria with the casing heading mechanism illustrated in last section, it is not difficult to figure out that the first inequality is intended to check if the design is a B-type solution and the second inequality is going to check if casing heading exits once the design is an A-type solution. To obtain these algebraic inequalities, Asheim made several assumptions, by which he mainly ignored the friction and acceleration components of pressure drop in the tubing. Since both friction and acceleration give the stabilizing effects to casing heading, the criteria of Asheim are conservative if his other assumptions were reasonable.

Alhanati *et al.* (1993) extended Asheim's criteria by taking account of different flow regimes for the surface injection choke and the bottomhole gas-lift valve. The interesting thing was that he used the mathematical method of Blick *et al.* and could derive the same result as Asheim got if same assumption was made. According to Alhanati *et al.*, wells operating in the critical flow regimes

of orifice, or throttling close regime of PPO/IPO valve, were always stable. This is illustrated in Figure 2-3.

Otherwise, the flow stability had to be checked with the corresponding criterion. Alhanati *et al.* made the same assumption as did by Asheim, which ignored the friction and acceleration effects for two-phase flow in the tubing. They agreed that this assumption made the criteria give conservative result. In their paper, Alhanati *et al.* also concluded that it was inadequate to tell casing heading by just using steady-state graphic analysis.

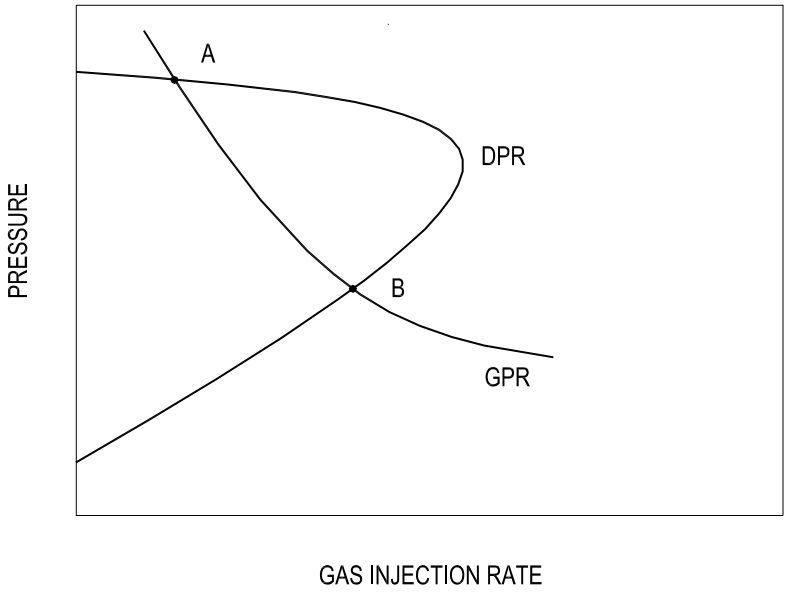

Figure 2-3 Node analysis: using unloading valve as operating valve.

Tinoco (1998) in her thesis verified Alhanati criteria with data from 25 unstable gas-lift wells that used IPO valve as injection valve. The unsatisfied comparison results motivated a determination on what role that friction played in the overall flow performance of the well. A new stability criterion was then developed by adding the friction component for tubing pressure calculation based on the same technique used by Alhanati *et al.* The main conclusion of Tinoco was that casing heading could also happen when the well was operated at throttling close regime of IPO valve.

Tinoco's new criteria were able to predict unstable gas-lift operated at IPO throttling close regime by 80%. However, she did not explain physically why her new criteria improved the accuracy compared with Alhanati's criteria by considering friction in the calculation. Normally friction has a stabilizing effect to the instability, thus Alhanati's criteria should be more conservative than

Tinoco's new criteria. But it was just the opposite according to the results of Tinoco. And this was not properly explained.

Another weak point in Tinoco's thesis was that she did not graphically show the steady-state solutions. So, we have no idea on how the IPO valve discharge performance curve intersected with the GPR of the well. Normally, the steady-state solution located in the throttling close regime of PPO/IPO valve should be B type solution. This was why Alhanati *et al.* concluded that it should be always stable.

The criteria discussed in this section might have been provided as practical methods for the design of stable gas-lift system, but they never substitute the more advanced approaches dealing with unstable well flow. Even just answer yes or no to the stability check, the accuracy of available criteria is far from satisfied since researchers had to inevitably make some simplification during derivation of the criteria as we have seen from the review.

Today even the adoptability of the criteria should be doubted since modern wells are much more complicated in both completion and flow. The simplified models and assumptions used for deriving criteria might have lost their rationality. Let's take a look at the performance of the latest Tinoco's criteria. She used both her criteria and Tang's dynamical gas-lift unloading simulator to check the stability of the 25 unstable wells. Even though Tang's simulator was also quite simple in flow model, results showed that the dynamical simulator predicted 84% to be unstable, while Tinoco's new criteria predicted only 76% to be unstable. For those wells operating under throttling close regime of gas-lift valve, the performance of Tinoco's criteria was even worse.

2.1.4 Dynamic simulation

Besides the accuracy worry, another main drawback for all the criteria is that they can only answer whether the well is stable or not. They cannot tell how unstable it will be. Clearly, the best way of judging and helping to remedy the unstable problem is to construct full transient simulator. But this view could not be accepted some years ago.

Ahanati *et al*. made comments on the dynamical gas-lift simulator in their paper as such, "No matter how accurate such a simulator can be made, it is surely not convenient for design purpose. What one needs are simple and reliable criteria that can be easily incorporated into design program". This is definitely not the case today. The data preparation for a transient simulator will not be more complicated and difficult than that of using so-called simplified criteria, but the outputs from such a simulator are much more abundant, which make the simplified criteria be too inferior to bear

comparison. Although there is still some undergoing research work, searching for a better stability criterion is not prioritized anymore.

The development of dynamic gas-lift simulators has been almost in parallel with the evolution of stability criteria. But unlike the developing process of stability criteria, in which the latecomers followed and improved the work of predecessors, the simulator development was rather independent. We cannot find any inherent connection among different simulators worked out by different people. So, the emerged simulators, listed below in the sequence of appearing time, are all isolated cases. Some simulators might be developed not for, or not limited to the purpose of solving casing heading; for example, several of them were initially developed mainly for simulating unloading process. But they are still included in this review since normally they should also be able to simulate casing heading if they can simulate the unloading process properly.

Grupping, *et al*. (1984) wrote a computer program to simulate casing heading of continuous gas-lift system and analysed the merits of several stabilization methods. To calculate the pressure losses in the tubing string, the main factors taken into account were the relative amounts of liquid and free gas, and their densities at the prevailing pressure. Except this, they did not give detailed description of their model and program.

According to Grupping *et al*., the program successfully reflected the casing heading cycle in the test case. Based on that, parametric studies were performed, which investigated the effects on stability by reducing downhole orifice port size, reducing flow bean and changing surface gas injection. Grupping *et al*. further suggested that continuous gas-lift wells should be equipped with downhole packer and an interchangeable bottomhole orifice. And for a long-term solution of the heading problem, the capacities of the gas-lift and water injection facilities should be balanced since they believed that casing heading occurred mostly when reservoir pressure decreased. There was no further publication on the application of the program afterwards, so its performance and fate are unknown.

Capucci and Serra (1991) developed a transient unloading simulator. The two-phase flow in the tubing was modelled by drift-flux approach. The mass exchange between the liquid and gas phase was ignored. The simulator considered only the simple condition of single tubing and casing size in vertical wellbore. A check valve at the bottom of the tubing string was assumed to suppress back flow. Capucci and Serra demonstrated the simulator's applications in simulating transient unloading process, but no gas-lift instability cases were attempted.

Caralp *et al*. (1993) developed a gas-lift simulator to determine the salient dynamic properties exhibited by the flow model when applied to a hypothetic well. The flow model was based on slug flow that was assumed as the main flow pattern in the tubing. The simulator could reveal the existence of stable oscillations that set in through a supercritical Hopf bifurcation. Caralp *et al*. also gave the guidelines for the selection of running conditions of a gas-lift process. It seems that the simulator was developed just for research purpose rather than being applied to practical gas-lift design and operation. So, no field application cases were reported.

Ter Avest and Oudeman (1995) developed real gas-lift simulator that could be used to aid in the diagnoses of gas-lift problem. The simulator was used to study poor lift gas performance, evaluate quantitatively the effectiveness of remedial measures and optimize unloading procedures. The simulator calculated the local pressure drop along the tubing with multiphase flow correlations. But the hold-up was dynamically calculated based on the mass balance and mass exchange between phases.

Ter Avest and Oudeman showed three field cases of applying their simulator. One case was about casing heading, the other two were related to unloading process and multipoint gas injection. For the casing heading simulation, the simulator gave promising results that matched the well data very well. The simulation even indicated that there was some erosion of the injection valve and the well could be stabilized by installing a valve with a smaller port size. The case study demonstrated that the injection valve port size could be determined from dynamical analysis. Costly wire-line operations to replace the injection valve, which was often on a trial-and-error basis, could therefore be minimized. Unfortunately, except the application cases, Ter Avest and Oudeman did not give more detailed information on the model and the simulator itself.

Gamaud *et al*. (1996) mentioned a gas-lift simulator in their paper, which was used to give training to personnel. According to Gamaud *et al*., the simulator had widened the knowledge of gas-lift operators and proved to efficiently answer to field personnel needs. No more information on the model and simulator was supplied.

Tang and Schmidt (1998) developed a comprehensive dynamic simulator to simulate unloading process. The simulator was based on a simplified two-phase flow drift-flux model, in which only near vertical dispersed flow pattern was considered. The simulator incorporated a transient model to calculated heat transfer in the wellbore. The simulator could be used for the wells with multi tubing and casing size.

Tang and Schmidt not only used the simulator to simulate unloading process, but also applied it to unstable continuous gas-lift wells. Tang simulated three gas-lift wells to check the performance of the simulator in judging stability, among which one was unstable and the other two were stable. He also applied Asheim's criteria to the same wells and obtained conservative results. This once again demonstrated the advantageous of dynamical simulator over simplified stability criteria.

The main drawbacks of Tang and Schmidt's simulator were that, first its flow model was too simple to handle complicated two-phase flow in some wells; second the explicit numerical scheme was used for solving the dynamical model. The first drawback limited its application to the wells with various multiphase flow structures along their complicated trajectory, and the second one added suspicion on its numerical stability and simulating time cost.

EPS has introduced a dynamical gas-lift simulator DynaLift™ to address the opportunity to improve the performance of gas-lift wells through a better understanding of the gas-lift unloading process combined with detailed performance modelling of valves. The simulator can also predict and diagnose heading and "multipointing" problem. Proposed workover solutions can then be developed and tested to ensure the problem is rectified and the correct valves chosen.

Shauna *et al*. (2000) used this simulator in their design of gas-lift during the development of Angola Kuito field. The main task involved in the design was to ensure well flow stability by choosing the right orifice size. The simulator was used to check the well stability at different operating conditions that involve the changing of gas injection rate, water-cut, productivity index and reservoir pressure. It was also used to evaluate the severity of possible well fluctuations under certain design and operation conditions for ensuring that the system could continue to produce without problem when fluctuation occurred.

According to Shauna *et al*., all the above purposes were realized by using the simulator. The details of the flow model and the capabilities of the simulator were not addressed in their paper. No field data was given to validate their gas-lift design.

From above introduction, we have seen the necessity and status of developing transient gas-lift simulation tools. A dynamical gas-lift simulator can help the gas-lift engineers to check the stability of their designs, diagnose the unstable problems and rectify the stabilizing measures. It can also supply operator necessary information on transient gas-lift operation such as

unloading before it is commissioned. Besides, the simulator can be used to give training to gas-lift personnel.

It is also advised that there is still some way to go for such a simulator to meet the demand of field requirements in both functionality and performance. To improve or create new gas-lift simulator, the following aspects have to be emphasized in the future.

1. Transient multiphase flow model is the core part for gas-lift simulator. To have an accurate model is the basic requirement for capturing the gas-lift dynamics. The weakest point for most of the existing simulators is that they use simplified two-phase flow models, or even quasi-transient model. This probably is the main reason for the simulators not having been widely accepted so far.

2. The performances of all kinds of gas-lift valves are also very important since they are involved in the transient gas-lift processes. The simulators should include the characteristics of all kinds of valves, which should be precisely calibrated and modelled.

3. A gas-lift well does not produce in an isolated manner. It dynamically interacts with other wells within the production system. The interactions could come from both gathering network and gas distribution network. A dynamic simulator should have the function of simulating network flows. All the aforementioned simulators have no this capability.

2.1.5 Role and practice of active control

As we have seen from previous sections, conventional methods for stabilizing the wells include wellhead choking, increasing gas injection and reducing the injection valve port size. But all these methods can only stabilize the wells by sacrificing the optimization. Wellhead choking will impose high backpressure to the well flow, thus reduce production. Increasing gas injection will change optimized operation point and require more capacity for compression and distribution system. Reducing the operating valve port size will increase the pressure in annulus, which requires high compressor discharge pressure and could also result in reopen of unloading valves. Besides, the replacement of the operating valve is sometimes very costly and even forbidden.

Even a proper design is selected to avoid instability, the problem still exists since the reservoir condition is always changing and the original design might gradually become inadaptable to the changes. So, it is difficult to get a gas-lift design that can assure stability for the whole gas-lift production life. This consideration drives people to look for alternative methods that can easily

stabilize the well and sustain the production optimum simultaneously. Active control applied on the unstable gas-lift wells is such a method that can satisfy both requirements. Compared with the conventional methods, the active control approach has at least following advantages.

1. It can stabilize the production near the optimum.

2. It is a flexible method that can be easily adjusted for different wells at different production period.

3. The basic measurements and actuator needed by the control are often available in the fields even for the old ones.

Blick *et al*. might be the pioneers who introduced feedback control to stabilize the naturally flowing wells suffering casing heading problem. In order to analyse the unstable phenomenon, the unsteady equations of motion for flow out of the reservoir, flow out of the annulus and flow up the tubing were derived and then solved by the Laplace transform method. Their analysis produced a characteristic equation whose coefficients allowed one to determine if a particular well was stable or unstable.

If the well were unstable, it would be possible to use a feedback controller to stabilize the well. Blick *et al*. found that the negative feedback control structure, which sensed tubing head pressure and then activated the opening of production choke, was theoretically possible to stabilize the well in some situations. Further on, Blick *et al*. performed root locus stability analysis for the feedback controller to find out the range of controller parameters. Unfortunately, Blick *et al*. did not give further information on the practical application of their control design even though their method was demonstrated based on a hypothetical well.

In 1990 Elf Exploration and Production developed a sequence-based control system for automatic handling of single wells and whole field operation. The system was based on universal sequences and fuzzy logic without any computation. Based on the measurements on the wells, the control system dynamically adjusted surface gas injection choke and production choke in such a way that it maximized and stabilized the wellhead temperature, whilst minimizing the lifting gas rate. The control stabilized operating points that were unstable under standard operation through an enhanced path during unloading and transition. The instability was field proven to be path dependent. In case of substantial flow variations, the adjustments on the well were modified immediately to bring the well back to its normal regime. These technologies have been used for nearly ten years on more than 200 wells,

which have increased the average oil production from 5 to 20% and decreased gas lift usage from 5 to 20%.

Der Kinderen *et al*. (1998) introduced a feedback control system to unstable gas-lift wells. The system was called DynaCon. The control strategy was based on stabilizing and minimizing the casing head pressure of an unstable gas-lift well. Two cascaded PID control loops are used to achieve that strategy. The inner loop used casing head pressure as input and the production choke position as output. This loop stabilized the annulus pressure by manipulating the production choke.

This control mechanism was based on that, when the injection rate was fixed at the surface, a constant annulus pressure guaranteed a constant downhole gas injection rate. For example, if the annulus pressure dropped, it indicated that the tubing took too much gas from annulus. This could be counter-acted by increasing the tubing pressure at the injection point, which was achieved by reducing the opening of the production choke. The inner control loop required a set point for annulus pressure which was generated by the second PID loop. The system had been demonstrated in a model gas-lift system of Shell in Rijswijk. Promising result was obtained. Field test was proposed and no result has been published so far.

Jansen *et al*. (1999) suggested a new model-based automatic control approach for unstable gas-lift wells. The suggestion heavily relied on dynamic gas-lift well models, and could be viewed as further development of the control concept of Elf Exploration and Production. The idea behind the new model-based control concept was to analyse and design stabilizing controllers, and if applicable, estimators based on a dynamic model of the system. By using such model-based concept it was possible to stabilize the pressures, temperatures and flow rates of a gas-lift well in an operating point that was unstable in open loop. The model-based stabilizing controller made sure that the control error, the difference between the optimal reference operating point and the real operating point, at any time was kept at a minimum. An appealing feature of the model-based stabilizing controller was that it was able to stabilize gas-lift wells with different available measurements on the wells. Jansen *et al*. demonstrated the concept through dynamic simulation, but no field application was reported.

The core part of Jansen's proposal was the dynamic model of gas-lift well. For the purpose of being used in control analysis, controller design and state estimation, the model should be low dimensional or simplified. Jansen *et al*. created such a non-linear lumped parameter model that involved three ordinary differential equations conserving masses in casing and tubing. The model was improved by Dvergsnes and Imsland (2000) later, which also

included energy balance and friction loss along the tubing. The model was able to capture the main dynamics of unstable gas-lift well, might easily be linearized for linear controller design and could be tuned to fit measured real time series of well flow parameters.

But due to the simplification, the controllers designed based on the model are not reliable. They must be tested and adjusted before being transferred to practical use. That is why a dynamic simulator based on the real model is often needed to test the controller. This adds another reason to the necessity and additional requirement to the function of developing dynamic gas-lift simulator as discussed in previous section.

Gisle ***et al***. (2000) used a commercial available multiphase flow simulator to test different feedback control structures on gas-lift wells. The controllers were designed based on trial-and-error. Two different control structures that activated the production choke were tested for a single open loop unstable gas-lift well. One structure sensed the bottomhole pressure and the other used casing head pressure as input. Results showed that both control structures could stabilize the well, but the first one that used bottomhole pressure as input gave a lower stable downhole pressure. Besides, Gisle ***et al***. also tried to control a two-well system, in which the total lifting gas was fixed and gas robbing between the two wells would occur if no control were applied. Successful results were also obtained. All the simulations were based on a hypothetic gas-lift well. No field application has been attempted so far.

As mentioned earlier, active control is a cost-effective alternative to the conventional remediation methods of unstable gas-lift. But the application of the technology is just at its starting stage. Most of the reviewed cases were based on theoretical analysis and hypothetic well test. So, the robustness and reliability of the active control approach still need to be verified on real wells so that the concept can be widely accepted and applied.

2.2 Pressure-drop type oscillation

As discussed in last section, a positive system feedback to perturbations can be derived for solution A under certain conditions but not for solution B. So, an A-type solution could be statically unstable and a B-type solution is statically stable. Normally this is correct for vertical wells. But sometimes, under certain conditions, a positive feedback can also be derived for a B-type solution for horizontal wells. So, whether the perturbations around a steady-state solution can get a positive feedback from the system is not only dependent on the manner how the two steady-state curves intersect each other.

2.2.1 Introduction

The pressure-drop type oscillation is such a kind of example. Originally, this instability was identified in nuclear and power engineering. Even though it has not been addressed in petroleum engineering, it is believed that it can also happen in oil wells. The concept of this instability is illustrated in Figure 2-4, in which a flow system is sketched. Water is pumped into a surge tank charged by air at the top, and then further to a vertical heated pipe where it is vaporized.

The pump characteristic curve and the two-phase pipe flow characteristic curve are plotted in the same plane. The intersection of the two curves gives the steady-state solution. Since around the solution point, the tangent of pump characteristic curve is less than that of pipe flow characteristic curve, the solution should be statically stable. But if we include the dynamics of the surge tank, this is not true.

Assuming that the surge tank experiences a negative pressure perturbation, both the inflow and outflow of the surge tank will increase according to the characteristic curves. Since the outflow will increase more than that of inflow, the pressure in the tank will continue to decrease, that is, the pressure perturbation gets a positive feedback from the system. So, the system will be statically unstable and migrate towards point A.

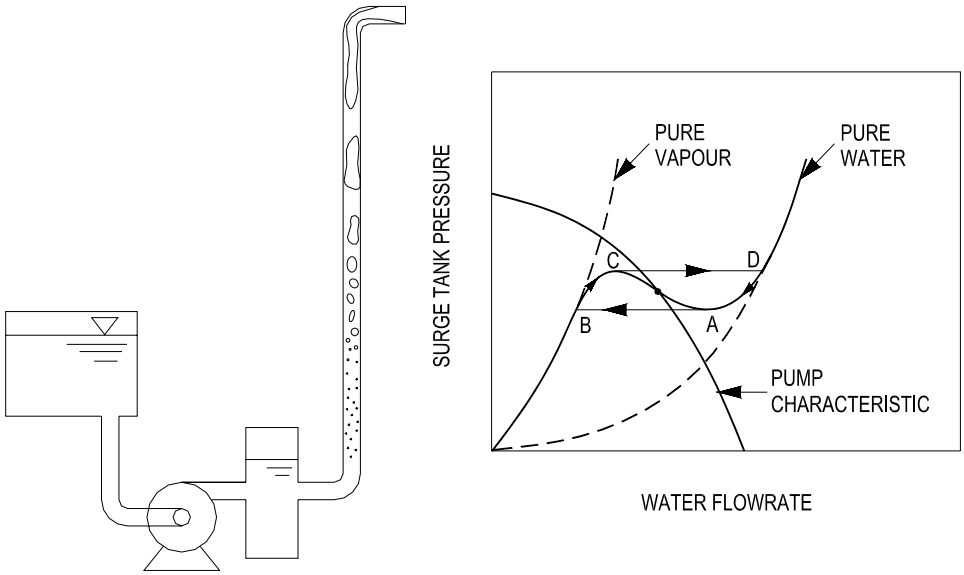

Figure 2-4 Pressure-drop type instability.

Because there is no other statically stable solution and the flow discrepancy will continuously make the pressure in the buffer tank decrease, the excursion process will then jump from point A to point B. At point B, since the inflow is less than the outflow, the pressure in the surge tank will increase. When the pressure reaches point C, the excursion process jumps to point D. Just as opposite as point B, the inflow is higher than the outflow at point D, and thus the pressure starts to decrease. This trend will continue until the pressure reaches point A. From there, the process will repeat itself along the limit cycle ABCD.

The compressible volume that is essential for the occurrence of the pressure-drop oscillations is not necessary to be a surge tank. The internal compressibility of two-phase flow in the horizontal section can sometimes be sufficient large for generating this type of oscillations.

2.2.2 Conditions of occurrence in gas-lift wells

First, the equilibrium point or the steady-state determined by the well inflow performance relationship (IPR) and tubing performance relationship (TPR) should be located at the negative slope of the TPR curve as shown in Figure 2-5.

Second, there should be a compressible volume in the upstream of the tubing to act as a surge tank, for example, this could be the horizontal section filled with both gas and liquid in a horizontal well as shown in Figure 2-6.

In principle, the pressure-drop type oscillation can occur in both natural flowing wells and gas-lift wells as long as the above two necessary conditions are satisfied. But, in practical operations, the pressure-drop type oscillations are rarely encountered in oil wells because the two necessary conditions are too harsh to be satisfied simultaneously. At least so far we have not found any publication that discusses it. So, this instability does not have the common sense for most of gas-lift wells, thus it is not discussed further in this dissertation.

However, it should be emphasized that the possibility of such instability cannot be totally ruled out; particularly in those situations when U-shape well trajectory is presented and reservoir pressure is also depleted.

Another important observation here is that an analogue can be found between the riser based severe slugging and the pressure-drop type oscillation. Many basic characteristics of the severe slugging can be explained by the mechanism of pressure-drop type oscillations.

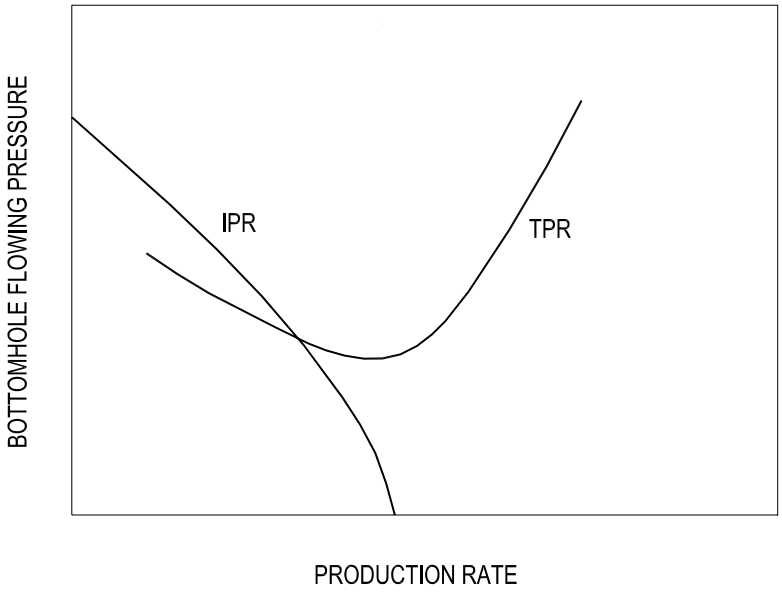

Figure 2-5 Well performance curves

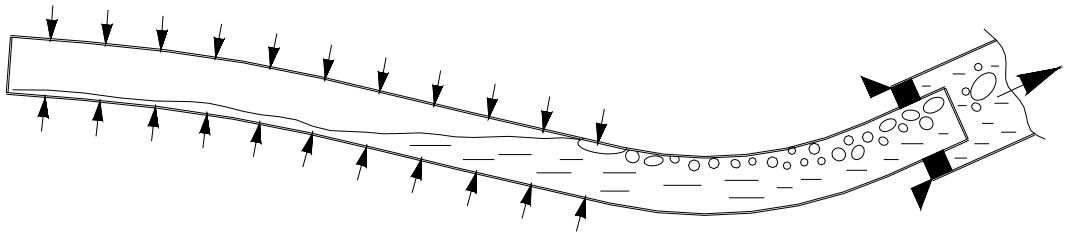

Figure 2-6 Gas and liquid segregation at the V-shape horizontal wellbore

2.3 Summary

From the above reviews and discussions, it is made clear that casing heading is triggered by the system positive feedback to its bottom gas injection perturbation. It is impossible to occur in those gas-lift wells where friction is the dominant factor for the flow within tubing. For gravity dominant systems, the occurrence depends on many factors. An A-type solution in Figure 2-1 is a necessary condition for casing heading. So, to thoroughly eliminate casing heading, we can choose the B-type gas-lift design as long as it is feasible.

Developing casing heading criteria not only supplied simple tools for gas-lift engineers to check the stability of their designs, but also resulted in many useful conclusions that led them to solve casing heading problem. Those basic conclusions include

1. Increasing gas injection rate increases stability.

2. Increasing productivity index increases stability.

3. Wellhead choking increases stability.

4. Increasing gas injection pressure by using a smaller port size orifice increases stability.

5. Smaller annulus volume increases stability.

Dynamic simulation and active control of casing heading are two new diagnosing and stabilizing approaches. But their applications are still in initial stages. Field application reports are rare even though publications based on hypothetical wells are available.

Pressure-drop type oscillation is another possible static instability that may occur most likely in depleted horizontal wells. Even though this instability has not been widely addressed in petroleum engineering, it definitely can occur if certain conditions can be satisfied. However, in this dissertation when discussing field reports of unstable gas-lift, it is assumed that pressure-drop type oscillation is not the reason. This is because the unstable gas-lift wells from the field reports are either vertical wells or horizontal wells with under-saturated oil at its horizontal sections.

3 DYNAMIC GAS-LIFT INSTABILITY: AN EMERGING ISSUE

3.1 New gas-lift instability problem

As mentioned in first chapter, unstable gas-lift production is undesired in practical field operation. Whenever it happens, it should be solved in an effective and efficient manner. However, since the unstable gas-lift production could be due to different reasons, the investigators must recognize the type of flow instability on hand before he can perform analysis or apply remediation.

For example, as it is shown in the review of casing heading, active control is an effective and efficient approach that is getting more and more active in solving unstable gas-lift problems. To apply active control to a certain unstable gas-lift well, one may need to know why the well is unstable, what kind of instability it is, can we use a first principle model to describe the instability, and so on. In this respect, it is therefore very important to identify the instability that could happen in a gas-lift system since different instabilities may have different characteristics and require different control design to stabilize it.

To carry out this identification, the first we should do is to distinguish between the local instability such as hydrodynamic slugging and systematic instability such as casing heading. Furthermore, if it is systematic instability, we should know whether it is static instability or dynamic instability. This procedure definitely requires that we know very clearly about all the instability types and their characteristics.

Static gas-lift instabilities, particularly the casing heading studies have already been reviewed and discussed in last chapter. It is concluded that normally in a vertical well the A-type solution in Figure 2-1 is a necessary condition for casing heading and the B-type solution is a sufficient condition for not casing heading. So, if the gas-lift design requires the well produce at solution A, then the well will be very possible, but not necessary, to be unstable. To avoid casing heading, the B-type solution should be selected when it is suitable to do so. But the question now is: “Is it possible for a statically stable solution such like B to be dynamically unstable?”

The answer to this question is “yes”. This means a system that has a negative feedback mechanism to flow perturbations around a steady-state solution could also be unstable. Xu and Golan mentioned in their paper that even if a steady-state solution was statically stable, it might not satisfy the dynamic

stability criterion, so it might still be dynamically unstable. Even though they used the classical definitions of static and dynamic instability, the deduction is still valid here in terms of the new definitions presented in the first chapter. This is because we do have some evidence from field reports, which support the answer.

3.1.1 Field observations

Alhanati *et al*. (1993) gave a field example describing a new gas-lift instability that was different with casing heading. Their description is cited as below.

> *"Some of the wells included in the Prudhoe Bay data exhibited instabilities, sometimes severe, that can not be explained by the mechanism* (casing heading) *described in the introduction. For instance, there were wells with huge oscillations in the tubing pressure with little oscillation in the casing pressure. Because the gas flow rate through the surface choke was constant all the time, the nearly constant casing pressure implies approximately constant flow rate through the gas-lift valve. The only possible sources of these particular instabilities that we can think of are those attributed to vertical two-phase flow in pipes under certain conditions. Although we are aware of some studies in this area, we know of no practical criteria that can be used to predict this type of instability. The normal solutions used to control "regular" gas-lift instability* (casing heading) *may not work for these cases."*

Clearly, the gas-lift wells described above had B-type solutions (statically stable) since the gas injection rates through their operating valves were almost constant. This can be easily plotted and figured out in a graph like Figure 2-1. The interesting thing was that, despite the steady-state solutions being statically stable, the wells could still be dynamically unstable and sometimes even severe.

Tinoco (1998) collected some data from 25 unstable gas-lift wells in Tia Juana field located in the eastern part of the Maracaibo basin in Venezuela. All of the wells used IPO valves as gas-lift operation valve. Some of them were operated within the throttling close regime of the valve, which normally should be casing heading free due to the statically stable operation design. Unfortunately they were not!

Tinoco treated all the unstable phenomena as casing heading problem without distinguishing them with the mechanism of casing heading. This might explain why the results were far from satisfied when she checked the stability

even with her improved casing heading criteria. Another important hint was that Tinoco did not explain physically why the wells were casing heading when the gas injection valves were operated under throttling close regime. It seemed to be too farfetched to take all unstable phenomena as casing heading. There might be something else in the background.

Some other dynamic gas-lift instability evidence involves the application of the newly developed gas-lift valve based on nozzle-venturi principle. The background of developing the new valve is briefly introduced below.

To thoroughly eliminate casing heading, we may change the property of solution A by reducing the port size of injection orifice. This is illustrated in Figure 3-1, from which we can see clearly that the tangent value of GPR can be larger than that of DPR if using an orifice with a small enough port size.

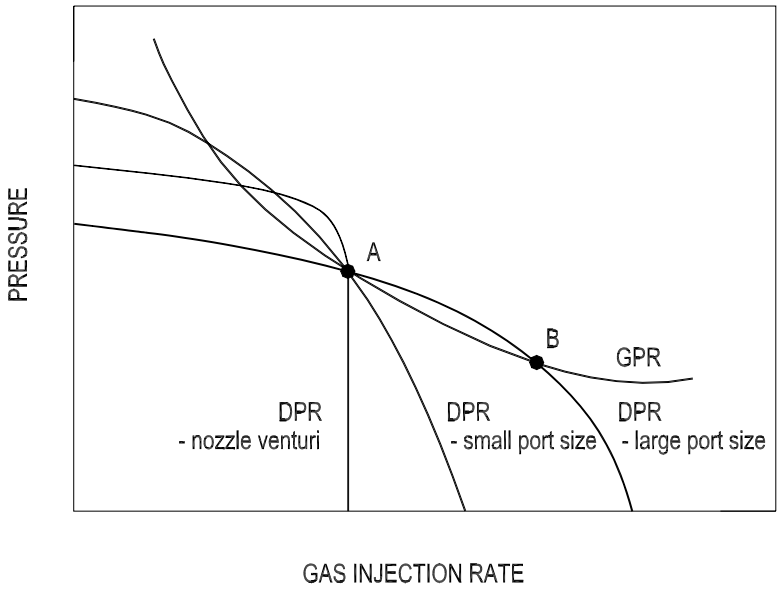

Figure 3-1 Node analysis: effects of changing orifice size and using nozzle-venturi valve.

But this stabilizing option has its drawback. It needs to increase the annulus pressure. This means that a higher discharge pressure is required for the gas compressor. Besides, increasing annulus pressure may also result in the reopen of unloading valves, particularly the IPO valve. So, the aforementioned approach for avoiding casing heading is not practically favourable.

To tackle the problem of increased annulus pressure, Tokar *et al.* (1996) suggested a new type of operating valve based on the nozzle-venturi principle. Compared with orifice valve, the new valve has two attractive features. First, it needs a much smaller pressure difference across the valve to attain critical flow. Second it needs a much lower annulus pressure to get a B-type solution. These two features can be easily figured out in Figure 3-1.

According to Tokar *et al*., the pressure difference for the new valve to get critical flow is about 10% of the upstream pressure, only one fourth of that of orifice. Tokar *et al*. used the new valve on a dual gas-lift well and successfully eliminated casing heading by critical gas injection. It therefore stabilized the whole well by cut off the fluctuation interaction between the two strings.

Due to its attractive performance, the nozzle-venturi valve has been selected in more and more modern gas-lift well designs. In the meantime, it is also used to replace orifice for the unstable gas-lift wells. Since a B-type solution is already sufficient for casing heading not to happen, it is not necessary to make the valve to work under critical flow regime even though it is normally selected so. As long as the parameter of nozzle-venturi valve is properly selected, casing heading should be eliminated no matter whether the gas injection is critical. Thus, there must be some other reasons if the well is still unstable after the nozzle-venturi valve is installed.

Faustinelli *et al*. (1999) shared their experiences of using nozzle-venturi valve to solve casing heading problem. They replaced the orifice valves in seven unstable gas-lift wells with nozzle-venturi valves. All the wells are located offshore Lake Maracaibo. Among the seven wells, five was successfully stabilized after the nozzle-venturi valve had been installed. Two wells were unfortunately still unstable. One of them was observed to be unstable in both casing and tubing pressures and the other only in tubing pressure. Faustinelli *et al*. explained that the failed stabilization for the two wells attributed to sub-critical gas injection and gas liquid slip in tubing respectively. Cleary, their explanations were ambiguous and inconvincible. But the real interesting observation was, for a B-type solution, the well could also be dynamically unstable no matter the gas injection was critical or not.

Another case of applying the nozzle-venturi valve to remove casing heading was from Brage field of North Sea. Approximately 16 gas-lift wells were installed the valve and casing heading was successfully removed or avoided in that field. Unfortunately, eliminating casing heading does not necessarily mean that the well is unconditionally stable. Damped casing flow oscillations sometimes did not result in the expected oscillation damping in the tubing side. Operators gradually find that those gas-lift wells equipped with venturi

gas-lift valves can still exhibit periodic unstable flow behaviours, particularly when the reservoir pressure is depleted.

Recent reports from Brage field of North Sea show that many wells are subject to severe flow oscillations in tubing due to unknown reasons. The periodic varies from 20 minutes to 2 hours, and bottomhole flowing pressure oscillation amplitudes change from 5 to 10 bar from well to well. The phenomenon is definitely different with hydrodynamic slugging in the normal sense. Figure 3-2 shows the oscillations of oil, gas and water flow rates at the wellhead for one of the unstable wells.

The aforementioned cases significantly demonstrated that a statically stable steady-state solution could be sometimes dynamically unstable. There might be many more such field cases not being reported due to the reason that they are very easy to be misinterpreted as casing heading when gas injection is sub-critical since the phenomenon in appearance is very close to casing heading. This might also explain why there is no publication so far to discuss about this newly identified unstable phenomenon.

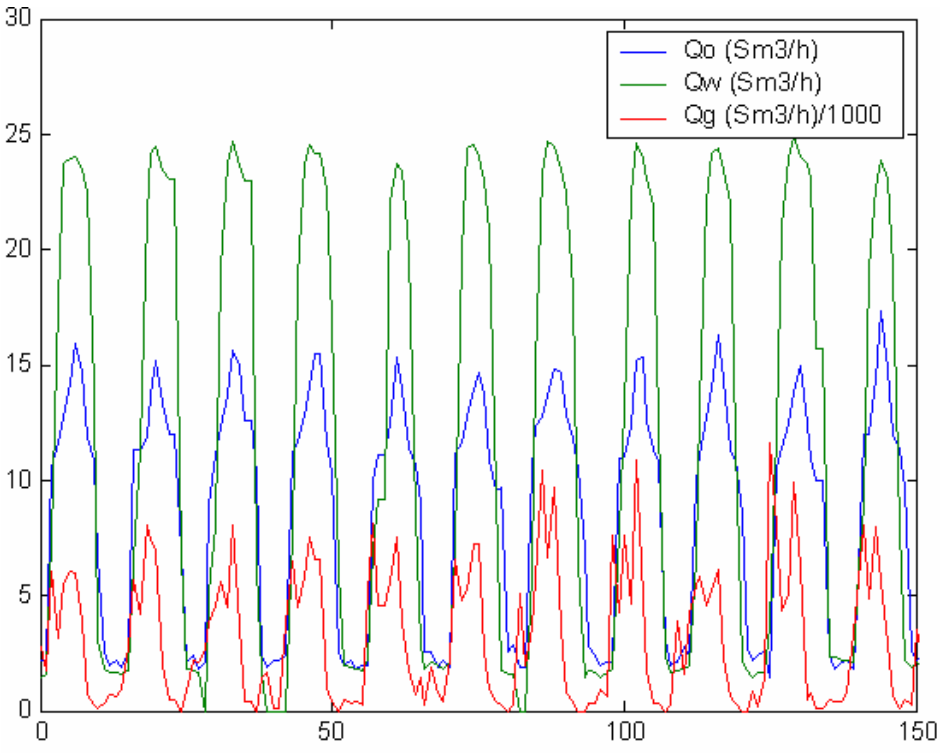

Figure 3-2 Oscillating wellhead flow rate of one of unstable Brage gas-lift wells. X-axis is time in minutes. Courtesy Norsk Hydro AS

3.1.2 Unstable airlift pumping

Some other evidence of Xu and Golan's deduction can be found in airlift pumping process. An airlift pump has the same principle as a gas-lift well. A typical airlift pump, as shown in Figure 3-3, consists of a vertical riser pipe and an air injection conduit. The riser is partially submerged in a liquid and the compressed air is injected into the riser through an injection device near its bottom. Because the density of the air-liquid mixture in the riser is less than that of the surrounding liquid, a pumping action is caused by hydrostatic pressure difference. Thus, the two-phase mixture is elevated and discharged at the top of the riser.

According to Zenz (1993), the applications of airlift pumps have included the handling of hazardous fluids, the design of bioreactors, the recovery of archaeological artefacts, recycle aeration in sludge digesters, deep-sea mining and the recovery of manganese nodules from ocean floor.

An airlift pump differs from a gas-lift well in four aspects.

1. The flow path of an airlift pump is order-of-magnitude shorter than a gas-lift well.

2. The riser pipe inlet normally is open and without any restriction.

3. Due to its small scale, the flow inlet effect, depending on the air injection method, plays an important role in pump performance.

4. The air injection conduit size is quite small comparing with the riser pipe.

Since the air injection conduct is very small, its buffer effect could be ignored, thus the air injection at the bottom of vertical riser can be taken as constant.

It is clear that the pumping process has a self-controlling character (negative feedback) in terms of the stability, since a small disturbance, which increases the liquid inflow, causes an increase of the density of the air-liquid mixture, which has a slowing down effect, and vice versa. But for certain combinations of the submergence ratio and air injection rate, the self-control mechanism may be breakdown and airlift pump becomes unstable. In this case, the flow at the discharge fluctuates strongly, which cannot be accepted in many applications.

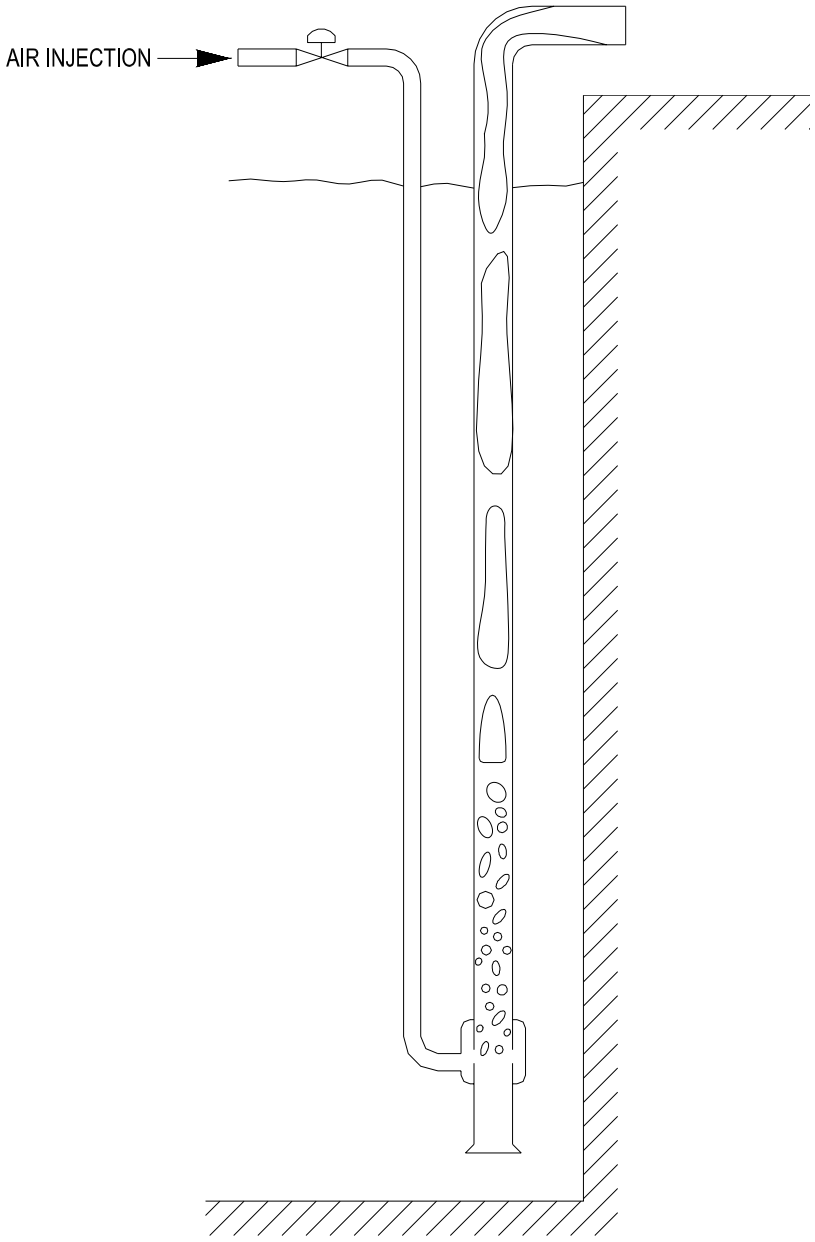

Figure 3-3 An airlift pump.

Hjalmars (1973) carried out a preliminary analysis to find out the origin of the instability. He assumed an incompressible, isothermal and frictionless system with a constant air injection rate at the riser lower end. With these assumptions, an analytical perturbation analysis was conducted based on homogeneous model for air-water two-phase flow in the riser. It was found that a small time-dependent liquid inflow perturbation around its steady-state value satisfied a linearized second order retarded difference-differential equation, in which a time-lag term presented. Due to the time-lag, the self-control mechanism of airlift pump was delayed and instability might set in.

Hjalmars developed a stability criterion by solving the system characteristic equation analytically. The criterion gave the relationship of different parameters of airlift pump such as the submergence ratio and air injection rate. Even it was a preliminary study, the results still gave a reasonable approximation of the critical submergence ratio, at which the pump started to be unstable with a given air injection rate. The predicted oscillation frequency was also in agreement with observations. Although Hjalmars did not show explicitly in his paper, it was clear from his derivation and solution that the unstable phenomenon could be labelled as density-wave instability. Hjalmars' pioneering work initiated the study of airlift pump instability despite that he made some assumptions in the analysis, which resulted in no greater quantitative significance of the solution.

Since the analytical solution was neither subject to numeric instability, nor numeric diffusion, it provided references against which dynamic simulators could be tested if its accuracy could be improved. Asheim (2000) made an effort on this. He extended Hjalmars' analysis by including wall friction and interface slippage so that the solution could be used to verify the performances of dynamic simulators when simulating vertical two-phase transient flow.

A hypothetic 25 m deep, 0.2 m ID airlift pump was analysed and simulated for comparison. The pump was arbitrarily applied a high system pressure of 100 bar. By doing so, the air expansion effect could be ignored since the pressure drop along the riser was too small compared with system pressure. Thus, the system could be considered incompressible as it was assumed in the analysis. Results showed that the commercial dynamic simulator OLGA (v3.4) gave quite different predictions compared with the analytical solution, whilst an experimental numerical simulator, developed by the author, exhibited satisfying performances.

Asheim ended up with a similar dynamic equation with Hjalmars. But, instead of using Hjalmars' solution, he resorted to numerical method to find out the roots of the characteristic equation, which in principle could have an infinite

number of solutions. The details of the numerical method were unfortunately not presented in the paper. Since zero was always a root of the derived characteristic equation, the corresponding linear dynamic system only had a neutral stability. This was also not addressed when comparison had been made. Besides, including slippage was necessary for improving the accuracy, but this damaged the perfection of the “analytical” since approximation had to be made so that the perturbed momentum equation could be integrated along the riser.

For small diameter airlift pump, assumptions of homogenous flow and neglecting wall friction are unrealistic. Moreover, air compressibility effect directly related to the volume of injection conduit should be considered when air injection regulating valve has to be kept outside the liquid that could be contaminated with hazardous substances. De Cachard *et al*. (1998) investigated the stability of a small diameter airlift pump, in which liquid was sucked by a U-tube from a head tank instead of liquid basin. The inertia effect of the liquid in the U-tube was included in the analysis. A slug-churn flow model was used for describing two-phase flow in the riser pipe. The assumption of incompressible flow in the riser was still kept, but the compressibility of the air in the injection conduit was considered. Both linear analysis and experiments were conducted and results were compared.

De Cachard *et al*. observed interesting phenomena when changing the air injection rate at some combinations of geometry and submergence ratio. When the air rate is low, the flow was unstable. Increasing air rate tended to make the system stable, but it then became unstable again when the air rate reached to a certain level. Besides, during the process, sub-critical instability might also happen, which was only observed from experiments and could not be estimated by linear analysis. Stability effects of inertia and friction, volume of air injection conduit and submergence ratio were also studied. The system tended to be stable by increasing the length and reducing the diameter of the suction pipe. Increasing the volume of air injection conduit strongly destabilized the pump, whilst increasing submergence ratio gave the opposite effect.

De Cachard *et al*. did not explain the physical background in details about the phenomena they observed except that density-wave instability was mentioned and thought to be the reason of the oscillations. Despite that the linear analysis gave similar parametric trend for instabilities compared with experiments, the quantitative prediction of the stability thresholds showed a systematic error in the non-conservative direction. This might be due to the assumption of incompressible flow in the riser.

To investigate the influence of air bubble expansion and relative velocity on the performance and stability of an airlift pump, Apazidis (1985) carried out mathematic analysis and experimental work based on a model pump. The height of the model pump was just 0.49 m and the inner diameter was 13 mm. Compressibility and slippage were both considered in the linear stability analysis. Wall friction and air conduit volume effect were still ignored. Results of linear analysis were compared with experimental observations.

Apazidis showed that the prediction of stability threshold based on Hjalmars' method, which did not consider air expansion and phase slippage, was quite inaccurate compared with experimental observations from the model airlift pump. Fist of all, Hjalmars' method failed to predict the local minimum of the critical submergence ratio, instead, it gave a monotonous trend when increasing air rate from low to high. Second, there was a drastic difference between the prediction and experimental results. Apazidis' analysis, which considered air expansion and relative velocity, agreed quite well with the experimental observations both in parametric trend and in numbers.

Since there were no experimental results based on other real scale airlift pumps, Apazidis could not give further series results to demonstrate the influence of air bubble expansion and relative velocity on the stability of airlift pump. He could only concluded that the air expansion and relative velocity had a big influence on the stability of the model pump without giving more detailed discussion. His paper also implied that the influence could vary from pump to pump depending on their sizes.

Apazidis also observed significant difference in the model pump's performance when changing injected air bubble size by adding detergent to water from both analysis and experiments. Injecting air with smaller bubbles could improve the pump's performance significantly, e.g. a 10 to 40% reduction in the submergence ratio at the same values of air and water flow rates had been observed when reducing the diameter of the air bubble from 2 mm to 1 mm. But the bubble size effect on large-scale airlift pump was not as strong as in the model airlift pump.

There were three main defectives in Apazidis' work. First, he compared the steady-state solution of his mathematic model with the experimental results without considering the influence of instability on the discharged water rates. Second, he did not consider the effects of air expansion and relative velocity separately, thus no further conclusions were given on each effect respectively. Third, the instability of the model airlift pump was determined visually instead of using precise measurements. The pump was said to be unstable when there was a periodic emptying and refilling of the riser. In fact this is too conservative for the instability. However, Apazidis gave a quite

concise mathematic formulation in the linear stability analysis. The way he did the analysis is going to be adopted in this dissertation with some modifications.

There were also some other studies on the airlift pump instability, which mainly or purely concentrated on the experimental observations. Sekoguchi *et al*. (1981) conducted experimental investigation on the characteristics of airlift pump instability. The experiment system consisted of an air-water separator and a constant head tank, which were connected by a 25.9 mm I.D. U-tube and a water-return tube. The height of the two-phase flow riser was about 6.2 m. The pressure in the separator and head tank was controlled constant below atmosphere reference by a vacuum pump. Tested submergence ratios were from 0.363 to 0.980. The air injection rate was controlled constant near the injection device, thus the air injection conduit could be ignored from the pump instability. The air rate was well controlled even when the flow within the riser fluctuated strongly.

Various instability phenomena were observed from the experiments. Sekoguchi *et al*. classified them into four types depending on whether they were periodic and whether a reverse flow of feed water was observed. Type I, corresponding to low air injection rate, was just random fluctuation accompanied by an occasional reverse flow. Type II showed clear periodic oscillations, in which, an air slug as long as the riser and many short air slugs alternately occupied the riser. Type III gave the transitional flow from type II to type IV, whose periodicity was obscure and reverse flow was still observed. Type IV was just random fluctuation without reverse flow.

Type II was the main unstable phenomenon discussed by Sekoguchi *et al*. Based on the observation, they concluded that the periodic phenomenon in the experiment was a self-excited oscillation induced by a flow rate fluctuation due to the compressibility of gas in the two-phase mixture and the reverse flow to the head tank of feed water. The basic characteristic of the typical periodic flow (type II) was that, two different flow patterns alternatively appeared in the riser in every half period. Sekoguchi *et al*. also showed that the unstable phenomenon was likely to happen at lower submergence ratio, and would disappear as the submergence ratio approached unity. Another interesting conclusion was that flow oscillation promoted the pumping action of water in the experiments especially in the case of small submergence ratios.

Sekoguchi *et al*. gave the detailed description of the self-excited oscillation cycle, which, they thought, attributed to gas compressibility in the two-phase region within the riser. But the interesting thing was that they mentioned in the paper the transit time of air-water mixture under unstable flow conditions was

comparable to the period of void fraction oscillation, which was also called continuity wave or density wave sometimes.

Tramba *et al*. (1995) also did visual study on airlift pump instability. The experiment system they used consisted of a 1.65 m riser partially submerged in a tank of water. Air was injected from the lower end of the riser duct. To obtain a better view of the unstable phenomenon, a plexiglass riser with rectangular cross section of 9x2 cm was used in the experiment. The motions of fluid in the riser were recorded using a high-speed video system, which had a recording speed up to 400 f/s (frames pr second). Before the experiments, they already knew that two-phase flow in the airlift pump could be unstable, resulting in periodic emptying and refilling of the riser and the onset of this behavior depended on the submergence ratio and injected air rate. So, the main purpose of the visual study was to capture the phenomenon and look at it in detail.

Tramba *et al*. recorded the experiments with low submergence ratios (from 0.17 to 0.31). They observed that the generation of an unstable cycle occurred in the region around the air injector. The main characteristic of the two-phase flow structure, during the generation of the cycle, was an air pocket that was a gradually increasing volume of air above the injector, in which water was entrained and dispersed in the form of droplets. The sequence of events closed with a burst-like expansion of the air pocket at the top of the riser duct. In Figure 3-4, this can be seen clearly from the sketches of the two-phase flow in the riser duct at different stages of the oscillation cycle. Tramba *et al*. gave a detailed description of the cycle from stage to stage in their paper.

Tramba's *et al*. work was pure visual study without too much discussion on the theoretic background. But the sketches they produced from the experiments' observation were quite persuasive in demonstrating airlift density-wave instability.

Alimonti *et al*. (1992) did steady-state airlift modelling for the design of its control system. The model was compared with experimental data and a good agreement was obtained. The purpose of the control system design was to keep the liquid flow around its desired value in spite of the immeasurable external influences. The desired value was related to an operating point corresponding to a maximum economical airlift resulting from a steady-state optimization of the pumping system. Their starting point was that the airlift pump was open-loop stable.

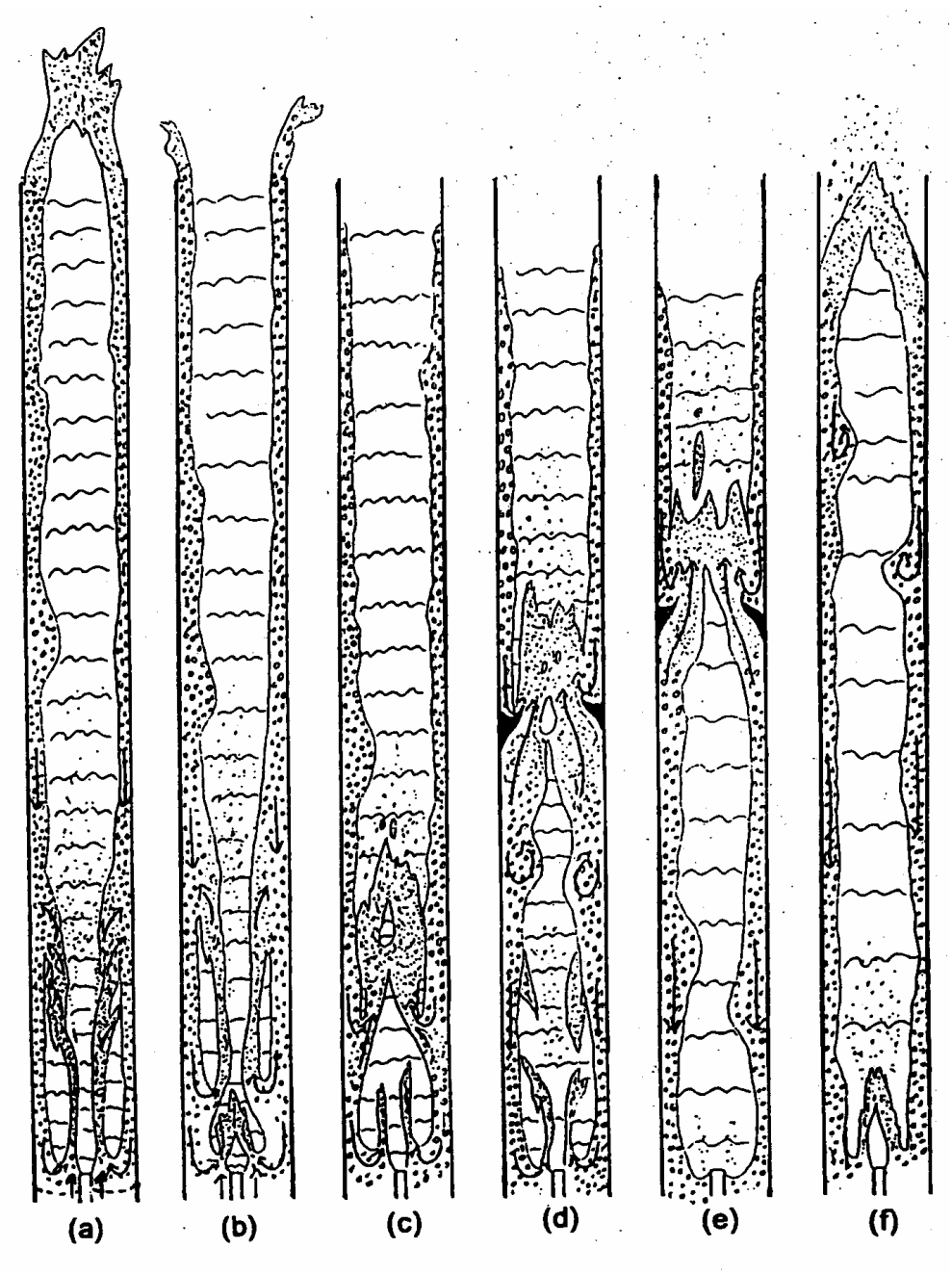

Figure 3-4 A sketch of unstable airlift pumping cycle. Courtesy Tramba *et al*.

The objective could be achieved by control the air injection rate according to Alimonti *et al*. The control scheme they suggested was a true model-reference system where the feedback signal forced the process output to track the model output. They concluded that the proposed model based control system allowed fulfilment of rejection of parameter variations, stability of the closed-loop system and low sensitivity of time response to the actual operating conditions of the pump. Clearly, the starting point and purpose of the control design of Alimonti *et al*. was different with that of active control for unstable gas-lift wells.

The above review shows that a statically stable airlift pumping design can be dynamically unstable and the instability is system related. Even though an airlift pump is not exact the same as a gas-lift well, the common principle of the two processes remind us of the importance of the above observations and their potential hints in solving similar gas-lift instability problem.

3.2 Density-wave propagation and dynamic instability

As mentioned by Alhanati *et al*., the dynamic instability observed in gas-lift wells is related to that of vertical two-phase flow in pipes under certain conditions. If we ignore those instability types induced by thermal effects, the dynamic instability in a two-phase flow system with constant inlet and outlet pressures is characterized as density-wave type oscillation.

Density-wave type oscillation or density-wave instability as just mentioned in the unstable airlift pumping review is related to kinematic wave propagation phenomena, which sometimes is also called continuity wave or void wave. When density-wave instability happens, fluid waves of alternative higher and lower density mixtures travel through the system. The concept of density-wave instability can be explained by the simplified concentrated pressure-drop model as shown in Figure 3-5.

In the model, the air injection rate is assumed constant. The liquid level and pressure at the outlet are both fixed so that the total pressure drop across the system is kept constant at all times. If ignore the pressure drop along the tube, the total pressure drop across the system concentrates on the inlet and exit restrictions. It is also assumed that the flow rate of this system is low and the restrictions at both inlet and outlet are strong functions of mixture density.

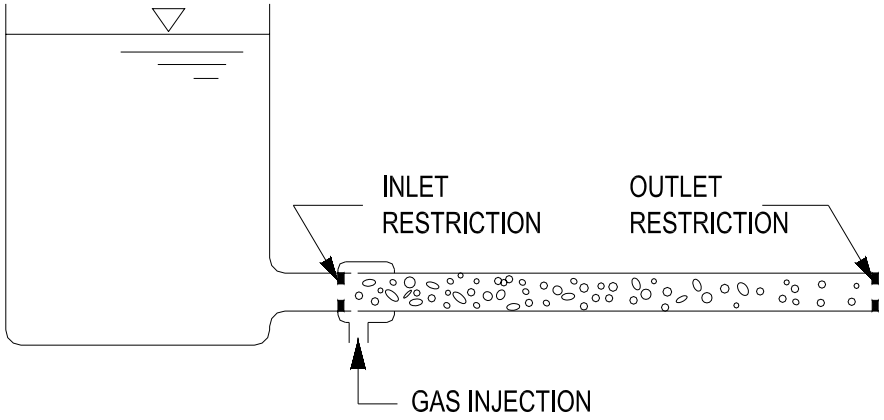

Figure 3-5 Illustration of density-wave instability in a horizontal system.

Suppose that, at time zero, the exit restriction pressure drop undergoes a sudden infinitesimal drop from its steady-state value, thus the pressure drop through the exit restriction will decrease and this decrease is propagated to the inlet almost instantaneously at the speed of sound. Since the total pressure drop across the system is constant, then the pressure drop at the inlet restriction will increase. As a result, the inlet liquid velocity is increased infinitesimally. Since the air injection rate is constant, the fluid mixture at inlet thus obtains a higher density than normal almost at time zero. The wave of higher density mixture is set to travel along the horizontal tube. After a certain period Δt, it reaches the exit restriction, and then causes an infinitesimal increase to the pressure drop at exit restriction due to higher density. This on the contrary will decrease the inlet velocity and result in a lower density fluid mixture at the inlet.

Once again, it takes another Δt time for the wave of lower-density mixture to travel through the tube. When it arrives at the exit restriction, another infinitesimal decrease for the pressure drop across the exit restriction is triggered and the process repeats itself. So, when density wave occurs, it takes one high and one low wave to make one cycle. It is therefore concluded that the periods of density-wave oscillations are roughly equal to twice of the transit time of fluid particle flowing through the system.

The occurrence of density-wave instability relies on the delayed system negative feedback to the flow perturbations. This is clearly demonstrated in the above illustration, in which the damping to flow oscillation from the exit restriction is delayed by a time-lag Δt. This out-of-phase effect between the pressure drop and flow rate change is the core concept of density-wave instability.

For the system in Figure 3-5, making the exit restriction much larger than the inlet restriction decreases the stability. Naturally, if we relatively increase the restriction that is in-phase with the flow rate change, for example, the inlet restriction in the above system, stability will be improved.

Svanholm (1989) derived an analytical instability criterion for the system in Figure 3-5, which shows that the system is unstable if the pressure drop at the outlet restriction is about the twice of that at the inlet. If the system is unstable, the infinitesimal perturbation is expected to grow to a limit cycle oscillation. Otherwise, it will be gradually dampened.

Unlike the pressure-drop type oscillations, density-wave instability does not require an upstream compressible volume in the flow path, and its corresponding steady-state solution is located on the positive slope of TPR curve. As having been reviewed, the dynamic instability observed in airlift pumping process attributes mainly to density-wave oscillations. This also emphasizes the importance of density-wave instability and indicates its possible existence in gas-lift wells.

3.3 About the investigation of this dissertation

It is shown from the review in last chapter that casing-heading problem has been widely investigated. We are now very clear about its mechanism, characteristics and stabilizing methods. But for the new observed unstable gas-lift phenomenon, which has a dynamic instability background, has not been touched by the researchers. We have not got any publication that discuss about it from the literature survey in petroleum area even though some people might have realized the possible existence of such instability in gas-lift wells.

For instance, Alhanati *et al*. not only described the new instability phenomenon, but also pointed out that it was related to that of vertical two-phase flow in pipes under certain conditions. Unfortunately, they did not go further beyond that.

Asheim also noticed the dynamic instability in airlift pumping process when he investigated casing heading problem, but he was not optimistic about the possibility for such instability to occur in gas-lift wells since the inflow mechanism of a gas-lift well was considerably more complicated than an airlift pump and the friction damping would be much larger in a gas-lift well because of out-of-magnitude-larger flow length. He expected that deep wells favour excursive rather than sinusoidal variations. However, in his another paper, Asheim added that this should follow as a result from the stability analysis, rather than an á-priori assumption.

3.3.1 Tasks of this study

Today the new observed instability becomes more and more common in gas-lift wells that produce from depleted reservoir, particularly after the nozzle-venturi type of gas-lift valve was installed. Some unstable gas-lift wells even face the fate of shut-in due to the gradually increased fluctuation. So, field operators are anxiously to know why their wells are unstable and how to deal with it.

Appeal of investigating the new phenomenon also comes from control engineers who attempt to stabilize those wells by active control. In fact, some of the unstable wells were already installed feedback controllers. However as we know, due to lack of knowledge and information of the instability, not all the controllers gave successful stories. It might be possible that the controller designed to control systematic instability, was mistakenly installed on a well with normal hydrodynamic slugging since sometimes it is difficult to distinguish between local and systematic instabilities without knowing them in advance.

In respond to the appealing of both field operators and control engineers, this dissertation aims at verifying the occurrence of dynamic instability in gas-lift wells and investigating its characteristics upon presence. As mentioned earlier, density-wave instability is the only form of dynamic instability in a pressure-pressure boundary two-phase flow system if we discard those instabilities due to thermal effects and acoustic-type oscillations. So, the task of the rest of this dissertation is to investigate the existence of density-wave instability in gas-lift wells and its characteristics.

3.3.2 Considerations and assumptions

This study is more qualitatively oriented. It does not look at any concrete unstable well. Instead, it mainly concentrates on the common fundamentals of gas-lift instabilities. To make the results of this investigation be with common sense, it is therefore necessary to simplify the gas-lift well system and ignore the unimportant factors to the occurrence of instabilities. Besides, some reasonable assumptions have to be made so that the research work can concentrate on the main tasks. For example, air and water are used as test fluids instead of hydrocarbon gas and oil so that the complicated PVT behavior of the reservoir fluid can be ignored. This definitely simplifies the research work.

The other main simplifications made in this study are as followings.

1. A vertical well with single tubing diameter is assumed. It is believed that any instability occurring in a vertical well will definitely appear in

horizontal and deviated wells. So, to investigate the instabilities in a vertical well is more representative.

2. Unloading valves are removed from the well. Even though unloading valves often join the dynamic process, they give no influence on the mechanism of the instability to be discussed.

3. An isothermal system is assumed since heat transfer and other thermal effects are not key factors to flow instabilities here.

With the above simplifications, the gas-lift well illustrated in Figure 1-1 can be abstracted into the system shown as Figure 3-6, which mainly consists of two vertical pipes. The right-hand pipe represents the annulus and the left-hand pipe represents the tubing. Lifting gas is injected from left-hand pipe to the right-hand pipe through injection valve. Three boundary conditions for the simplified system are specified as followings.

1. On the annulus side, the gas injection rate at the surface injection choke is constant.

2. On the tubing head, outlet pressure is thought to be constant.

3. At the bottom of the well, a steady-state linear inflow performance relationship is applied, which means the influx is proportional to the drawdown from the reservoir to the wellbore. The ratio between influx and drawdown is called productivity index (PI).

Obviously, the first boundary condition is reasonable since most of gas-lift wells are operated under certain gas-injection rate and it should be controlled constant as we have discussed previously.

The second boundary condition might not be always applicable to practical wells since many wells are connected with a surface or seabed gathering system that can create many possibilities for the wellhead pressure to be in continuous variation. But it is a natural assumption of the arbitrary system considered in this study, which does not include the gathering system and the transport flow line. Even for a production system, this is still a reasonable boundary condition in terms of identifying the instability source if we are sure it comes from the well, which means the occurrence of the instability is independent on the downstream flow even though it might affect the appearance of unstable phenomenon.

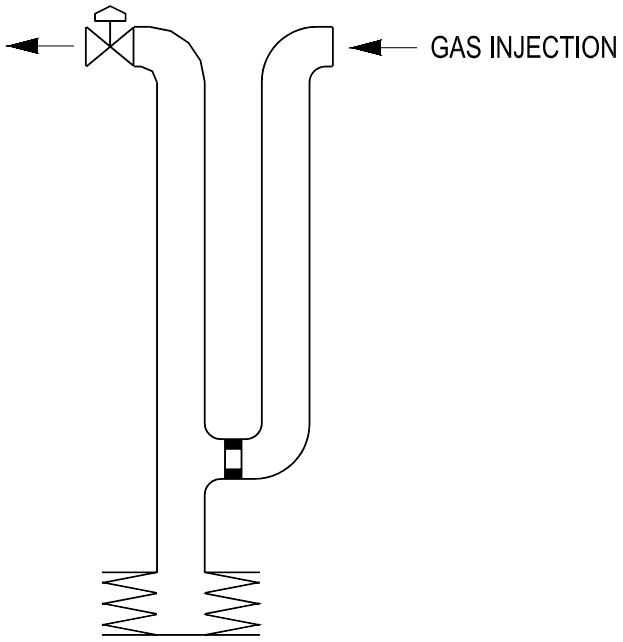

Figure 3-6 A simplified gas-lift model with non-critical gas injection.

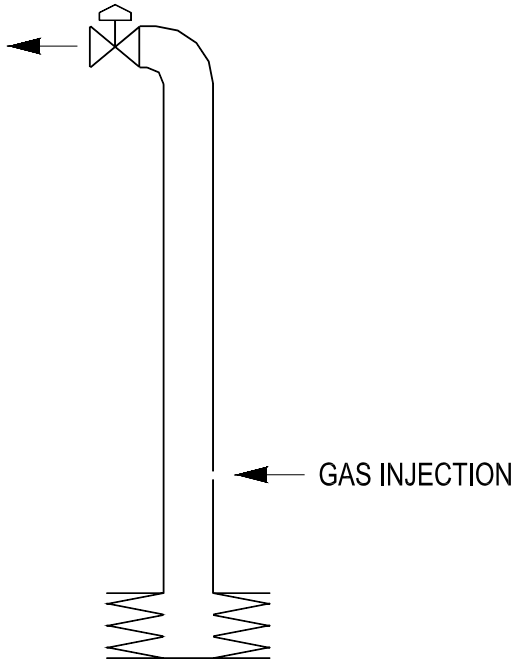

Figure 3-7 A simplified gas-lift model with critical gas injection.

But for those instabilities relying on the dynamic interactions between the well flow and surface pipe flow, the production system must be considered as a whole rather than being separated by set a constant wellhead pressure. But this is out of the scope of this dissertation.

The only disputable boundary condition is the third one that assumes a steady-state inflow performance relationship for the flow from reservoir to the wellbore. The reservoir dynamic flow properties are ignored by using such a boundary condition. Strictly speaking, this is not a proper assumption when discussing well dynamics. There were already some disputes over this issue when casing heading was investigated. For example, Hasan *et al*. claimed that it was oversimplified to use steady-state inflow performance to implement the dynamic gas-lift simulation as Tang did. He suggested that, for simplicity, one should use transient analytical reservoir flow solution for single-phase flow and analytical pseudo-pressure formulation for two-phase flow. Unfortunately, Tang replied Hasan with that the transient response of reservoir could be ignored since the response of the reservoir was too slow to be comparable with the change in the wellbore. Obviously, Tang made a wrong deduction with the correct observation.

Asheim (2000) also addressed the importance of the dynamic properties of the compressible reservoir. He derived an analytical dynamic inflow solution for single-phase flow and suggested that it provide proper well boundary condition for stability analysis of gas-lift wells.

Even though the importance of the reservoir dynamic response to the bottomhole pressure variation is well acknowledged, it is still ignored in this study. There are two main considerations for this.

1. As introduced, the density-wave instability is caused by the system delayed negative feedback response to any flow perturbation at the inlet. The function of reservoir dynamic properties here is to create more time delay. Therefore the investigation result would be conservative in terms of instability if it were ignored. At the same time, since this research is qualitatively oriented, ignoring the time-delay effect of the reservoir does not change the nature of the instability, as it is believed that the density-wave instability is mainly a result of the flow in the tubing.

2. The delay effect caused by the reservoir dynamic response is also sometimes very weak so that it can be ignored in stability analysis. Particularly, for the wells having high PIs and producing from high permeability reservoirs, the reservoir dynamic response is very close

to steady-state prediction if the bottomhole flowing pressure oscillation frequency is low.

The above two points are supported by the calculation illustrated in Appendix A. Thus, the steady-state IPR assumption for the inflow is also reasonable for the study in this dissertation.

The gas-lift well in Figure 1-1 can even further simplified as shown in Figure 3-7 if critical gas injection at the bottom is attained. In fact, this is the main target system of interest in most of our investigations here since many new gas-lift wells are equipped with nozzle-venturi type of gas injection valve, which is normally operated at its critical flow regime.

3.3.3 Methodology

In this dissertation, a combined approach, which includes both theoretical analysis and numerical simulations, is adopted to carry out the tasks. For theoretical analysis, linear stability analysis is applied to the simplified gas-lift system. Whilst, a commercial available dynamic multiphase flow simulator is used to conduct the numerical simulation.

Obviously, the dynamic system to be investigated has a non-linear nature. The stability of a steady-state solution of a non-linear process can be determined by solution perturbation approach, which linearizes the process model around the solution and analyses the linearized model for stability. If the linear analysis indicates stability of the solution, then the corresponding non-linear system will also be stable in the vicinity of this solution. If the linear analysis indicates instability of the solution, then the original non-linear system will be unstable.

Due to the limitation of “vicinity”, the real threshold between the stable and unstable regime for the non-linear process might not be exactly the same with the result from linear analysis. But this does not compose a topic here since this study mainly aims at finding out instability in a more qualitative manner rather than pursuing the numeric accuracy.

As discussed in the review of casing heading study, dynamic simulation has many advantageous in determining the instability and revealing its behaviours. So, using dynamic simulation should be the best way to conduct the research work. Unfortunately, the performances of the commercial available dynamic multiphase flow simulators are still not quite satisfied. This reduces the confidence about the results obtained from the simulation. For this consideration, it is therefore determined to use the combined investigation approach so that the result from simulation and linear analysis can be

crosschecked. The linear analysis may also give some useful hints to the simulations so that the simulation work can be more efficient.

Choosing an independent simulation tool rather than discretizing the same model used in linear analysis also gives us confidence about the final conclusions if the linear analysis and numerical simulation can get reciprocal support.

Besides, both methods are verified against casing heading problem before being used to investigate the density-wave instability. Since both casing heading and density-wave instability are slow transient process, if any tool can deal with one phenomenon, it has no reason to be unable to deal with another. So, this verification also increases the confidence about the methods, thus the results worked out of them.

By adopting the above methodology, the final conclusions will be convincible if both methods can give the same answer or similar parametric trend.

4 DENSITY-WAVE INSTABILITY IN A VERTICAL SYSTEM

4.1 Introduction

In last chapter, the origin of density-wave instability in horizontal systems has been explained by using a simple example as sketched in Figure 3-5. We know very clear why and how the density wave can trigger instability in the horizontal system, in which pressure drop is assumed to take place only at inlet and outlet restrictions. We also know that the increase or decrease of the instability depends mainly on the relationship between inlet and outlet restrictions. From the horizontal system, it is concluded that outlet choking normally increase instability.

But in a vertical system, all these are not as clear as in the horizontal case. For the simplified gas-lift well, besides the inlet and outlet restrictions, gravity effect has to be taken into account as well as the friction loss along the tubing. We are not very sure about why and how the instability occurs since it is hard to tell the relationships between the instability and the different pressure drop components without studying them in detail. For example, in the simplified gas-lift system, can we say choking increases instability as it does in the horizontal case?

To understand “why” instead of just knowing stable or unstable is extremely important for us to deal with the instability in practical operations. This chapter is therefore intended to figure out the basic features of density-wave instability in the simplified gas-lift system so that we can understand why it occurs and what are the effects of different pressure drop components. This study also serves as the foundation and guide for further comprehensive linear analysis and numerical simulations, which have to resort to numerical approach instead of giving explanation of the background analytically.

It is necessary to make some assumptions in order to get an analytical solution for the vertical system as Svanholm did for the horizontal system. In the following analysis, an incompressible system is assumed since the origin of density-wave instability does not necessarily require a compressible system. Besides, the two-phase flow in the tubing is assumed homogeneous so that those complicated two-phase flow structures can be dropped from the analysis. It is believed that the basic features of the density-wave instability derived from such a system are still qualitatively correct for a real compressible two-phase vertical flow system.

The following analyses in this chapter are enlightened by the work of Svanholm and Hjarmars who respectively analyzed the horizontal two-phase flow system and unstable airlift pumping process, which have been introduced and reviewed in last chapter. Particularly, the analyses in this chapter follow the basic framework of Hjarmars' analyses. There are three main differences between this study and the work did by Hjarmars.

1. First, the open end of an airlift pump is replaced by a linear reservoir inflow performance relationship.

2. Second, the pressure-drop due to friction loss was not considered by Hjarmars since normally the flow path of an airlift pump was so short that the friction loss could be ignored. This on the contrary is the main concern in a gas-lift well due to its out-of-magnitude long flow path compared with an airlift pump. The friction loss along the well path thus is too large to be ignored.

3. Third, the outlet restriction (choke) is included in this study.

Because of the aforementioned differences, the final model, as well as the solving procedure and the final results of the system will be different with what Hjarmars got.

4.2 Derivation of system dynamic perturbation model

Since the system is incompressible, the flow in the annulus is dropped from the analysis. The corresponding system considered in this analysis is as sketched in Figure 3-7. Besides, the gas injection point is assumed very close to the bottom of the well.

Based on all the assumptions, a dynamic gas-lift model for the corresponding system is built as below.

The continuity equation of two-phase flow in the tubing writes

$$\rho'_{m,t} + (\rho_m u_m)'_z = 0 \qquad \textbf{4-1}$$

The momentum balance of two-phase flow in the tubing gives

$$\rho_m u'_{m,t} + \rho_m u_m u'_{m,z} + \rho_m g + f\frac{\rho_m u_m^2}{2D} + p'_{T,z} = 0 \qquad \textbf{4-2}$$

For incompressible flow,

$$u'_{m,z} = 0 \qquad \textbf{4-3}$$

Considering 4-3, Equation 4-1 and 4-2 become

$$\rho'_{m,t} + u_m \rho'_{m,z} = 0 \qquad \textbf{4-4}$$

$$\rho_m u'_{m,t} + \rho_m g + f \frac{\rho_m u_m^2}{2D_T} + p'_{T,z} = 0 \qquad \textbf{4-5}$$

At the bottom of the well, the inflow performance relationship gives

$$q_l\big|_{z=0} = \frac{J(p_R - p_{wf})}{\rho_l} \qquad \textbf{4-6}$$

The injection rate for lifting gas is constant, that is

$$q_g\big|_{z=0} = q_{inj} \qquad \textbf{4-7}$$

At the exit of the tubing, choke equation writes

$$q_m\big|_{z=L} = kA_c \sqrt{\frac{2(p_{wh} - p_{sep})}{\rho_m}} \qquad \textbf{4-8}$$

Rewrite Equation 4-6, 4-7 and 4-8 in terms of velocity, we have

$$u_{sl}\big|_{z=0} = \frac{J(p_R - p_{wf})}{A_T \rho_l} \qquad \textbf{4-9}$$

$$u_{sg}\big|_{z=0} = \frac{q_{inj}}{A_T} \qquad \textbf{4-10}$$

$$u_m\big|_{z=L} = k \frac{A_c}{A_T} \sqrt{\frac{2(p_{wh} - p_{sep})}{\rho_m}} \qquad \textbf{4-11}$$

We define

$$u_m = \bar{u}_m + \delta u_m \qquad \textbf{4-12}$$

$$\rho_m = \bar{\rho}_m + \delta \rho_m \qquad \textbf{4-13}$$

$$p_T = \bar{p}_T + \delta p_T \qquad \textbf{4-14}$$

where $\bar{u}_m$, $\bar{\rho}_m$ and $\bar{p}_T$ represent the steady-state solution and are independent of time, δu_m, $\delta \rho_m$ and δp_T represent the perturbations of velocity, density and pressure respectively and are functions of both location and time. Substituting Equation 4-12, 13 and 14 into system Equations 4-3, 4-4 and 4-5 and separating the steady-state and perturbation terms, we get

$$\bar{u}'_{m,z} = 0 \qquad \textbf{4-15}$$

$$\bar{\rho}'_{m,z} = 0 \qquad \textbf{4-16}$$

$$\bar{\rho}_m g + f\frac{\bar{\rho}_m \bar{u}_m^2}{2D_T} + \bar{p}'_{m,z} = 0 \qquad \textbf{4-17}$$

and

$$(\delta u_m)'_z = 0 \qquad \textbf{4-18}$$

$$(\delta\rho_m)'_t + \bar{u}_m(\delta\rho_m)'_z = 0 \qquad \textbf{4-19}$$

$$\bar{\rho}_m(\delta u_m)'_t + \delta\rho_m \cdot g + f\frac{\bar{\rho}_m \bar{u}_m \cdot \delta u_m}{D_T} + f\frac{\bar{u}_m^2 \cdot \delta\rho_m}{2D_T} + (\delta p_T)'_z = 0 \qquad \textbf{4-20}$$

The perturbation equations are already linearized by ignoring the second-order perturbation terms. From Equation 4-15 and 4-16, we see that $\bar{u}_m$ and $\bar{\rho}_m$ are also independent of *z*.

From 4-18, we have

$$\delta u_m = \delta u_m\big|_{z=0} \qquad \textbf{4-21}$$

By definition,

$$u_m = u_{sl} + u_{sg} \qquad \textbf{4-22}$$

then,

$$\delta u_m = \delta u_{sl} + \delta u_{sg} \qquad \textbf{4-23}$$

thus,

$$\delta u_m\big|_{z=0} = \delta u_{sl}\big|_{z=0} + \delta u_{sg}\big|_{z=0} \qquad \textbf{4-24}$$

By considering Equation 4-10, we get

$$\delta u_{sg}\big|_{z=0} = 0 \qquad \textbf{4-25}$$

Substituting Equation 4-24, 4-25 into 4-21, we obtain

$$\delta u_m = \delta u_{sl}\big|_{z=0} \qquad \textbf{4-26}$$

Using the method of characteristics, we get the solution of Equation 4-19 that takes the form

$$\delta\rho_m = \mathrm{f}(\zeta) \tag{4-27}$$

where $\zeta = z - \bar{u}_m t$.

If writes $\varepsilon = \delta u_{sl}\big|_{z=0}$, then Equation 4-20 becomes

$$\bar{\rho}_m \varepsilon_t' + \mathrm{f}(\zeta) g + f\frac{\bar{\rho}_m \bar{u}_m \varepsilon}{D_T} + f\frac{\bar{u}_m^2 \mathrm{f}(\xi)}{2D_T} + (\delta p_T)_z' = 0 \tag{4-28}$$

For simplicity, we assume a constant number for the friction factor in this study. Integration of Equation 4-28 along the tubing gives

$$\begin{aligned}\bar{\rho}_m L_T \varepsilon_t' + \left(g + f\frac{\bar{u}_m^2}{2D_T}\right)(\mathrm{F}(L_T - \bar{u}_m t) - \mathrm{F}(-\bar{u}_m t)) + f\frac{\bar{\rho}_m \bar{u}_m L_T \varepsilon}{D_T} \\ + \delta p_T(L_T) - \delta p_T(0) = 0\end{aligned} \tag{4-29}$$

By differential and ordering Equation 4-29, we get

$$\begin{aligned}\bar{\rho}_m L_T \varepsilon_{tt}'' - \bar{u}_m\left(g + f\frac{\bar{u}_m^2}{2D_T}\right)(\mathrm{f}(L_T - \bar{u}_m t) - \mathrm{f}(-\bar{u}_m t)) + f\frac{\bar{\rho}_m \bar{u}_m L_T}{D_T}\varepsilon_t' \\ + (\delta p_T(L_T))_t' - (\delta p_T(0))_t' = 0\end{aligned} \tag{4-30}$$

The real form of density perturbation term can be found from the following derivation. By definition,

$$\rho_m = \frac{\rho_g q_g + \rho_l q_l}{q_g + q_l} \tag{4-31}$$

then,

$$\mathrm{f}(\zeta) = \delta\rho_m = \frac{\partial \rho_m}{\partial q_g}\delta q_g + \frac{\partial \rho_m}{\partial q_l}\delta q_l \tag{4-32}$$

At the bottom of the tubing, $\delta q_g\big|_{z=0} = 0$, thus,

$$\mathrm{f}(-\bar{u}_m t) = \frac{\partial \rho_m}{\partial q_l}\delta q_l\bigg|_{z=0} = \frac{(\rho_l - \rho_g) q_{inj} A_T}{(q_{inj} + \bar{q}_l)^2}\varepsilon(t) \tag{4-33}$$

At $z = L_T$,

$$\mathrm{f}(L_T - \bar{u}_m t) = \frac{(\rho_l - \rho_g) q_{inj} A_T}{(q_{inj} + \bar{q}_l)^2}\varepsilon\left(t - \frac{L_T}{\bar{u}_m}\right) \tag{4-34}$$

The last two terms in Equation 4-30 can be calculated from the inflow performance relationship and choke equation respectively. Rewriting Equation 4-9, we get

$$p_{wf} = p_R - \frac{A_T \rho_l u_{sl}\big|_{z=0}}{J} \tag{4-35}$$

Equation 4-11 gives

$$p_{wh} = \frac{\rho_m u_m^2}{2k^2\left(\frac{A_c}{A_T}\right)^2} + p_{sep} = \frac{\rho_m u_m^2}{K} + p_{sep} \tag{4-36}$$

Then,

$$(\delta p_T(0))'_t = -\frac{A_T \rho_l}{J}\varepsilon'_t \tag{4-37}$$

$$(\delta p_T(L_T))'_t = \frac{\overline{u}_m^2}{K}(\delta \rho_m(L_T))'_t + \frac{2\overline{\rho}_m \overline{u}_m}{K}\varepsilon'_t \tag{4-38}$$

Introducing the real form of density perturbation, we get

$$(\delta p_T(L_T))'_t = \frac{\overline{u}_m^2}{K}\frac{(\rho_l - \rho_g)q_{inj}A}{(q_{inj} + \overline{q}_l)^2}\left(\varepsilon\left(t - \frac{L}{\overline{u}}\right)\right)'_t + \frac{2\overline{\rho}_m \overline{u}_m}{K}\varepsilon'_t \tag{4-39}$$

Substituting Equation 4-33, 4-34, 4-37 and 4-39 into Equation 4-30, we get

$$\begin{aligned}
&\overline{\rho}_m L_T \varepsilon''_{tt} + \left(f\frac{\overline{\rho}_m \overline{u}_m L_T}{D_T} + \frac{2\overline{\rho}_m \overline{u}_m}{K} + \frac{A_T \rho_l}{J}\right)\varepsilon'_t \\
&+ \overline{u}_m\left(g + f\frac{\overline{u}_m^2}{2D_T}\right)\frac{(\rho_l - \rho_g)q_{inj}A_T}{(q_{inj} + \overline{q}_l)^2}\left(\varepsilon(t) - \varepsilon\left(t - \frac{L_T}{\overline{u}_m}\right)\right) \\
&+ \frac{\overline{u}_m^2}{K}\frac{(\rho_l - \rho_{inj})q_g A_T}{(q_{inj} + \overline{q}_l)^2}\left(\varepsilon\left(t - \frac{L_T}{\overline{u}_m}\right)\right)'_t = 0
\end{aligned} \tag{4-40}$$

If define

$$t = \frac{L_T}{\overline{u}_m}\theta \tag{4-41}$$

and

$$\varepsilon(t) = \eta(\theta) \tag{4-42}$$

Equation 4-40 can be normalized as

$$\eta''_{\theta\theta} + C_1\eta'_\theta + C_2(\eta(\theta) - \eta(\theta-1)) + C_3(\eta(\theta-1))'_\theta = 0 \qquad \textbf{4-43}$$

where

$$C_1 = f\frac{L_T}{D_T} + \frac{2}{K} + \frac{\pi D_T^2 \rho_l}{4\bar{\rho}_m \bar{u}_m J}$$

$$C_2 = \frac{4L_T(\rho_l - \rho_g)q_{inj}}{\pi D_T^2 \bar{\rho}_m \bar{u}_m^3}\left(g + f\frac{\bar{u}_m^2}{2D_T}\right)$$

$$C_3 = \frac{4(\rho_l - \rho_g)q_{inj}}{\pi D_T^2 K \bar{\rho}_m \bar{u}_m}$$

In the above coefficients, steady-state solution of the system is required. By integrating Equation 4-17, we get

$$\bar{\rho}_m g L_T + f\frac{\bar{\rho}_m \bar{u}_m^2 L_T}{2D_T} + \bar{p}_{wh} - \bar{p}_{wf} = 0 \qquad \textbf{4-44}$$

in which, all the other parameters at steady-state can be expressed in terms of $\bar{u}_m$. Since $\bar{u}_m$ and $\bar{\rho}_m$ are independent of ***z***, then

$$\bar{u}_m = \frac{q_{inj} + \bar{q}_l}{A_T} \qquad \textbf{4-45}$$

thus,

$$\bar{q}_l = \bar{u}_m A_T - q_{inj} \qquad \textbf{4-46}$$

and,

$$\bar{\rho}_m = \frac{\rho_g q_{ing} + \rho_l \bar{q}_l}{q_{ing} + \bar{q}_l} = \frac{(\rho_g - \rho_l)q_{inj} + \rho_l \bar{u}_m A_T}{\bar{u}_m A_T} \qquad \textbf{4-47}$$

$$\bar{p}_{wh} = p_{sep} + \frac{\bar{\rho}_m \bar{u}_m^2}{2k^2\left(\frac{A_o}{A_T}\right)^2} = p_{sep} + \frac{(\rho_g - \rho_l)q_{inj}\bar{u}_m A_T + \rho_l \bar{u}_m^2 A_T^2}{2k^2 A_o^2} \qquad \textbf{4-48}$$

$$\bar{p}_{wf} = p_R - \frac{\rho_l \bar{q}_l}{PI} = p_R - \frac{\rho_l \bar{u}_m A_T - \rho_l q_{inj}}{J} \qquad \textbf{4-49}$$

Substituting Equation 4-46, 4-47, 4-48 and 4-49 into Equation 4-44, we get a third order polynomial of $\bar{u}_m$, which can be solved analytically.

$$\left(\frac{fL_T\rho_l A_T}{2D_T}+\frac{\rho_l A_T^3}{2k^2A_o^2}\right)\overline{u}_m^3+\left(\frac{fL_T(\rho_g-\rho_l)q_{inj}}{2D_T}+\frac{(\rho_g-\rho_l)q_{inj}A_T^2}{2k^2A_o^2}+\frac{\rho_l A_T^2}{J}\right)\overline{u}_m^2 + \left(\rho_l gL_T A_T-\frac{\rho_l q_{inj}A_T}{J}+p_{sep}A_T-p_R A_T\right)\overline{u}_m+(\rho_g-\rho_l)gL_T q_{inj}=0 \quad \textbf{4-50}$$

4.3 Stability criterion for incompressible vertical system

The derived Equation 4-43 represents the dynamic model of the system in terms of non-dimensional liquid inflow velocity perturbation. It is a second-order differential-difference equation. Since it only has zero and first order of the delay terms, it is also called as retarded second-order system, in which the change rate of the perturbation term is determined by its present and past values. Physically, it represents the propagation of density wave in the tubing since the inflow liquid flow rate perturbation is in analogue with the inlet density change. If consider its physical background, Equation 4-43 might be also called a second-order system with delayed feedback.

Equation 4-43 has an infinite number of solutions that take the form

$$\eta(\theta)=C\exp(\omega\theta) \quad \textbf{4-51}$$

where ω is a constant, in general a complex. If substituting the above solution into Equation 4-43, we can get the transcendental characteristic equation for ω, which is recognized as an exponential polynomial

$$(\omega^2+C_1\omega+C_2)e^{\omega}-C_2+C_3\omega=0 \quad \textbf{4-52}$$

where

$C_1, C_2, C_3 > 0$

Clearly, $\omega=0$ is a root of Equation 4-52. This means the dynamic system of Equation 4-43 has no asymptotic stability, or there is only marginal stability or neutral stability for the system. Also, the system is stable if C_2 and C_3 are small. Instability might be able to occur as a hopf bifurcation if C_2 and/or C_3 are large enough.

As long as other roots' real parts stay negative, Equation 4-43 is uniformly stable. To find out when the system switches itself from stable to unstable, we need the real part of any non-zero root to change its sign. Let's assume that

$$\omega=x+iy \quad \textbf{4-53}$$

$x=0$ with a non-zero real value y gives the criterion or switch of stability. Putting $\omega=iy$ into Equation 4-52, we get

$$H(iy) = (-y^2 \cos y - C_1 y \sin y + C_2 \cos y - C_2) + (-y^2 \sin y + C_1 y \cos y + C_2 \sin y + C_3 y)i = 0 \quad \textbf{4-54}$$

Separating the real and imaginary part, we have

$$-y^2 \cos y - C_1 y \sin y + C_2 \cos y - C_2 = 0 \quad \textbf{4-55}$$

$$-y^2 \sin y + C_1 y \cos y + C_2 \sin y + C_3 y = 0 \quad \textbf{4-56}$$

Now, the goal is to find non-zero real *y* so that the above two equations are satisfied. Rewriting 4-55 and 56, we get

$$(C_2 - y^2)\cos y - C_1 y \sin y = C_2 \quad \textbf{4-57}$$

$$(C_2 - y^2)\sin y + C_1 y \cos y = -C_3 y \quad \textbf{4-58}$$

Squaring and adding 4-57 and 58, we have

$$(C_2 - y^2)^2 + C_1^2 y^2 = C_2^2 + C_3^2 y^2 \quad \textbf{4-59}$$

Two solutions can be obtained

$$y^2 = 0 \quad \textbf{4-60}$$

and

$$y^2 = C_3^2 + 2C_2 - C_1^2 \quad \textbf{4-61}$$

The first solution is not of interest since the role of the zero root has been clarified. The second solution is what we are looking for. Clearly, from Equation 4-61, $C_3^2 + 2C_2 > C_1^2$ is a necessary condition for instability to happen since *y* should be a non-zero real number as required. To find out the exact boundary between stable and unstable regime, we need combine the Equation 4-57 and 58 as

$$\cos y = \frac{C_2(C_2 - y^2) - C_1 C_3 y^2}{(C_2 - y^2)^2 + C_1^2 y^2} \quad \textbf{4-62}$$

Substituting the solution 4-61 into 4-62, we obtain

$$\cos\left(\pm\sqrt{C_3^2 + 2C_2 - C_1^2}\right) = \frac{-C_2 C_3^2 - C_2^2 + C_1^2 C_2 - C_1 C_3^3 + C_1^3 C_3 - 2C_1 C_2 C_3}{C_3^4 + C_2^2 - C_1^2 C_3^2 + 2C_2 C_3^2} \quad \textbf{4-63}$$

Solving Equation 4-63 gives

$$2n\pi \pm \arccos\left(\frac{-C_2C_3^2 - C_2^2 + C_1^2C_2 - C_1C_3^3 + C_1^3C_3 - 2C_1C_2C_3}{C_3^4 + C_2^2 - C_1^2C_3^2 + 2C_2C_3^2}\right) = \pm\sqrt{C_3^2 + 2C_2 - C_1^2} \quad \textbf{4-64}$$

This represents a family of surface in the C_1, C_2 and C_3 space since the arc cosine term is multi-valued. On these surfaces, we have characteristic roots that cross the imaginary axis. Probably but not certainly they don't come back. Since the system is stable for small C_2 and C_3 with also considering that C_1, C_2 and C_3 are all positive, it will be the closest of these surfaces to the C_1 axis that gives stability and instability boundary. The further out surfaces just add more unstable roots. The closest surface to C_1 is

$$\arccos\left(\frac{-C_2C_3^2 - C_2^2 + C_1^2C_2 - C_1C_3^3 + C_1^3C_3 - 2C_1C_2C_3}{C_3^4 + C_2^2 - C_1^2C_3^2 + 2C_2C_3^2}\right) - \sqrt{C_3^2 + 2C_2 - C_1^2} = 0 \quad \textbf{4-65}$$

If we do not emphasize its quantitative significance, Equation 4-65 can even be further simplified to 4-67, particularly when C_1 is very large. For example, if we send the arc cosine term of Equation 4-65 to the right side of the equation and square both sides, then we can get

$$C_3^2 + 2C_2 = C_1^2 + \arccos^2\left(\frac{-C_2C_3^2 - C_2^2 + C_1^2C_2 - C_1C_3^3 + C_1^3C_3 - 2C_1C_2C_3}{C_3^4 + C_2^2 - C_1^2C_3^2 + 2C_2C_3^2}\right) \quad \textbf{4-66}$$

Assuming a well that is 1000 m in depth and 0.1 m in diameter, C_1^2 will at least be 10000 if friction factor equals 0.01, but the maximum value of the arc cosine term would be π^2 that can be ignored from the equation. In this way, Equation 4-66 can be simplified to

$$C_3^2 + 2C_2 - C_1^2 = 0 \quad \textbf{4-67}$$

Plotting this surface in the C_1, C_2 and C_3 space as shown in Figure 4-1, we will get the boundary between stable and unstable region of the system 4-43. The scale of each parameter in the figure is selected as such that the shape of the surface is clearly exhibited. In Figure 4-1, the system is unstable below the surface, and vice versa.

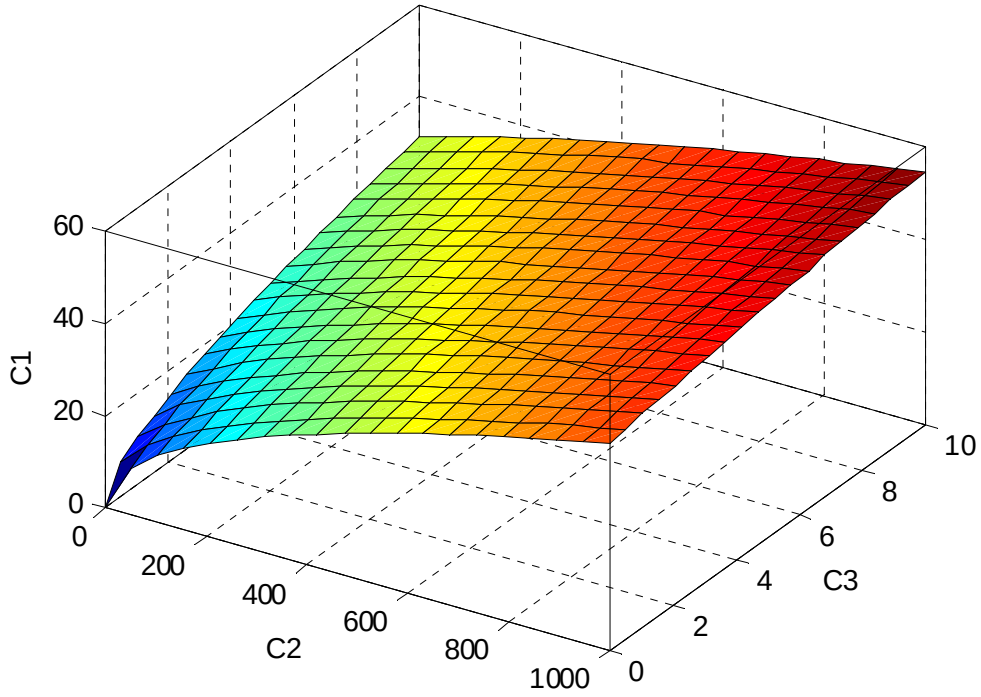

Figure 4-1 Neutral stability surface.

4.4 Discussions on the basic features

Equation 4-43 gives the mathematic description of density-wave transport dynamics in an incompressible vertical flow system. Since C_1, C_2 and C_3 are all positive numbers, Equation 4-43 should be a stable system if the delay items do not appear. This clearly demonstrates that if there is any instability, it comes from the delayed system feedback. This explains why such a vertical system could be unstable due to density-wave transport.

Mathematically the instability is going to happen as long as C_1, C_2 and C_3 satisfy the inequality 4-68.

$$\frac{C_3^2 + 2C_2}{C_1^2} > 1 \qquad \textbf{4-68}$$

Now, we can take a close look at the influence of different pressure drop components on the instability.

1. J represents the restriction of flow from reservoir to wellbore. This restriction is in-phase with flow rate change at the bottom of well. So, J only appears in C_1. If other parameters stay unchanged, a larger J

gives an unstable effect by reducing C_1. This implies that a system with a high reservoir pressure and a low J is more stable than the system with a low reservoir pressure and a high J even though they can be selected to produce the same amount of liquid using the steady-state linear inflow performance relationship.

2. The gravity term only appears at C_2. Since the hydrostatic pressure drop totally depends on density, its response to the liquid inflow rate perturbation is then partially delayed. This implies that a gravity dominant system is much easier to be unstable due to density-wave propagation since a gravity dominant system is more sensitive to the two-phase mixture density change.

3. The term of friction loss along the well appears in both C_1 and C_2. The pressure drop due to friction is dependent on the velocity and density of the two-phase mixture. So the friction loss change can be separated into two parts. One part is due to the change of velocity and the other part is due to the change of density. If there is a liquid inflow perturbation, then the friction due to velocity change will response immediately since the system is incompressible. This is why friction term appears in C_1. But the friction loss change due to density is partially delayed because of the transport of density wave. This explains why friction term also appears in C_2.

4. The same as the friction term, the pressure drop across the choke can be also separated into two parts. One part is in-phase with the flow rate change at the bottom of well, the other is completely delayed and out-of-phase with flow rate change at the bottom of well. This explains why the restriction terms of choke appear in both C_1 and C_3, which have stabilizing and destabilizing effects respectively.

5. But whether the pressure-drop components along the tubing or across the choke have a net stabilizing effects not only depends on the pressure-drop components themselves, but also rely on the inlet restriction of the well. This is because, after C_1 is squared, there are also three product terms of every two components besides the quadratic terms. In fact, the two product terms between the third term and the first two terms in C_1, are very important in determining the net effects of pressure-drop components along the tubing and across the choke.

6. If compare the tubing friction terms in C_1^2 (the quadratic term and the product with the third term) with that in C_2 (multiplied by 2), it is not difficult to figure out that the friction along the tubing in general has a

net effect of stabilization. This stabilizing effect will be weakened if the inlet restriction is small.

7. But, if compare the choke restriction terms in C_1^2 (the quadratic term and the product with the third term) with C_3^2, it is hard to tell the net effect of choking. The choking effect is heavily dependent on the inlet restriction term. If the system has a high *J* value, choking tends to give destabilizing effect, if the system has a low *J*, choking tends to give stabilizing effect. This might explain why in the nuclear engineering and powering engineering, the outlet restriction of the vertical vapour tube normally destabilize the system since the inlet restriction is much smaller compared with the well inflow. But for production wells, choking effect on density-wave instability should be evaluated case by case since at least no general rule can be derived from above simplified analysis.

4.5 Density-wave instability in incompressible systems

Although the derived the instability criterion gives the basic features of the density-wave instability in a vertical flow system, it can not be used as a practical criterion to judge the occurrence of the instability in a real compressible system. The instability can occur without the help of compressibility if the *J* value is very large, just like in the airlift pumping case. But, it is almost impossible to occur if compressibility is neglected when practical well parameters are adopted in the criterion since the *J* value is extreme small in a real oil well. Some north gas-lift wells have *J* in the magnitude of 10^{-6}. Following analysis shows why density-wave instability can not happen without including compressibility.

Since friction along tubing gives stabilizing effect, the system should be easier to be unstable if it is ignored. Also, for simplicity, outlet choke is removed from the system. So, the system is assumed to have inlet restriction and hydrostatic loss only. Then the left side of inequality 4-68 becomes,

$$\frac{C_3^2 + 2C_2}{C_1^2} = \frac{32J^2 g L_T \left(\rho_l - \rho_g\right)\overline{\rho}_m \alpha}{\pi^2 D_T^4 \rho_l^2} \qquad \textbf{4-69}$$

The right side of Equation 4-69 can be amplified further by replacing $\overline{\rho}_m$ with ρ_l, ignoring ρ_g, setting $\alpha = 1$ and eliminating g and π^2. Thus, the maximum value of the right side of Equation 4-69 will not larger than

$$\frac{32J^2 L_T}{D_T^4}$$

For a practical gas-lift well, L_T is in the 10^3 order-of-magnitude, D_T is in the 10^{-1} order-of-magnitude and J is in the 10^{-6} order-of-magnitude. If put these numbers in the above expression, we get a number that is in the 10^{-4} order-of-magnitude, which is far less than 1. Therefore, it is concluded that density-wave instability can not happen without the help of compressibility in a real gas-lift well.

Of course, we can perform concrete calculation based on the derived criterion and the solution of the steady-state to check if a practical well could be unstable without considering compressibility. But from above simplified analysis, this is not thought to be necessary.

4.6 Summary

1. The simplified gas-lift system under constant gas injection at the bottom of well can be modelled (around its steady-state solution) by a second-order differential-difference equation in term of non-dimensional inlet flow perturbation. It is also called as retarded second-order system. The model explains why the system can sometimes be unstable due to density-wave transport.

2. The derived stability criterion reveals some basic features of density-wave instability and offers useful hints for further comprehensive analysis. It is certain that the inlet restriction of a well and the friction loss along the tubing give the stabilizing effect to density-wave instability. But the net effect of choking is uncertain from the criterion. The criterion also implies that not only the pressure-drop components themselves, but also their interrelations will determine their influence on the instability. For example, the effect of choking to the instability is up to the magnitude of inlet restriction at the bottom of the well.

3. The criterion also quantitatively shows that the instability is unlikely to occur in an incompressible system if a reasonable well J value is applied. It is therefore concluded that density-wave instability can not happen in a real gas-lift well without the help of compressibility.

4.7 Nomenclature

A	Area, m^2
D	Diameter, m
f	Friction factor, -
g	Acceleration of gravity force, m/s^2
k	Valve coefficient, -

J	Mass productivity index, kg/s/Pa
L	Tubing length, m
P	Pressure, Pa
q	Volume flow rate, m^3/s
u	Velocity, m/s
α	Void fraction, -
ρ	Density, kg/m^3

Subscripts

g	Gas
inj	Injection
l	Liquid
m	Mixture
c	Choke
R	Reservoir
sep	Separator
sg	Superficial gas
sl	Superficial liquid
t	Time
T	Tubing
wf	Wellbore flowing
wh	Well head
z	Vertical coordinate

Superscripts

$\bar{}$	Steady-state
$'$	Derivation

5 LINEAR STABILITY ANALYSIS RESULTS

5.1 Introduction

In this chapter, linear stability analysis is performed to investigate the occurrence and characteristics of density-wave instability in the simplified gas-lift system.

The derived criterion in last chapter reveals some basic features of density-wave instability and offers useful hints for further comprehensive analysis and simulation. However, it also quantitatively shows that the instability is unlikely to occur in a hypothetical incompressible system when the practical productivity index is applied. This therefore initiates the complete linear stability analysis in this chapter, which considers compressibility. Even though the origin of density-wave instability does not rely on compressibility as mentioned previously, the compressibility sometimes plays key role for it to happen.

The following analyses follow the same linear analysis procedure used by the Apazidis who analyzed the unstable airlift pumping process by considering compressibility. His work has been reviewed in the third chapter. Compared with Apazidis' analyses, the main concerns of the study here are,

1. The almost non-restrictive open end of an airlift pump is not comparable with the inflow mechanism of a gas-lift well, which has a strong restriction to the flow from reservoir to the wellbore and bears main damping effect to density-wave flow oscillation as shown in last chapter. In the following analyses, it is specially emphasized since it also has long been the main reason for people to suspect the occurrence possibility of density-wave instability in gas-lift wells.

2. The pressure-drop due to friction loss was not considered by Apazidis since normally the flow path of an airlift pump was so short that the friction loss could be ignored. This on the contrary is the main concern in a gas-lift well due to its out-of-magnitude long flow path compared with an airlift pump. The friction loss along the well path thus is too large to be ignored, adding that it also has a damping effect on density-wave instability.

As concluded in last chapter, choking can either damp or trigger the instability depending on the value of productivity index. It is not included in the gas-lift model in this chapter; instead, its role will be studied by simulation in next

chapter. The same as in last chapter, homogenous two-phase flow model is assumed here. When considering the compressibility of the lifting gas, ideal gas law is applied. To make the analysis easier, air and water are used as lifting gas and reservoir fluid respectively. Mass exchanges between phases are ignored.

To make the analysis more concise, it is assumed that lifting gas is injected into the tubing at the bottom of well. This means the downstream pressure of gas injection valve equals the bottomhole flowing pressure of the well. With this simplification, the single-phase flow in the wellbore between the bottom of the well and the gas-injection point is ignored.

The analysis procedure used in this chapter is validated with casing heading problem. Results from both verification and investigation are discussed and summarized. The nomenclatures used in the analyses are given in the last part of the chapter.

5.2 Formulation of linear stability analysis

With all above assumptions, the linear stability analysis is formulated as followings.

5.2.1 Dynamic modeling of the simplified gas-lift system

The simplified gas-lift system sketched in Figure 3-6 is modeled. If the gas injection at the bottom of the well is critical as in Figure 3-7, the model of flow in the annulus does not enter into calculation.

For two-phase homogeneous flow in the tubing, mass balance for liquid and gas writes

$$[(1-\alpha)\rho_l]'_t + [(1-\alpha)\rho_l u_m]'_z = 0 \qquad \textbf{5-1}$$

$$(\alpha\rho_g)'_t + (\alpha\rho_g u_m)'_z = 0 \qquad \textbf{5-2}$$

Momentum balance for gas-liquid mixture gives

$$\rho_m u'_{m,t} + \rho_m u_m u'_{m,z} + \rho_m g + \frac{f}{2D_T}\rho_m u_m^2 + p'_{T,z} = 0 \qquad \textbf{5-3}$$

For flow in the annulus, mass balance equation writes

$$\rho'_{g,t} + (\rho_g u_g)'_z = 0 \qquad \textbf{5-4}$$

Momentum balance gives

$$\rho_g u'_{g,t} + \rho_g u_g u'_{g,z} - \rho_g g + \frac{f}{2D_A}\rho_g u_g^2 + p'_{A,z} = 0 \quad \textbf{5-5}$$

The density of two-phase mixture in the tubing is calculated by

$$\rho_m = \alpha\rho_g + (1-\alpha)\rho_l \quad \textbf{5-6}$$

Considering the ideal gas law and assuming liquid density is constant, Equation 5-1 to 5-5 become

$$\alpha'_t - (1-\alpha)u'_{m,z} + u_m\alpha'_z = 0 \quad \textbf{5-7}$$

$$\alpha p'_{T,t} + p_T\alpha'_t + \alpha p_T u'_{m,z} + \alpha u_m p'_{T,z} + p_T u_m \alpha'_z = 0 \quad \textbf{5-8}$$

$$\left(\alpha\frac{p_T}{RT} + (1-\alpha)\rho_l\right)u'_{m,t} + \left(\alpha\frac{p_T}{RT} + (1-\alpha)\rho_l\right)u_m u'_{m,z} + \left(\alpha\frac{p_T}{RT} + (1-\alpha)\rho_l\right)g + \frac{f}{2D_T}\left(\alpha\frac{p_T}{RT} + (1-\alpha)\rho_l\right)u_m^2 + p'_{T,z} = 0 \quad \textbf{5-9}$$

$$p'_{A,t} + p_A u'_{g,z} + u_g p'_{A,z} = 0 \quad \textbf{5-10}$$

$$p_A u'_{g,t} + p_A u_g u'_{g,z} - p_A g + \frac{f}{2D_A}p_A u_g^2 + RTp'_{A,z} = 0 \quad \textbf{5-11}$$

The boundary conditions of the system are given below. At the bottom of the well, we assume a linear reservoir inflow rate equation for the liquid.

$$u_{sl}^{in} = \frac{J(p_R - p_{wf})}{\rho_l A_T} \quad \textbf{5-12}$$

At the outlet of the well, pressure is assumed constant, that is

$$p_{sep} = Const. \quad \textbf{5-13}$$

At the casing head, lifting gas injection rate is assumed constant.

$$\dot{m}_g^{inj} = Const. \quad \textbf{5-14}$$

Then,

$$u_g^{in} = \frac{\dot{m}_g^{inj} RT}{p_A^{in} A_A} \quad \textbf{5-15}$$

For gas-lift valve, an orifice flow rate equation is given as

$$\dot{m}_g^o = C_D \frac{\pi}{4} D_o^2 p_u \sqrt{\frac{2}{RT}} \sqrt{\frac{k}{k-1}\left(\left(\frac{p_d}{p_u}\right)^{\frac{2}{k}} - \left(\frac{p_d}{p_u}\right)^{\frac{k+1}{k}}\right)} \quad \textbf{5-16}$$

The ratio of downstream and upstream pressures at critical flow is calculated by

$$\left(\frac{p_d}{p_u}\right)_{cr} = \left(\frac{2}{k+1}\right)^{\frac{k}{k-1}} \quad \textbf{5-17}$$

If gas injection at the bottom of well is critical like in Figure 3-7, $\dot{m}_g^o$ will be a constant value.

5.2.2 Steady-state solution

The steady-state solution to be analyzed for stability is calculated from the corresponding steady-state model of the system, which reads

$$(1-\overline{\alpha})\overline{u}_m' + \overline{u}_m\overline{\alpha}' = 0 \quad \textbf{5-18}$$

$$\overline{\alpha}\overline{p}_T\overline{u}_m' + \overline{\alpha}\overline{u}_m\overline{p}_T' + \overline{p}_T\overline{u}_m\overline{\alpha}' = 0 \quad \textbf{5-19}$$

$$\left(\overline{\alpha}\frac{\overline{p}_T}{RT} + (1-\overline{\alpha})\rho_l\right)\overline{u}_m\overline{u}_m' + \left(\overline{\alpha}\frac{\overline{p}_T}{RT} + (1-\overline{\alpha})\rho_l\right)g + \frac{f}{2D_T}\left(\overline{\alpha}\frac{\overline{p}_T}{RT} + (1-\overline{\alpha})\rho_l\right)\overline{u}_m^2 + \overline{p}_T' = 0 \quad \textbf{5-20}$$

$$\overline{p}_A\overline{u}_g' + \overline{u}_g\overline{p}_A' = 0 \quad \textbf{5-21}$$

$$\overline{p}_A\overline{u}_g\overline{u}_g' - \overline{p}_A g + \frac{f}{2D_A}\overline{p}_A\overline{u}_g^2 + RT\overline{p}_A' = 0 \quad \textbf{5-22}$$

Recombine Equation 5-19, 5-20 and 5-21, we get

$$\overline{p}_T' = \frac{-\left(\overline{\alpha}\frac{\overline{p}_T}{RT} + (1-\overline{\alpha})\rho_l\right)g - \frac{f}{2D_T}\left(\overline{\alpha}\frac{\overline{p}_T}{RT} + (1-\overline{\alpha})\rho_l\right)\overline{u}_m^2}{1-\left(\overline{\alpha}\frac{\overline{p}_T}{RT} + (1-\overline{\alpha})\rho_l\right)\overline{u}_m^2\frac{\overline{\alpha}}{\overline{p}_T}} \quad \textbf{5-23}$$

$$\overline{u}_m' = -\frac{\overline{\alpha u}_m}{\overline{p}_T}\overline{p}_T' \quad \textbf{5-24}$$

$$\overline{\alpha}' = -\frac{(1-\overline{\alpha})\overline{\alpha}}{\overline{p}_T}\overline{p}_T' \qquad \textbf{5-25}$$

Where

$$\overline{u}_m = \overline{u}_{sl} + \overline{u}_{sg} \qquad \textbf{5-26}$$

$$\overline{\alpha} = \frac{\overline{u}_{sg}}{\overline{u}_{sg} + \overline{u}_{sl}} \qquad \textbf{5-27}$$

and

$$\overline{u}_{sl} = \overline{u}_{sl}^{in} = \frac{J(p_R - \overline{p}_{wf})}{\rho_l A_T} \qquad \textbf{5-28}$$

$$\overline{u}_{sg} = \frac{\dot{m}_g^{inj} RT}{\overline{p}_T A_T} \qquad \textbf{5-29}$$

Equation 5-23, 5-24 and 5-25 can then be solved by integration. This is a boundary value problem (BVP). Equations 5-12 and 5-13 are its boundary conditions.

Similarly, if recombine Equation 5-21 and 5-22, we can get

$$\overline{p}_A' = \frac{\frac{\overline{p}_A}{RT} g - \frac{f}{2D_A}\frac{\overline{p}_A}{RT}\overline{u}_g^2}{1 - \frac{\overline{u}_g^2}{RT}} \qquad \textbf{5-30}$$

$$\overline{u}_g' = -\frac{\overline{u}_g}{\overline{p}_A}\overline{p}_A' \qquad \textbf{5-31}$$

Where

$$\overline{u}_g = \frac{\dot{m}_g^{inj} RT}{\overline{p}_A A_A} \qquad \textbf{5-32}$$

This is also a BVP with its boundary conditions as

$$\overline{u}_g^{in} = \frac{\dot{m}_g^{inj} RT}{\overline{p}_A^{in} A_A} \qquad \textbf{5-33}$$

$$\overline{\dot{m}}_g^o = \dot{m}_g^{inj} = C_D \frac{\pi}{4} D_o^2 \overline{p}_u \sqrt{\frac{2}{RT}} \sqrt{\frac{k}{k-1}\left(\left(\frac{\overline{p}_d}{\overline{p}_u}\right)^{\frac{2}{k}} - \left(\frac{\overline{p}_d}{\overline{p}_u}\right)^{\frac{k+1}{k}}\right)} \quad \textbf{5-34}$$

In Equation 5-34, the downstream pressure of the injection orifice equals to the bottomhole flowing pressure of the tubing, which is available from the steady-state solution of flow in tubing. The upstream pressure is the pressure at the annulus bottom where orifice is installed.

If the gas injection at the bottom of well is critical as in Figure 3-7, only the first BVP will be solved.

5.2.3 Solution perturbation and linearization

With known steady-state solution, the dynamic variables can be written in the perturbation forms like

$$\alpha = \overline{\alpha}[1+\varepsilon\lambda(z,t)] \quad \textbf{5-35}$$

$$u_m = \overline{u}_m[1+\varepsilon\beta(z,t)] \quad \textbf{5-36}$$

$$p_T = \overline{p}_T[(1+\varepsilon\psi(z,t)] \quad \textbf{5-37}$$

$$u_g = \overline{u}_g[1+\varepsilon\varphi(z,t)] \quad \textbf{5-38}$$

$$p_A = \overline{p}_A[1+\varepsilon\xi(z,t)] \quad \textbf{5-39}$$

$$u_{sl}^{in} = \overline{u}_{sl}^{in}[1+\varepsilon\eta(t)] \quad \textbf{5-40}$$

Substituting Equation 5-35~5-40 into 5-7~5-11 and neglecting the nonlinear terms in the perturbed variables, we get

$$\overline{\alpha}\lambda_t' - \overline{u}_m'\beta + (\overline{\alpha}'\overline{u}_m + \overline{\alpha u}_m')(\lambda+\beta) + \overline{\alpha u}_m\lambda_z' - (1-\overline{\alpha})\overline{u}_m\beta_z' \quad \textbf{5-41}$$

$$\overline{\alpha p}_T(\lambda_t'+\psi_t') + \overline{\alpha p}_T\overline{u}_m(\lambda_z'+\beta_z'+\psi_z') + (\overline{\alpha p}_T\overline{u}_m' + \overline{\alpha u}_m\overline{p}_T' + \overline{p}_T\overline{u}_m\overline{\alpha}')(\lambda+\beta+\psi) = 0 \quad \textbf{5-42}$$

$$\left(\overline{\alpha}\frac{\overline{p}_T}{RT} + (1-\overline{\alpha})\rho_l\right)\overline{u}_m\beta_t' + \frac{\overline{\alpha p}_T\overline{u}_m}{RT}(\lambda+2\beta+\psi)\overline{u}_m' + \left(\frac{\overline{\alpha p}_T\overline{u}_m^2}{RT} + (1-\overline{\alpha})\rho_l\overline{u}_m^2\right)\beta_z'$$
$$+[2(1-\overline{\alpha})\beta - \overline{\alpha}\lambda]\rho_l\overline{u}_m\overline{u}_m' + \left(\frac{\overline{\alpha p}_T}{RT}(\lambda+\psi) - \overline{\alpha}\rho_l\lambda\right)g \quad \textbf{5-43}$$
$$+\frac{f}{2D_T}\left(\frac{\overline{\alpha p}_T\overline{u}_m^2}{RT}(\lambda+2\beta+\psi) - \overline{\alpha}\rho_l\overline{u}_m^2\lambda + 2(1-\overline{\alpha})\rho_l\overline{u}_m^2\beta\right) + \overline{p}_T\psi_z' + \overline{p}_T'\psi = 0$$

$$\overline{p}_A\xi_t' + \overline{p}_A\overline{u}_g(\varphi_z' + \xi_z') + (\overline{p}_A\overline{u}_g' + \overline{p}_A'\overline{u}_g)(\varphi + \xi) = 0 \quad \textbf{5-44}$$

$$\frac{\overline{p}_A}{RT}\overline{u}_g\varphi_t' + \frac{\overline{p}_A\overline{u}_g}{RT}(2\varphi + \xi)\overline{u}_g' + \frac{\overline{p}_A\overline{u}_g^2}{RT}\varphi_z' - \frac{\overline{p}_A}{RT}\xi g + \frac{f}{2D_A}\left(\frac{\overline{p}_A\overline{u}_g^2}{RT}(2\varphi + \xi)\right) + \overline{p}_A\xi_z' + \overline{p}_A'\xi = 0 \quad \textbf{5-45}$$

The boundary conditions of the original system are converted to

$$\lambda(0,t) = \frac{(\mathrm{K}_1 + \mathrm{K}_2\mathrm{K}_3)(\overline{p}_{wf} - p_R)}{\overline{\alpha}(0)}\eta(t) + \frac{\mathrm{K}_2\mathrm{K}_4\overline{p}_u}{\overline{\alpha}(0)}\xi(L,t) \quad \textbf{5-46}$$

$$\beta(0,t) = \frac{(\mathrm{K}_5 + \mathrm{K}_6\mathrm{K}_3)(\overline{p}_{wf} - p_R)}{\overline{u}_m(0)}\eta(t) + \frac{\mathrm{K}_6\mathrm{K}_4\overline{p}_u}{\overline{u}_m(0)}\xi(L,t) \quad \textbf{5-47}$$

$$\psi(0,t) = \left(1 - \frac{p_R}{\overline{p}_{wf}}\right)\eta(t) \quad \textbf{5-48}$$

$$\psi(L,t) = 0 \quad \textbf{5-49}$$

$$\varphi(0,t) = -\xi(0,t) \quad \textbf{5-50}$$

$$\varphi(L,t) = \frac{(\mathrm{K}_7 + \mathrm{K}_8\mathrm{K}_4)\overline{p}_u}{\overline{u}_g(L)}\xi(L,t) + \frac{\mathrm{K}_8\mathrm{K}_3(\overline{p}_{wf} - p_R)}{\overline{u}_g(L)}\eta(t) \quad \textbf{5-51}$$

If gas injection is critical, they write

$$\lambda(0,t) = -\frac{\mathrm{K}_1(p_R - \overline{p}_{wf})}{\overline{\alpha}(0)}\eta(t) \quad \textbf{5-52}$$

$$\beta(0,t) = -\frac{\mathrm{K}_5(p_R - \overline{p}_{wf})}{\overline{u}_m(0)}\eta(t) \quad \textbf{5-53}$$

$$\psi(0,t) = \left(1 - \frac{p_R}{\overline{p}_{wf}}\right)\eta(t) \quad \textbf{5-54}$$

$$\psi(L,t) = 0 \quad \textbf{5-55}$$

Where

$$\mathrm{K}_1 = -\frac{\overline{\dot{m}}_g^o RT\rho_l J(p_R - 2\overline{p}_{wf})}{(J(p_R - \overline{p}_{wf})\overline{p}_{wf} + \overline{\dot{m}}_g^o RT\rho_l)^2} \quad \textbf{5-56}$$

$$\mathrm{K}_2 = \frac{RT\rho_l J(p_R - \overline{p}_{wf})\overline{p}_{wf}}{(J(p_R - \overline{p}_{wf})\overline{p}_{wf} + \overline{\dot{m}}_g^o RT\rho_l)^2} \quad \textbf{5-57}$$

$$\mathrm{K}_3 = \frac{\sqrt{\frac{2}{RT}}\pi D_o^2 C_D \sqrt{\frac{k}{k-1}}\overline{p}_u}{8\sqrt{\left(\frac{\overline{p}_{wf}}{\overline{p}_u}\right)^{\frac{2}{k}} - \left(\frac{\overline{p}_{wf}}{\overline{p}_u}\right)^{\frac{k+1}{k}}}}\left(\frac{2}{k}\overline{p}_{wf}^{\frac{2-k}{k}}\overline{p}_u^{-\frac{2}{k}} - \frac{k+1}{k}\overline{p}_{wf}^{\frac{1}{k}}\overline{p}_u^{-\frac{k+1}{k}}\right) \quad \textbf{5-58}$$

$$\mathrm{K}_4 = \sqrt{\frac{2}{RT}}\frac{\pi}{4}D_o^2 C_D\sqrt{\frac{k}{k-1}}\sqrt{\left(\frac{\overline{p}_{wf}}{\overline{p}_u}\right)^{\frac{2}{k}} - \left(\frac{\overline{p}_{wf}}{\overline{p}_u}\right)^{\frac{k+1}{k}}}$$
$$+\frac{\sqrt{\frac{2}{RT}}\pi D_o^2 C_D \sqrt{\frac{k}{k-1}}\overline{p}_u}{8\sqrt{\left(\frac{\overline{p}_{wf}}{\overline{p}_u}\right)^{\frac{2}{k}} - \left(\frac{\overline{p}_{wf}}{\overline{p}_u}\right)^{\frac{k+1}{k}}}}\left(-\frac{2}{k}\overline{p}_{wf}^{\frac{2}{k}}\overline{p}_u^{-\frac{2-k}{k}} + \frac{k+1}{k}\overline{p}_{wf}^{\frac{k+1}{k}}\overline{p}_u^{\frac{-2k-1}{k}}\right) \quad \textbf{5-59}$$

$$\mathrm{K}_5 = -\frac{J}{\rho_l A_T} - \frac{\overline{\dot{m}}_g^o RT}{\overline{p}_{wf}^2 A_T} \quad \textbf{5-60}$$

$$\mathrm{K}_6 = \frac{RT}{\overline{p}_{wf} A_T} \quad \textbf{5-61}$$

$$\mathrm{K}_7 = -\frac{\overline{\dot{m}}_g^o RT}{\overline{p}_u^2 A_A} \quad \textbf{5-62}$$

$$\mathrm{K}_8 = \frac{RT}{\overline{p}_u A_A} \quad \textbf{5-63}$$

Assuming the perturbation terms in 5-35~5-40 take the form

$$\lambda(z,t) = [\mathrm{A}_1(z) + i\mathrm{A}_2(z)]e^{\omega t} \quad \textbf{5-64}$$

$$\beta(z,t) = [\mathrm{B}_1(z) + i\mathrm{B}_2(z)]e^{\omega t} \quad \textbf{5-65}$$

$$\psi(z,t) = [\Psi_1(z) + i\Psi_2(z)]e^{\omega t} \quad \textbf{5-66}$$

$$\varphi(z,t) = [\Phi_1(z) + \Phi_2(z)]e^{\omega t} \quad \textbf{5-67}$$

$$\xi(z,t) = [\Pi_1(z) + i\Pi_2(z)]e^{\omega t} \quad \textbf{5-68}$$

$$\eta(t) = (c_1 + ic_2)e^{\omega t} \quad \textbf{5-69}$$

Where

$$\omega = x + iy \tag{5-70}$$

Substituting 5-64~5-69 into 5-41~5-45 and separate the real and imaginary part, we get

$$\begin{bmatrix} C_{1,1} & & C_{1,3} & & & & & & & \\ & C_{2,2} & & C_{2,4} & & & & & & \\ C_{3,1} & & C_{3,3} & & C_{3,5} & & & & & \\ & C_{4,2} & & C_{4,4} & & C_{4,6} & & & & \\ & & C_{5,3} & & C_{5,5} & & & & & \\ & & & C_{6,4} & & C_{6,6} & & & & \\ & & & & & & C_{7,7} & & C_{7,9} & \\ & & & & & & & C_{8,8} & & C_{8,10} \\ & & & & & & C_{9,7} & & C_{9,9} & \\ & & & & & & & C_{10,8} & & C_{10,10} \end{bmatrix} \begin{bmatrix} \mathrm{A}_1' \\ \mathrm{A}_2' \\ \mathrm{B}_1' \\ \mathrm{B}_2' \\ \Psi_1' \\ \Psi_2' \\ \Phi_1' \\ \Phi_2' \\ \Pi_1' \\ \Pi_2' \end{bmatrix} = \begin{bmatrix} b_1 \\ b_2 \\ b_3 \\ b_4 \\ b_5 \\ b_6 \\ b_7 \\ b_8 \\ b_9 \\ b_{10} \end{bmatrix} \tag{5-71}$$

For critical gas injection, it writes

$$\begin{bmatrix} C_{1,1} & & C_{1,2} & & & \\ & C_{2,2} & & C_{2,4} & & \\ C_{3,1} & & C_{3,3} & & C_{3,5} & \\ & C_{4,2} & & C_{4,4} & & C_{4,6} \\ & & C_{5,3} & & C_{5,5} & \\ & & & C_{6,4} & & C_{6,6} \end{bmatrix} \begin{bmatrix} \mathrm{A}_1' \\ \mathrm{A}_2' \\ \mathrm{B}_1' \\ \mathrm{B}_2' \\ \Psi_1' \\ \Psi_2' \end{bmatrix} = \begin{bmatrix} b_1 \\ b_2 \\ b_3 \\ b_4 \\ b_5 \\ b_6 \end{bmatrix} \tag{5-72}$$

The elements in 5-71 and 5-72 are listed as followings.

$$C_{1,1} = C_{2,2} = \overline{\alpha u}_m \tag{5-73}$$

$$C_{1,3} = C_{2,4} = -(1-\overline{\alpha})\overline{u}_m \tag{5-74}$$

$$C_{3,1} = C_{3,3} = C_{3,5} = C_{4,2} = C_{4,4} = C_{4,6} = \overline{\alpha p}_T \overline{u}_m \tag{5-75}$$

$$C_{5,3} = C_{6,4} = \frac{\overline{\alpha p}_T \overline{u}_m^2}{RT} + (1-\overline{\alpha})\rho_l \overline{u}_m^2 \tag{5-76}$$

$$C_{5,5} = C_{6,6} = \overline{p}_T \tag{5-77}$$

$$C_{7,7} = C_{7,9} = C_{8,8} = C_{8,10} = \overline{p}_A \overline{u}_g \tag{5-78}$$

$$C_{9,7} = C_{10,8} = \frac{\overline{p}_A \overline{u}_g^2}{RT} \tag{5-79}$$

$$C_{9,9} = C_{10,10} = \overline{p}_A \tag{5-80}$$

$$b_1 = -\overline{\alpha}(\mathrm{A}_1 x - \mathrm{A}_2 y) + \overline{u}_m' \mathrm{B}_1 - (\overline{\alpha}'\overline{u}_m + \overline{\alpha u}_m')(\mathrm{A}_1 + \mathrm{B}_1) \tag{5-81}$$

$$b_2 = -\overline{\alpha}(\mathrm{A}_2 x + \mathrm{A}_1 y) + \overline{u}_m' \mathrm{B}_2 - (\overline{\alpha}'\overline{u}_m + \overline{\alpha u}_m')(\mathrm{A}_2 + \mathrm{B}_2) \tag{5-82}$$

$$\begin{aligned} b_3 = {} & -\overline{\alpha p}_T[(\mathrm{A}_1 + \Psi_1)x - (\mathrm{A}_2 + \Psi_2)y] \\ & -(\overline{\alpha p}_T \overline{u}_m' + \overline{\alpha u}_m \overline{p}_T' + \overline{p}_T \overline{u}_m \overline{\alpha}')(\mathrm{A}_1 + \mathrm{B}_1 + \Psi_1) \end{aligned} \tag{5-83}$$

$$\begin{aligned} b_4 = {} & -\overline{\alpha p}_T[(\mathrm{A}_2 + \Psi_2)x + (\mathrm{A}_1 + \Psi_1)y] \\ & -(\overline{\alpha p}_T \overline{u}_m' + \overline{\alpha u}_m \overline{p}_T' + \overline{p}_T \overline{u}_m \overline{\alpha}')(\mathrm{A}_2 + \mathrm{B}_2 + \Psi_2) \end{aligned} \tag{5-84}$$

$$\begin{aligned} b_5 = {} & -\left(\overline{\alpha}\frac{\overline{p}_T}{RT} + (1-\overline{\alpha})\rho_l\right)\overline{u}_m(\mathrm{B}_1 x - \mathrm{B}_2 y) - \frac{\overline{\alpha p}_T \overline{u}_m}{RT}(\mathrm{A}_1 + 2\mathrm{B}_1 + \Psi_1)\overline{u}_m' \\ & -[2(1-\overline{\alpha})\mathrm{B}_1 - \overline{\alpha}\mathrm{A}_1]\rho_l \overline{u}_m \overline{u}_m' - \left(\frac{\overline{\alpha p}_T}{RT}(\mathrm{A}_1 + \Psi_1) - \overline{\alpha}\rho_l \mathrm{A}_1\right)g \\ & -\frac{f}{2D_T}\left(\frac{\overline{\alpha p}_T \overline{u}_m^2}{RT}(\mathrm{A}_1 + 2\mathrm{B}_1 + \Psi_1) - \overline{\alpha}\rho_l \overline{u}_m^2 \mathrm{A}_1 + 2(1-\overline{\alpha})\rho_l \overline{u}_m^2 \mathrm{B}_1\right) - \overline{p}_T' \Psi_1 \end{aligned} \tag{5-85}$$

$$\begin{aligned} b_6 = {} & -\left(\overline{\alpha}\frac{\overline{p}_T}{RT} + (1-\overline{\alpha})\rho_l\right)\overline{u}_m(\mathrm{B}_2 x + \mathrm{B}_1 y) - \frac{\overline{\alpha p}_T \overline{u}_m}{RT}(\mathrm{A}_2 + 2\mathrm{B}_2 + \Psi_2)\overline{u}_m' \\ & -[2(1-\overline{\alpha})\mathrm{B}_2 - \overline{\alpha}\mathrm{A}_2]\rho_l \overline{u}_m \overline{u}_m' - \left(\frac{\overline{\alpha p}_T}{RT}(\mathrm{A}_2 + \Psi_2) - \overline{\alpha}\rho_l \mathrm{A}_2\right)g \\ & -\frac{f}{2D_T}\left(\frac{\overline{\alpha p}_T \overline{u}_m^2}{RT}(\mathrm{A}_2 + 2\mathrm{B}_2 + \Psi_2) - \overline{\alpha}\rho_l \overline{u}_m^2 \mathrm{A}_2 + 2(1-\overline{\alpha})\rho_l \overline{u}_m^2 \mathrm{B}_2\right) - \overline{p}_T' \Psi_2 \end{aligned} \tag{5-86}$$

$$b_7 = -\overline{p}_A(\Pi_1 x - \Pi_2 y) - (\overline{p}_A \overline{u}_g' + \overline{u}_g \overline{p}_A')(\Phi_1 + \Pi_1) \tag{5-87}$$

$$b_8 = -\overline{p}_A(\Pi_2 x + \Pi_1 y) - (\overline{p}_A \overline{u}_g' + \overline{u}_g \overline{p}_A')(\Phi_2 + \Pi_2) \tag{5-88}$$

$$\begin{aligned} b_9 = {} & -\frac{\overline{p}_A}{RT}\overline{u}_g(\Phi_1 x - \Phi_2 y) - \frac{\overline{p}_A \overline{u}_g}{RT}(2\Phi_1 + \Pi_1)\overline{u}_g' + \frac{\overline{p}_A}{RT}\Pi_1 g \\ & -\frac{f}{2D_A}\left(\frac{\overline{p}_A \overline{u}_g^2}{RT}(2\Phi_1 + \Pi_1)\right) - \overline{p}_A' \Pi_1 \end{aligned} \tag{5-89}$$

$$b_{10} = -\frac{\overline{p}_A}{RT}\overline{u}_g(\Phi_2 x + \Phi_1 y) - \frac{\overline{p}_A \overline{u}_g}{RT}(2\Phi_2 + \Pi_2)\overline{u}_g' + \frac{\overline{p}_A}{RT}\Pi_2 g - \frac{f}{2D_A}\left(\frac{\overline{p}_A \overline{u}_g^2}{RT}(2\Phi_2 + \Pi_2)\right) - \overline{p}_A'\Pi_2 \quad \textbf{5-90}$$

The boundary conditions for BVP 5-71 are

$$\mathrm{A}_1(0) = \frac{(\mathrm{K}_1 + \mathrm{K}_2\mathrm{K}_3)(\overline{p}_{wf} - p_R)}{\overline{\alpha}(0)}c_1 + \frac{\mathrm{K}_2\mathrm{K}_4\overline{p}_u}{\overline{\alpha}(0)}\Pi_1(L) \quad \textbf{5-91}$$

$$\mathrm{A}_2(0) = \frac{(\mathrm{K}_1 + \mathrm{K}_2\mathrm{K}_3)(\overline{p}_{wf} - p_R)}{\overline{\alpha}(0)}c_2 + \frac{\mathrm{K}_2\mathrm{K}_4\overline{p}_u}{\overline{\alpha}(0)}\Pi_2(L) \quad \textbf{5-92}$$

$$\mathrm{B}_1(0) = \frac{(\mathrm{K}_5 + \mathrm{K}_6\mathrm{K}_3)(\overline{p}_{wf} - p_R)}{\overline{u}_m(0)}c_1 + \frac{\mathrm{K}_6\mathrm{K}_4\overline{p}_u}{\overline{u}_m(0)}\Pi_1(L) \quad \textbf{5-93}$$

$$\mathrm{B}_2(0) = \frac{(\mathrm{K}_5 + \mathrm{K}_6\mathrm{K}_3)(\overline{p}_{wf} - p_R)}{\overline{u}_m(0)}c_2 + \frac{\mathrm{K}_6\mathrm{K}_4\overline{p}_u}{\overline{u}_m(0)}\Pi_2(L) \quad \textbf{5-94}$$

$$\Psi_1(0) = \left(1 - \frac{p_R}{\overline{p}_{wf}}\right)c_1 \quad \textbf{5-95}$$

$$\Psi_2(0) = \left(1 - \frac{p_R}{\overline{p}_{wf}}\right)c_2 \quad \textbf{5-96}$$

$$\Psi_1(L) = 0 \quad \textbf{5-97}$$

$$\Psi_2(L) = 0 \quad \textbf{5-98}$$

$$\Phi_1(0) = -\Pi_1(0) \quad \textbf{5-99}$$

$$\Phi_2(0) = -\Pi_2(0) \quad \textbf{5-100}$$

$$\Phi_1(L) = \frac{(\mathrm{K}_7 + \mathrm{K}_8\mathrm{K}_4)\overline{p}_u}{\overline{u}_g(L)}\Pi_1(L) + \frac{\mathrm{K}_8\mathrm{K}_3(\overline{p}_{wf} - p_R)}{\overline{u}_g(L)}c_1 \quad \textbf{5-101}$$

$$\Phi_2(L) = \frac{(\mathrm{K}_7 + \mathrm{K}_8\mathrm{K}_4)\overline{p}_u}{\overline{u}_g(L)}\Pi_2(L) + \frac{\mathrm{K}_8\mathrm{K}_3(\overline{p}_{wf} - p_R)}{\overline{u}_g(L)}c_2 \quad \textbf{5-102}$$

The boundary conditions for BVP 5-72 are

$$A_1(0) = \frac{K_1(\bar{p}_{wf} - p_R)}{\bar{\alpha}(0)} c_1 \quad \textbf{5-103}$$

$$A_2(0) = \frac{K_1(\bar{p}_{wf} - p_R)}{\bar{\alpha}(0)} c_2 \quad \textbf{5-104}$$

$$B_1(0) = \frac{K_5(\bar{p}_{wf} - p_R)}{\bar{u}_m(0)} c_1 \quad \textbf{5-105}$$

$$B_2(0) = \frac{K_5(\bar{p}_{wf} - p_R)}{\bar{u}_m(0)} c_2 \quad \textbf{5-106}$$

$$\Psi_1(0) = \left(1 - \frac{p_R}{\bar{p}_{wf}}\right) c_1 \quad \textbf{5-107}$$

$$\Psi_2(0) = \left(1 - \frac{p_R}{\bar{p}_{wf}}\right) c_2 \quad \textbf{5-108}$$

$$\Psi_1(L) = 0 \quad \textbf{5-109}$$

$$\Psi_2(L) = 0 \quad \textbf{5-110}$$

5.2.4 Determination of stability

Equation 5-71 thus describes the system's response to an arbitrary applied perturbation such as the inlet flow variation. The stability of the system is determined by the sign of x, which is the dimensionless attenuation factor of the perturbation amplitude. If $x > 0$, the system is unstable, and if $x < 0$, the system is stable. $x = 0$ gives the neutral stability.

Equation 5-71 and its boundary conditions compose a BVP. It can be solved either for checking the stability of certain settings by looking at the sign of x, or for finding the boundary between stable and unstable regime by setting $x = 0$.

BVP 5-71 can also be solved by Matlab® BVP solver.

5.3 Matlab® BVP solver

The linear analysis procedure described in last section is coded in Matlab®. It involves two BVPs. One is looking for the system steady-state solutions, and the other is checking the stability of the system linearized perturbation equations. Matlab® BVP solver is used to solve the two BVPs.

5.3.1 Matlab® BVP function bvp4c

The solver is shipped as a standard Matlab® function named as bvp4c. According to Matlab® manual, bvp4c is a finite difference code that implements the 3-stage Lobatto IIIa formula.

This is a collocation formula and the collocation polynomial provides a C1-continuous solution that is fourth-order accurate uniformly in the interval of integration. Mesh selection and error control are based on the residual of the continuous solution. The collocation technique uses a mesh of points to divide the interval of integration into subintervals. The solver determines a numerical solution by solving a global system of algebraic equations resulting from the boundary conditions, and the collocation conditions imposed on all the subintervals. The solver then estimates the error of the numerical solution on each subinterval. If the solution does not satisfy the tolerance criteria, the solver adapts the mesh and repeats the process.

The user must provide the points of the initial mesh as well as an initial approximation of the solution at the mesh points. The detailed description of numeric method adopted in the solver is given by Shampine *et al*.

5.3.2 Method of continuation

The convergence of the program bvp4c is much dependent on the users' first guess. So, once a reasonable solution is obtained for one case, continuation method should be used when solving new cases, which helps to make the solving procedure more easily to converge.

For example, if we have found a reasonable solution for one case and we want to study a new case that has different parameters with the first one, the solution for the first case should be used as the first guess for the new case. If the parameters of the two cases are too different, one or more in-between cases have to be calculated in order to get a reasonable first guess for the new case.

5.3.3 Calculation example: results of the steady-state solution

As a demonstration, an example of using the Matlab® BVP solver is given, which calculates the steady-state solution for system in Figure 3-6. Table 5-1 gives the parameters used in the demo calculation.

To solve the steady-state problem, two-step has to be taken. First, flow in the tubing is solved with the boundary condition of constant gas injection rate at the bottom and constant pressure at the top.

Table 5-1 Parameters for the demo calculation.

Parameter	Value
Well depth, m	2500
Tubing diameter, m	0.125
Annulus hydraulic diameter, m	0.2
Orifice diameter, m	0.008
Gas injection rate, kg/s	1.0
Reservoir pressure, Pa	1.8e7
Wellhead pressure, Pa	1.0e6
System temperature, K	300
Productivity index, (kg/s)/Pa	4E-6
Friction factor, -	0.015
Water density, kg/m^3	1000

Second, once bottom hole flowing pressure is calculated, orifice equation 5-34 is used to calculate the upstream pressure of orifice at the annulus side. This pressure serves as a boundary condition for flow in the annulus, while the other boundary condition for annulus is the constant gas injection at the casing head.

The calculated results are given in Figure 5-1 and Figure 5-2. In fact, when performing linear stability analysis, for each case, such kind of steady-state calculation must be done first.

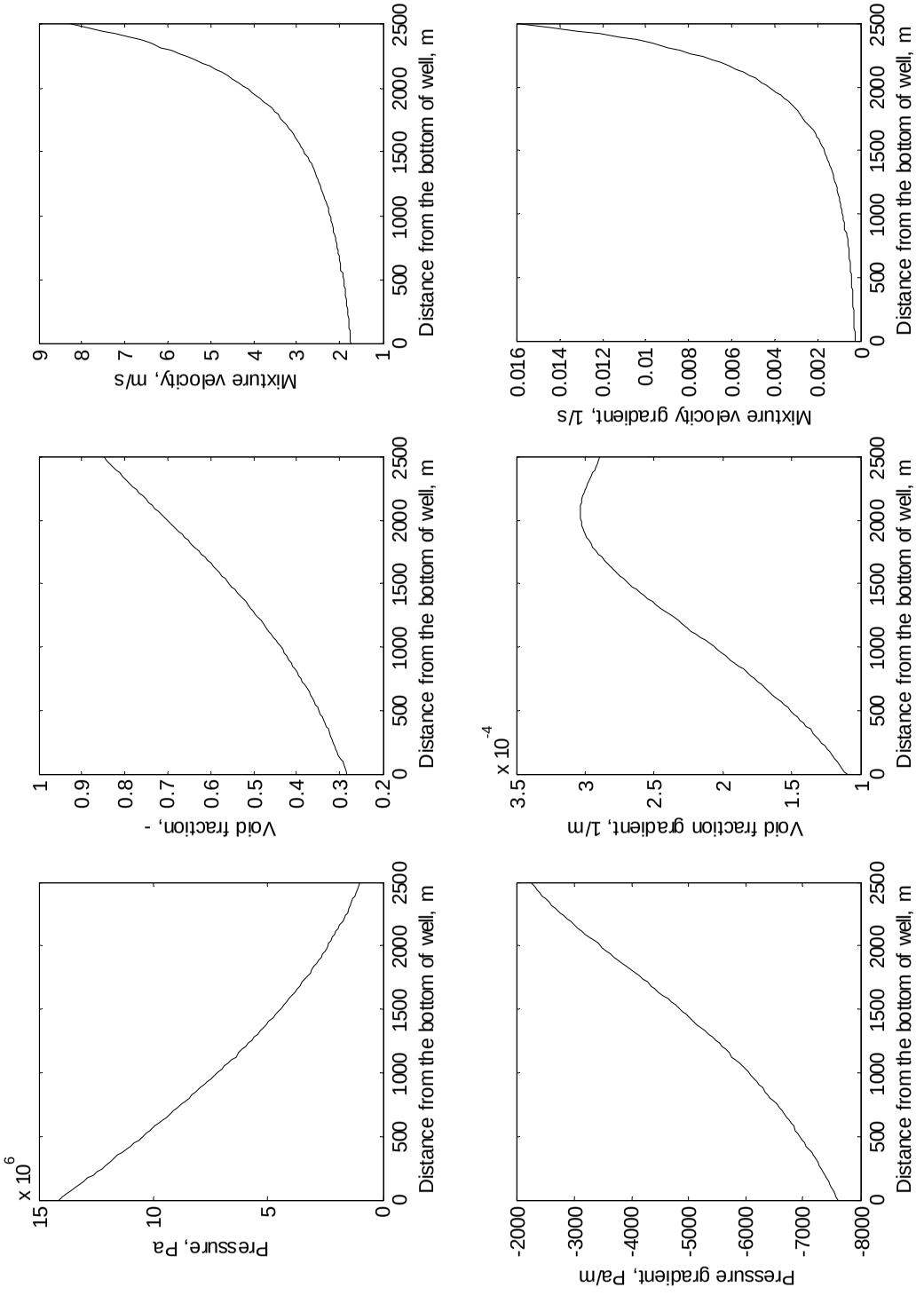

Figure 5-1 Steady-state solution for flow in the tubing.

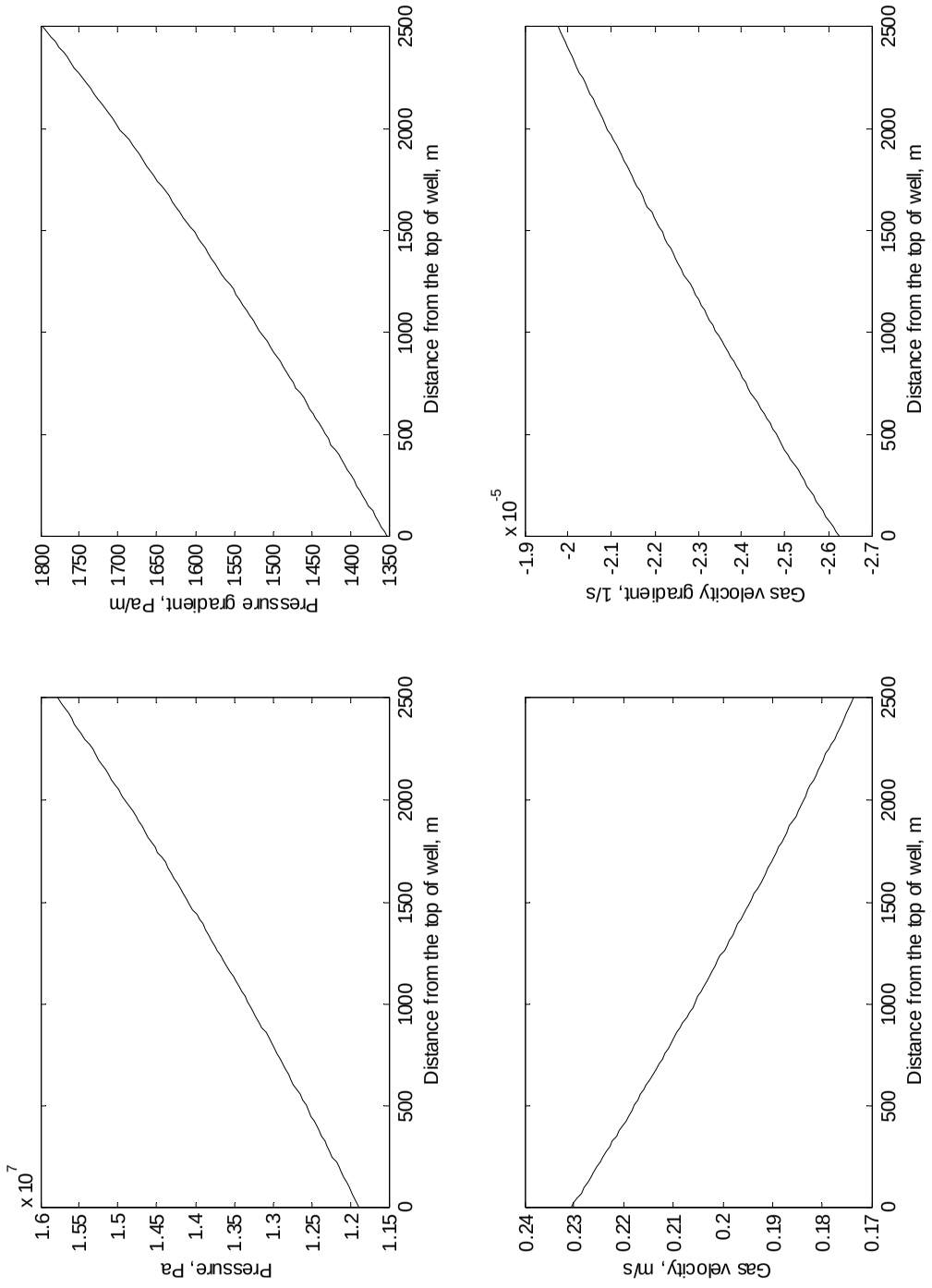

Figure 5-2 Steady-state solution for flow in the annulus.

5.4 Results of linear stability analysis

The linear stability analysis results are presented in this section. Before the analysis procedure is applied to investigate the occurrence of density-wave instability, it has been validated against casing heading problem.

5.4.1 Validating analysis procedure against casing heading

As it is concluded in the second chapter, casing heading has been extensively investigated by many researchers and its basic characteristics are now clear. Therefore it can be used as a target to validate the analysis procedure formulated in the second section of this chapter.

Table 5-1 gives a base case in studying the casing heading problem. Based on this, four parametric studies have been carried out. The four parameters are gas injection rate, orifice diameter, productivity index and hydraulic diameter of annulus. The results are given in Figure 5-3, in which the parametric trend of casing heading for each parameter is plotted.

The upper-left plot shows the attenuation factor versus gas injection rate. At low gas injection rate, the attenuation factor is positive, which means the system is unstable. The attenuation factor decreases with the increasing of gas injection rate. If the gas injection rate is high enough, it turns to be negative, which means the system is stable.

The upper-right plot shows the attenuation factor versus orifice size. For orifice with smaller diameter, the attenuation factor tends to be negative and vice versa. So, the system is stable for smaller orifice and unstable for larger orifice. The plot also shows that, when orifice diameter is too large, the attenuation factor tends to level off. This means the instability is saturated with the orifice size.

The lower-left plot shows the attenuation factor versus productivity index. In the normal range of productivity index, the attenuation factor tends to decrease with increasing of productivity index. This means the system moves towards to the stable direction. When the productivity index is extremely low, the system shows an opposite trend, in which lower productivity index tends to make the system stable. This corresponds to the situation when liquid production is very low, and so does the hold-up level in the tubing.

The lower-right plot shows the attenuation factor versus annulus hydraulic diameter. For very small diameter, the attenuation factor is negative, which means the system is stable. If increase the diameter, the attenuation factor increases to become positive. This means the system moves towards the unstable direction.

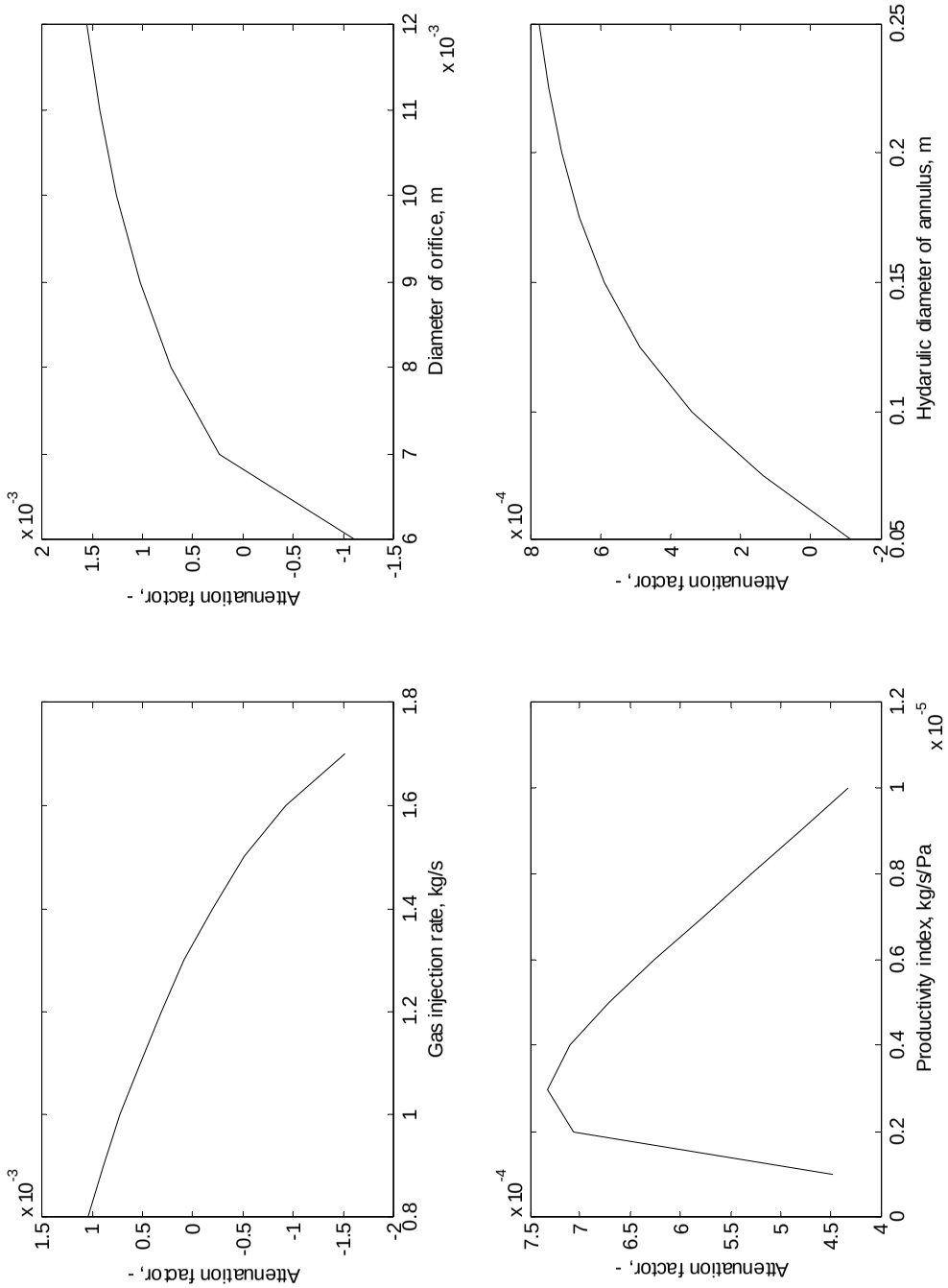

Figure 5-3 Casing heading parametric trend

The results of analysis agree quite well with the main conclusions of casing heading studies. This means the linear stability analysis procedure adopted in this chapter successfully reveals the main characteristics of casing heading, and therefore is reliable to be used for further analysis tasks.

5.4.2 Occurrence of density-wave instability

As discussed in the third chapter, dynamic instability (density-wave instability) can happen no matter the downhole gas injection is critical or non-critical. But if the gas injection is non-critical, there is a possibility for casing heading. This is shown in section 5.4.1. So, if we investigate the occurrence of density-wave instability in a non-critical gas injection system, then each time when instability is detected, we have to clarify whether it is casing heading or density-wave instability. This will involve more calculation work. To avoid this, this investigation concentrates only on the system with critical downhole gas injection, in which, once instability is detected, it should be density-wave instability. This corresponds to the system sketched in Figure 3-7.

The well parameters used in this investigation are abstracted from some typical unstable gas-lift wells in one of the North Sea field. These are given in Table 5-2.

Table 5-2 Well parameters used in the investigation

Parameter	Value
Well depth, m	2500
Tubing diameter, m	0.125
Well outlet pressure, bara	10
Productivity index, kg/s/Pa	4E-6

In order to get a whole picture of the possible instability, this investigation covers a wider range of gas injection rate and reservoir pressure. For example, the reservoir pressure is from 50 to 260 bara. To check the stability of the simplified system, Equation 5-72 together with its boundary conditions 5-103~5-110 has to be solved.

Figure 5-4 is the result of the stability check at different gas injection rate. The result is quite surprising. The instability does exist in the system at certain parameter settings. In the figure, the “+” sign represents positive value of the dimensionless attenuation factor x, and vice versa. Thus those operating points marked by “+” are unstable. The figure shows that when reservoir pressure is high, at normal gas injection rate, the system is stable. But when the reservoir pressure is depleted, even at high gas injection rate, the well still

could be unstable. This implies that the density-wave instability is likely to occur at the decline stage of the field.

It is not difficult to interpret the results showed in Figure 5-4. As a common sense, high flow rates can cause high friction loss, which normally dampens oscillations in vertical well flow. This corresponds to the area of high gas injection rates and high reservoir pressures in the figure. For the low reservoir pressures and low gas injection rates, gravity becomes the dominant factor for the two-phase flow in the tubing, which can often cause instability. For example, a small inflow rate change may result in the big change of the hold-up profile along the tubing, which therefore causes big change in pressure drop, and furthermore can cause larger flow variations at the bottom of the well. This is exactly the case for density-wave oscillations.

Figure 5-4 also indicates that at very low reservoir pressure, the unstable range in terms of gas injection rate shrinks itself. This could be explained by the very low hold-up when liquid rate is too low. At this situation, even if there is a change in inlet flow rate, the hold-up only varies in a low level, which is not likely to create too big change in the hydrostatic pressure drop.

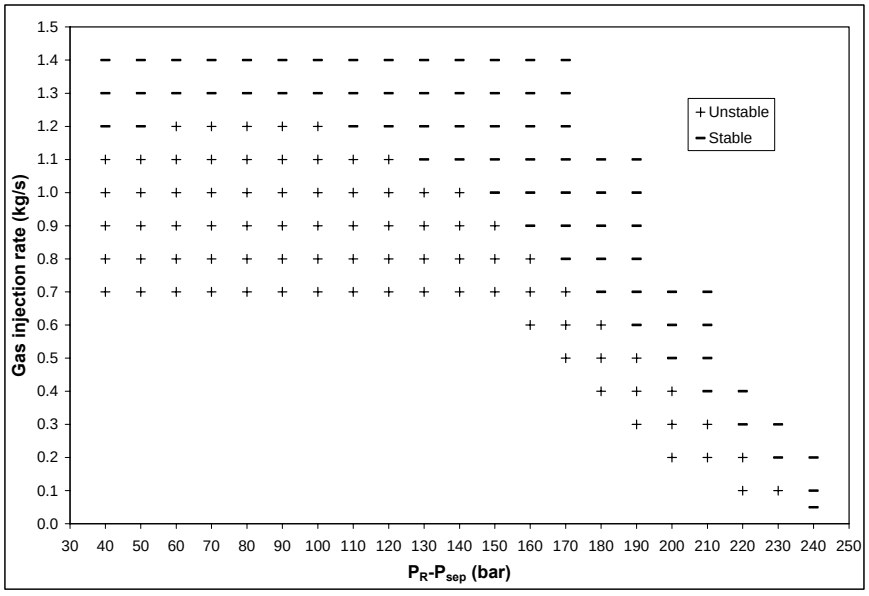

Figure 5-4 Map of density-wave instability.

One important observation here is that, when the reservoir pressure is between 70 and 110 bara, the system has a big possibility to be unstable.

This is exact what has been observed from the unstable gas-lift wells in the North Sea field, where the well data were abstracted.

This investigation clearly demonstrates that density-wave instability can happen in a gas-lift well, particularly when reservoir pressure is depleted.

5.4.3 Characterizing density-wave instability

To investigate the how other parameters affect the instability, parametric study has been performed. In this study, neutral stability is searched by setting $x = 0$, in which the Matlab® code calculates the gas injection rate that satisfies the neutral stability for a given reservoir pressure. The parameters considered in the parametric study are the four in Table 5-2. Their variation ranges are given in Table 5-3.

Table 5-3 Parameters used in characterizing density-wave instability.

Parameter	Value range
Well depth, m	2000~3000
Tubing diameter, m	0.1~0.15
Well outlet pressure, bara	5~20
Productivity index, kg/s/Pa	2~8E-6

In order to facilitate comparison among different cases, dimensionless system total pressure drop is used as x-axis in the following plots instead of the system pressure drop. The dimensionless total pressure drop is calculated by dividing the system pressure drop with the hydrostatic head of liquid column in the filled-up tubing.

Effect of productivity index. The first parameter studied is the productivity index, which represents the inflow restriction. Figure 5-5 gives the results. When the productivity index is changed from 2E-6 to 8E-6 kg/s/Pa, the regime of unstable production expands, particularly when reservoir pressure is low. However, for high reservoir pressures, the exciting effect on instability by increasing PI value is not as significant as it is for lower reservoir pressures. This is due to that higher productivity index also results in higher flow rate, particularly when reservoir pressure is high. The damping effect of friction due to high flow rate therefore compensates the exciting effect.

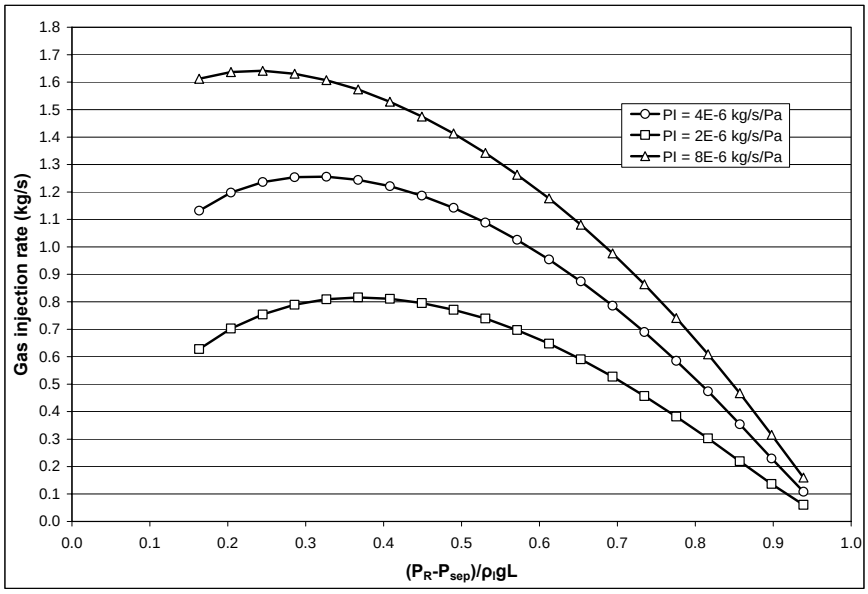

Figure 5-5 Effect of productivity index.

One important result here is that the effect of productivity index on density-wave instability is just opposite with its effect on casing heading. To remove instabilities from production wells, one may think of applying well stimulation, which increases productivity index. However, this should be done based on the clear knowledge of the type of instability for the unstable wells; otherwise the stimulation action may make the problem even worse according to the results in Figure 5-5.

Figure 5-5 also shows that when increasing productivity index, the value of dimensionless system pressure drops corresponding to the maximum gas injection rates on the curves shift to the left direction.

Effect of tubing diameter. The second parameter studied is the tubing diameter. Three diameters, 0.1, 0.125 and 0.15 m, are tested. Results of this study are given in Figure 5-6. As expected, small diameter tends to give stable effect due to increased friction damping. The suggestion of inserting coiled tubing into the production string to reduce the flow area should be a possible solution to reduce density-wave instability based on the results in Figure 5-6.

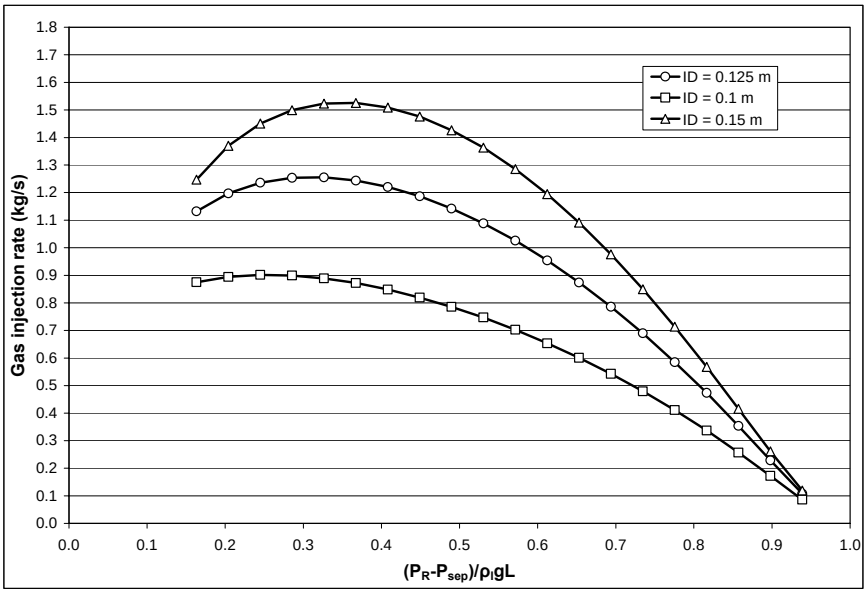

Figure 5-6 Effect of tubing diameter.

Just as opposite as in Figure 5-5, the dimensionless pressure drops corresponding to the maximum gas injection rates on the curves shift to the right direction when tubing diameter is increased.

Effect of system pressure. The third parameter studied is the system pressure. The backpressure of the system is increased from 5 to 20 bara. The results are shown in Figure 5-7. The results indicate that, under the same system pressure drop, high average system pressure increases instability. This is quite obvious in the low reservoir situation. Increasing system pressure basically reduces the volume flow rate in the tubing, which reduces friction loss. This effect is stronger when the system pressure is already low, for example in the situation of low reservoir pressure. But if the system pressure is already very high, increasing a lit bit backpressure has no significant effect on the stability.

The results suggest that, when the gas-lift well is unstable due to density-wave instability, reducing the backpressure might be an efficient way to remove the instability from system, particularly when the reservoir pressure is relatively low and there is a possibility to reduce wellhead backpressure.

The dimensionless system pressure drops corresponding to the maximum gas-injection rates on the curves do not shift with the change of system pressure.

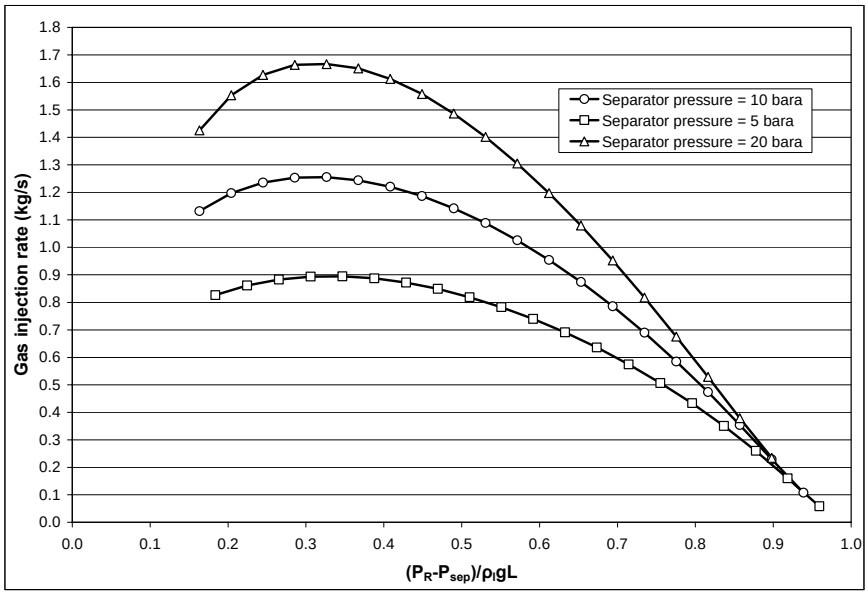

Figure 5-7 Effect of system pressure.

In last chapter, it is concluded that density-wave instability will not happen if neglecting compressibility. However the results shown in Figure 5-7 indicate that the system tends to be more unstable if reduce compressibility by increasing system pressure. The two conclusions seem conflict. In fact, they are not. The conclusion from last chapter means that compressibility is a necessary condition for density-wave instability to happen, while the conclusion from Figure 5-7 implies that density-wave instability will not monotonically increase with the compressibility, at low system pressure level, the compressibility gives stable effect.

Effect of well depth. The last parameter studied is the well depth. Since many field reports of unstable gas-lift operation indicate that the instability tends to occur in deeper gas-lift wells. So, this investigation tries to find out if this observation is generally correct. Three different well depths, 2000, 2500 and 3000 m are tested and results are given in Figure 5-8.

The results demonstrate that, for deeper gas-lift well, there is a bigger chance for density-wave instability to happen. This means that at the same gas injection rate, deeper well will have a wider unstable range for reservoir pressure than that of shallower wells. Therefore, one may have more chance to see the instability in deeper wells rather than shallower wells.

The dimensionless system pressure drops corresponding to the maximum gas-injection rates on the curves shift to the left direction.

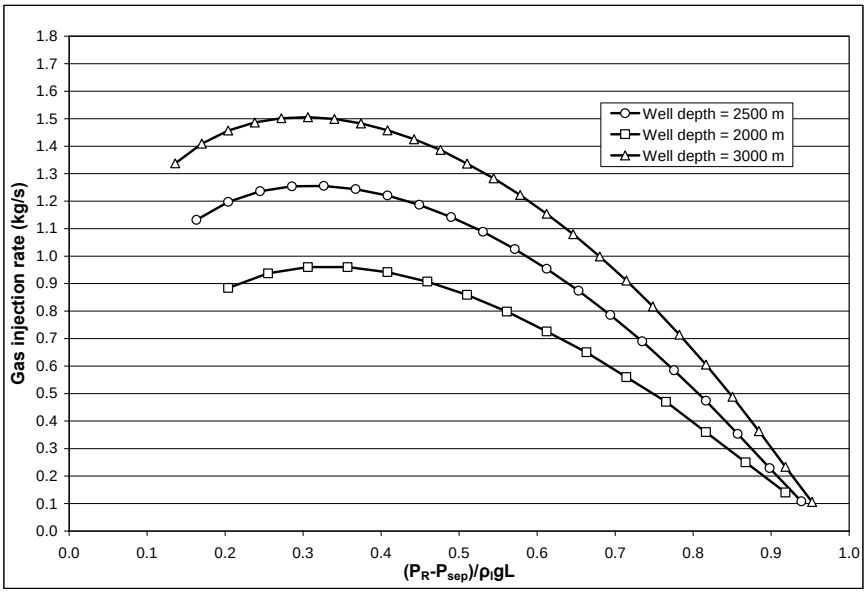

Figure 5-8 Effect of well depth.

5.4.4 More discussion of the characterization results

In last chapter, the effect of each parameter on the density-wave instability can be discussed independently since an analytical solution is available. For example, when discussing the effect of productivity index, all the other parameters can be assumed unchanged. However, this can not be done in this analysis and the numerical simulation in next chapter. When changing the productivity index, other parameters such as flow rate, mixture density, etc… will also change. So, the conclusions from this analysis are only valid to the corresponding parameter range, which is believed to be representative for most situations.

However, if the parameter is far outside the range of interest, the result might be different. For example, if continue to increase the productivity index, we may gradually see the instability regime shrinks, which implies that the effect of high flowrate takes over the control.

5.5 A necessary condition for density-wave instability

One of the important observations here is that the density-wave instability will not happen if the dimensionless total pressure drop is greater than one. This means that, in the simplified gas-lift system in Figure 3-7, if without the help of gas-lift, the well has the capability of natural flowing (single phase water flow), density-wave instability will not happen no matter how low the gas injection rate will be. So, a necessary condition for density-wave instability to happen is

$$\frac{p_R - p_{sep}}{\rho_l g L} < 1 \qquad \textbf{5-111}$$

The physical explanation of this phenomenon is not very clear. This is the first time for this conclusion is deduced. However, this is not the first time for one observes it from experiment. Sekoguchi ***et al***. found in their experiments for unstable airlift pumping that the unstable phenomenon was likely to happen at lower submergence ratio, and would disappear as the submergence ratio approached unit. Unfortunately, they did not explain the reason for this.

The conclusion here implies that, in the practical operation, those wells that can still produce without the supplement of gas-lift are unlikely to experience density-wave instability.

5.6 Summary

1. Linear stability analysis has been applied to the gas-lift system. The analysis procedure is validated against casing heading problem first. Satisfied results are obtained from the validating calculation. The adopted linear analysis procedure is then reliable for being used in further investigations.

2. Density-wave instability is able to occur in the simplified gas-lift system whose main parameters are abstracted from real unstable gas-lift wells. Parametric studies show that increasing productivity index, tubing diameter, system pressure and well depth can increase density-wave instability.

3. One of the important observation here is that density-wave instability is very unlikely to happen in those wells that still can naturally flowing without the supplement of gas-lift.

4. The results of density-wave instability investigation in this chapter also emphasize the importance of compressibility comparing with the conclusion from last chapter. In fact, compressibility is a necessary condition for density-wave instability to happen in gas-lift wells.

5.7 Nomenclature

A	Area m^2
C	Coefficient, -
D	Diameter, m
f	Friction factor, -

g	Acceleration of gravity, m/s^2
J	Mass productivity index, kg/s/Pa
K	Ratio of specific heat capacity, -
L	Tubing length, m
m	Mass flow rate, kg/s
P	Pressure, Pa
R	Air constant, J/kg/K
u	Velocity, m/s
x	Dimensionless perturbation amplitude attenuation factor, -
y	Angular frequency of perturbation, -
α	Void fraction, -
ρ	Density, kg/m^3
ε	Infinitesimal, -
λ	Perturbation term for void fraction, -
β	Perturbation term for velocity, -
η	Perturbation term for inlet liquid superficial velocity, -
ψ	Perturbation term for pressure, -

Subscripts

A	Annulus
Cr	Critical
D	Downstream
g	Gas
l	Liquid
m	Mixture
o	Orifice
R	Reservoir
sl	Liquid superficial
t	Time
T	Tubing
U	Upstream
wf	Well flowing
z	Vertical coordinate

Superscripts

$\bar{}$	Steady-state
´	Derivation
inj	Injection
in	Inflow

6 DYNAMIC SIMULATION RESULTS

6.1 Introduction

The linear stability analysis results from last chapter show that density-wave instability can happen in depleted gas-lift wells. However, the analysis can not show how the instability looks like in practical operations. To demonstrate the unstable flow behaviour, numerical simulation is performed in this chapter.

In order to get an independent cross-check with the linear stability analysis results, a commercial available dynamic multiphase flow simulator is used to carry out the simulation tasks instead of discretizing the homogenous two-phase flow model used in last chapter. The simulator, which is called OLGA®2000, was originally developed to simulate dynamic two-phase hydrocarbon flow in pipelines.

OLGA is based on a modified two-fluid model, in which separate continuity equations for gas, liquid bulk and liquid droplets are applied. The continuity equations are coupled through interfacial mass transfer. Only two momentum equations are used, one for the continuous liquid phase and one for the combination of gas and liquid droplets. The velocity of any entrained liquid droplets in the gas phase is given by a slip relation. One mixture energy equation is applied and both phases are at the same temperature. This yields six conservation equations to be solved, which are three for mass, two for momentum and one for energy.

Two basic flow regime categories, distributed flow and separated flow, are adopted to describe the two-phase flow structures. The former contains bubble and slug flow, the latter includes stratified and annular-mist flow. Transition between the regime categories is determined by minimum slip concept combined with additional criteria.

OLGA uses a semi-implicit numerical solution scheme, which allows relatively long time steps and is well suited for simulating rather slow mass flow transients. This is important for the simulation of very long transport lines, where typical transient process can take hours or even days and requires long time steps in order to save simulation time.

Since OLGA was commercialized, it has been extensively verified against data from both experimental loops and practical pipelines. Its application range has been continuously expanding. Particularly in recent years, it is more and more used in simulating well flow dynamics. However, very limited

publications can be found for discussing its performance in simulating well flow dynamics. This might be due to the difficulties in doing experiments and collecting accurate data in real production wells.

If OLGA simulation can reveal the density-wave oscillations and give the similar characterization results as we get from linear analysis, it will give strong support to the basic conclusions obtained from the analysis. However, alternatively speaking, using OLGA to simulate density-wave oscillations is also a good example to qualitatively verify the performance of the simulator since we are more confident about the linear analysis results as the method has been validated by casing heading problem.

Casing heading could also be a good example to be used to check the performance of the simulator. So, as did in last chapter, before the simulator is used to reveal the density-wave oscillation, it is used to simulate the cyclic behaviour of casing heading.

If positive results are obtained from the simulations of the two instabilities, which are based on different mechanisms, it at least indicates that OLGA is capable of capturing the dynamics of typical unstable flow phenomena in vertical two-phase flow system even though the verification here only has qualitative significance.

6.2 Set up a well within OLGA®2000

There are two ways to set up a well model in OLGA®2000. One is that the tubing is contained in a casing just like the well looks like. The other is that, the annulus is modelled as an equivalent pipe by using its hydraulic diameter just like the simplified gas-lift model in Figure 3-6.

The first model should be used when heat transfer calculation is the main concern since it gives the correct heat transfer model between tubing and annulus. However, in this dissertation, the simplified model is used and heat transfer calculation settings is simplified or even neglected since it has little effect on flow instabilities.

6.3 Simulating casing heading

Casing heading is simulated first in order to see if the simulator can reproduce the limit cycle. For this purpose, a hypothetic vertical well model is built within OLGA®2000.

The well parameters are abstracted from some typical gas-lift wells in the North Sea field. So, the well settings are reasonable even though it is hypothetic. The main parameters of the well and the reservoir are:

- Well depth: 2100 m
- Tubing inner diameter: 0.125 m
- Annulus hydraulic diameter: 0.2 m
- Production choke size: 0.07 m
- Gas-lift valve diameter: 0.0125 m
- Reservoir pressure: 150 bara
- Reservoir temperature: 108 °C
- Reservoir fluid: GOR = 80 Sm^3/Sm^3, Water-cut = 0
- Lifting gas density at standard condition: 1.19 kg/m^3
- Oil density at standard condition: 810 kg/m^3

A base case for casing heading is simulated first. The main settings of the base case are:

- Separator pressure: 15 bara
- Mass productivity index: 2.47E-6 kg/s/Pa
- Opening of the production choke: 100%
- Gas injection rate: 0.6 kg/s

The result of the base case simulation is shown as in Figure 6-1. From the figure, we can see that, when casing heading happens, both pressure in annulus and in tubing are in oscillation and so does the oil production rate. The periodic time and amplitude of the oscillation are tremendously larger than normal hydrodynamic slugging. So, it is more dangerous and needs more attention.

During the oscillation, the downstream pressure of gas-lift valve sometimes is higher than the upstream pressure, then the gas injection stops. When pressure in the annulus side is built up and higher than that in the tubing side, gas injection is recovered. Accordingly, the variation of surface oil rate in Figure 6-1 can be separated into three phases.

The first phase corresponds to the situation when gas injection stops. During this period, the well produces naturally at a low rate. This can be seen in the plot, for example between 5 hours and 5.5 hours. The second phase is the liquid blow-out period that corresponds to the recovery of gas injection. During this period, a bulk of liquid is pushed out of the tubing by the lifting gas in an acceleration manner, which is indicated by the oil production peak in the plot. After liquid blow-out, the lifting gas reaches the wellhead and the well enters the third phase. In this phase, there is a continuous gas injection from annulus even though it gradually decays. During this period, the production rate is relatively high due to high proportion of gas in the tubing. When gas injection

stops, the well goes back to the first phase and starts another cycle. The three phase production is a typical phenomenon for casing heading.

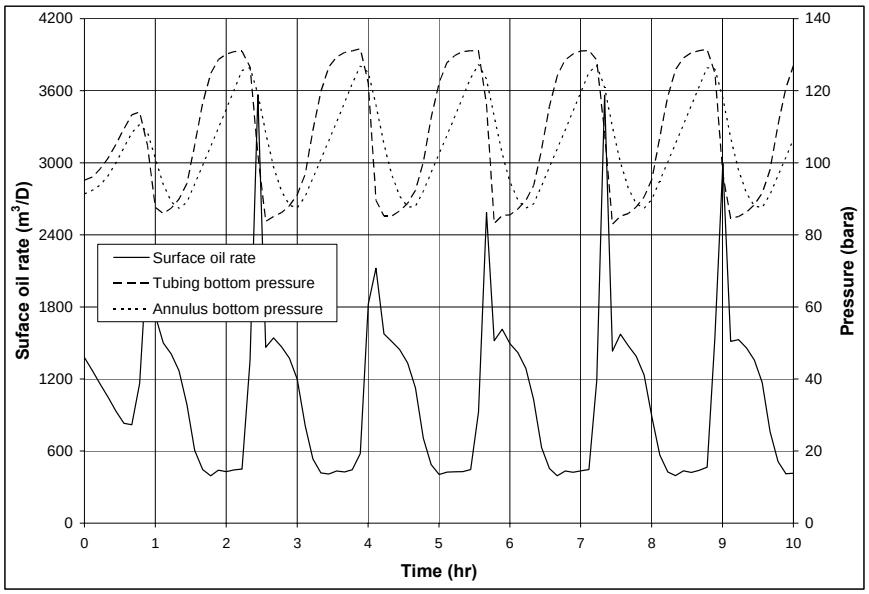

Figure 6-1 Base case simulation results.

6.3.1 Characterizing casing heading

Casing heading is characterized by applying parametric study on the base case. The effects of changing gas injection rate, orifice size, productivity index, choke opening and system pressure are investigated.

Effect of gas injection rate. First we see the effect of changing gas injection rate. Results are shown in Figure 6-2, in which the bottomhole flowing pressures are plotted for different cases. Besides the base case, another two cases with different gas injection rates (0.7 and 0.8 kg/s) are simulated while all other parameters and boundary conditions are kept the same as in the base case.

The results show that the oscillation amplitude is decreased and the frequency is increased when increasing gas injection rate from 0.6 kg/s to 0.7 kg/s. The well is stabilized when gas injection rate reaches 0.8 kg/s. This means that increasing gas injection rate can stabilize the well. This attributes to two factors caused by increased gas injection. One is the increased friction loss due to increased flow rate in the tubing. Another is that high gas rate can make the flow in the annulus more stiff, thus reduces the delay effect.

However, strictly speaking, increasing gas injection does not always increase stability. The well is capable of natural flowing as indicated in Figure 6-1. We can imagine that the well will produce stably without gas-lift. When gas-lift is added, then the instability starts to appear and will increase with the increasing of gas injection rate. The amplitude of the oscillation should level off and gradually decrease if increasing the gas injection further. What the Figure 6-2 shows is just the situation after the level-off. This part should be the normal operation range for most gas-lift wells in practice. So the conclusion here is practically correct. But one may possibly see that there is no significant improvement on the unstable gas-lift by adding more lifting gas in certain situation, particularly when the lifting gas rate is within the range of level-off as just explained.

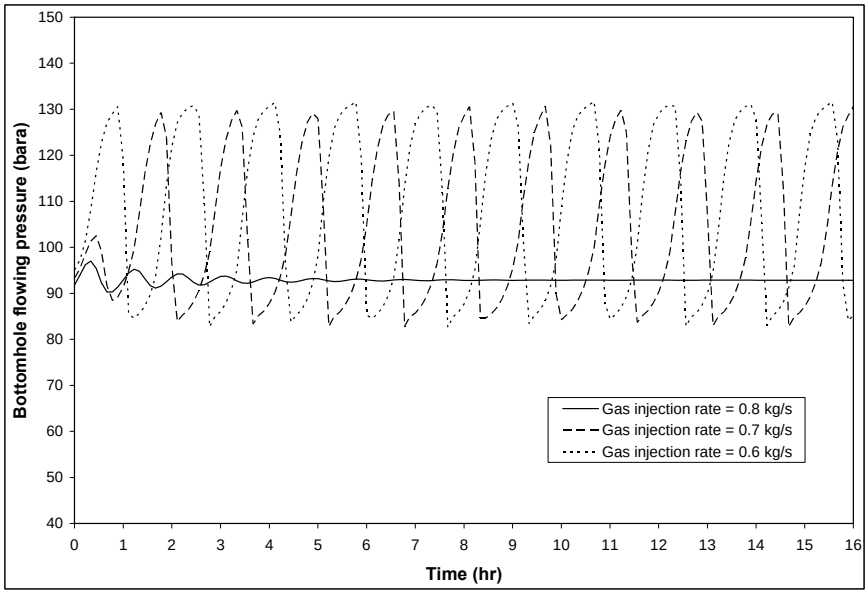

Figure 6-2 Effect of gas injection rate.

Effect of orifice size. The effect of gas-lift valve size is also investigated. Besides the gas-lift valve used in the base case, another two valve sizes, 0.01 and 0.02 m, are tested in the simulation to see their effects on the instability. Figure 6-3 gives the results of these simulations.

The port size of gas-lift valve has a strong impact on well stability. Valve with smaller port size can increase stability since it can suppress big flow variations. Figure 6-3 shows the time series of bottomhole flowing pressures for the three cases. It is clear that the oscillation amplitude is decreased when

using smaller size orifices. When the diameter of gas-lift valve is only 0.01 m, the well is stabilized.

The reason why using smaller orifice can stabilize casing heading has been explained in Chapter 3, which corresponds to Figure 3-1. The simulation here demonstrates the previous explanation.

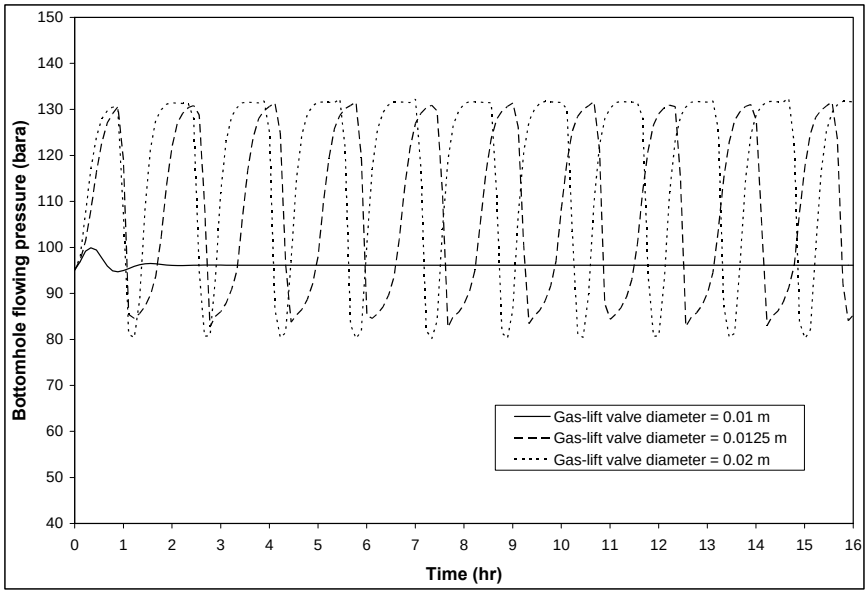

Figure 6-3 Effect of orifice size.

Effect of productivity index. The third parameter that has been investigated is the productivity index. Changing the productivity index also can change the stability of the well. As discussed in Chapter 2, casing heading is a static instability based oscillation, which means the system has a positive feedback to any flow perturbations around the steady-state solution. For example, a sudden increase of gas injection from annulus to tubing will decrease the hydrostatic pressure drop by decreasing mixture density, thus promotes the instability. Therefore, a higher productivity index should have a stabilizing effect by supplying more reservoir fluid to compensate the mixture density reduction. On the other hand, a higher productivity index will also result in high flow rate in the well. This of course also helps in stabilizing.

This is also clearly demonstrated by the simulation. Figure 6-4 shows the effects of productivity index. Three cases including the base case are given in the figure. Increasing productivity index reduces the oscillation amplitude and the well becomes stable when it is big enough. In this simulation, the well is stabilized when the productivity index is tripled from the base case.

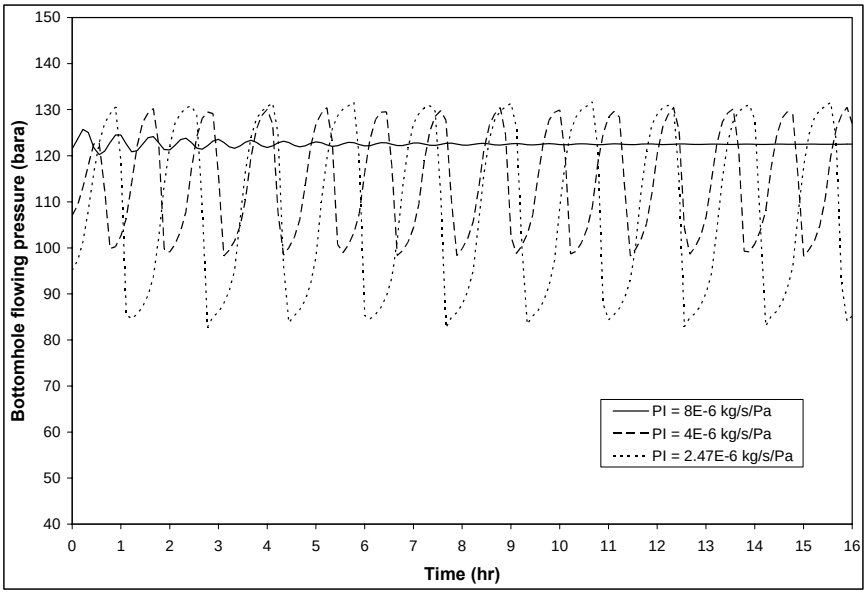

Figure 6-4 Effect of productivity index.

Effect of Choking. Choking is the most used pragmatic way of stabilizing unstable wells. The role of choking relies on that smaller choke opening can increase friction loss for the whole system. Choking effect on casing heading is simulated here and Figure 6-5 gives the simulation results for three cases with different choke openings.

The three cases have 20%, 40% and 100% opening respectively. Results show that choking decreases instability. When the choke opening is about 40%, the oscillation amplitude is already significantly reduced. Continuing to close the choke down to 20%, the well is stabilized.

So, in practical operation, when casing heading is confirmed, applying choking should be able to reduce the oscillation and even stabilize the well. One important point that should be emphasized here is that the stabilizing effect comes from the additional friction loss across the choke, instead of the increased back pressure. This can be further clarified when studying the separator pressure effect as below.

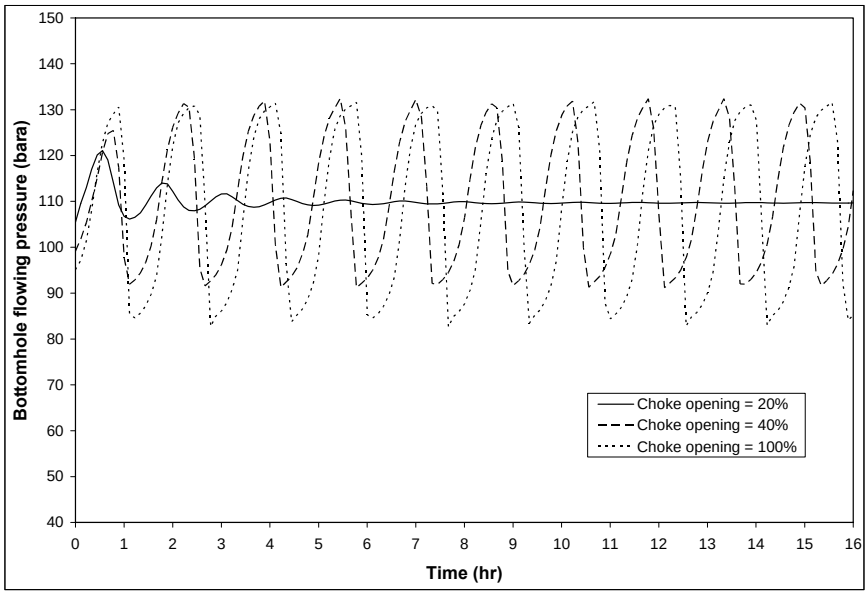

Figure 6-5 Effect of choking.

Effect of separator pressure. The separator pressure is changed to the see the response of casing heading to different back pressure. All the other parameters of the well are kept the same as in the base case except that the separator pressure is changed to 30 bara first, and then to 40 bara. The two cases together with the base case simulation results are plotted in the same plane for comparison. Figure 6-6 shows the results. This time, instead of plotting the time series of bottomhole flowing pressure, surface oil rate is plotted.

From the figure, we can see that none of the cases can give stable production, and there is no clear indication that the well flow tends to be stable when separator pressure is increased even though the average production rate is reduced due to increased wellhead back pressure. This implies that increasing separator pressure is not an option to stabilize the well in practical operations.

Discussions. To explain the reasons why choking can stabilize the well while increasing wellhead back pressure cannot, we have to understand the stabilizing mechanism. For casing heading, the instability relies on two facts. The first is that the two-phase flow in the tubing is gravity dominant. The second is that the flow in annulus is very compressible and there is an annulus volume effect that can result in a delayed response of the pressure in the annulus to the changed gas discharge rate. The two combined effects result in the casing heading cycle. So, to stabilize the well, any of these two facts has to be modified.

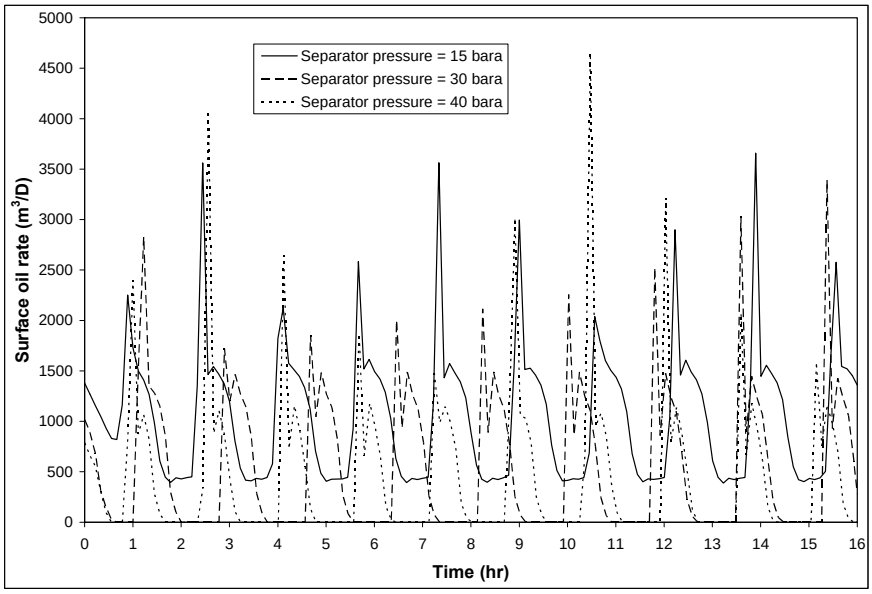

Figure 6-6 Effect of separator pressure.

Obviously choking can make the system less gravity dominant by increasing friction, but increasing well head back pressure does not help in modify this fact. Figure 6-7 shows the steady state simulation results of production rate versus gas injection rate. The solid line represents the result of the base case, the dashed line is the result with 20% choke opening and the dotted line is with 30 bara separator pressure. Other settings of the latter two cases are the same as in the base case.

If look at the sensitivity (derivative) of the production rate to the gas injection rate at a certain point, for example under 0.6 kg/s gas injection, it is found that both the solid line and dotted line have almost the same sensitivity, but for the dashed line, the production is less sensitive to the gas injection rate. This explains why increasing separator pressure will not stabilize the well.

Although increasing separator pressure could reduce the density difference between gas and oil, it cannot result in significant increase in friction loss. On the contrary, the opposite possibility exits, which could increase the sensitivity of production rate to gas injection rate and therefore make the unstable flow even worse.

In fact, in Figure 6-6, the surface oil rate oscillation amplitude increases for the case with 40 bara separator pressure comparing with the base case where the separator pressure is only 15 bara.

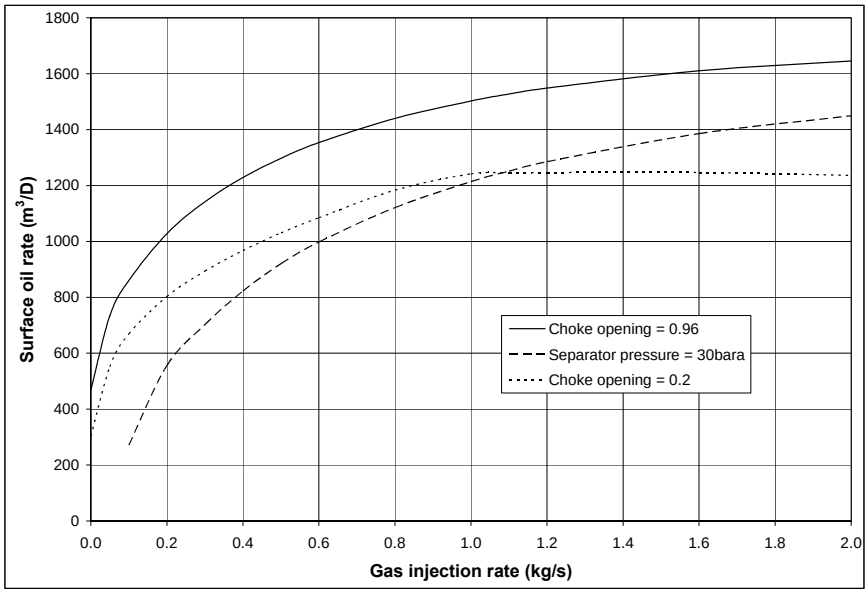

Figure 6-7 Lift performance relationships under different well settings.

6.3.2 Simulating gas robbing in dual gas-lift

The concept of dual gas-lift is that two tubing strings are contained in the same casing as shown in Figure 6-8. The two tubing strings may produce from different payzones. The two tubing strings share the same lifting gas source. Lifting gas is diverted into annulus by flow control valve on the casing top, and then injected into two tubing strings through gas-lift valves in the side pocket mandrels.

The total gas injection rate is split into two strings according to the gas-lift valve sizes, the annulus pressure and the tubing pressures. Obviously, the gas injection rate to each string could be different from each other.

Sometimes it is difficult to make the dual gas-lift operate under predefined gas split rates. The gas split scenario normally is planned based on steady-state calculation. However, the calculated scenario may be statically unstable. In practice, it is often observed that all the amount of lifting gas is sucked by one tubing string and leave another in starvation of lifting gas. This phenomenon is called gas robbing.

In order to simulate this phenomenon, a dual gas-lift well model was set up in OLGA®2000. It is assumed that the two tubing produce from two isolated payzones that have the same reservoir pressure and temperature as in the base case of casing heading simulation. The productivity indexes of the two

payzones are slightly different. For tubing 1, the productivity index is 2.7 kg/s/Pa; for tubing 2, it is 2.71 kg/s/Pa. The other main parameters of the well are the same as in the base case except that the hydraulic diameter of the annulus is reduced to 0.156 m.

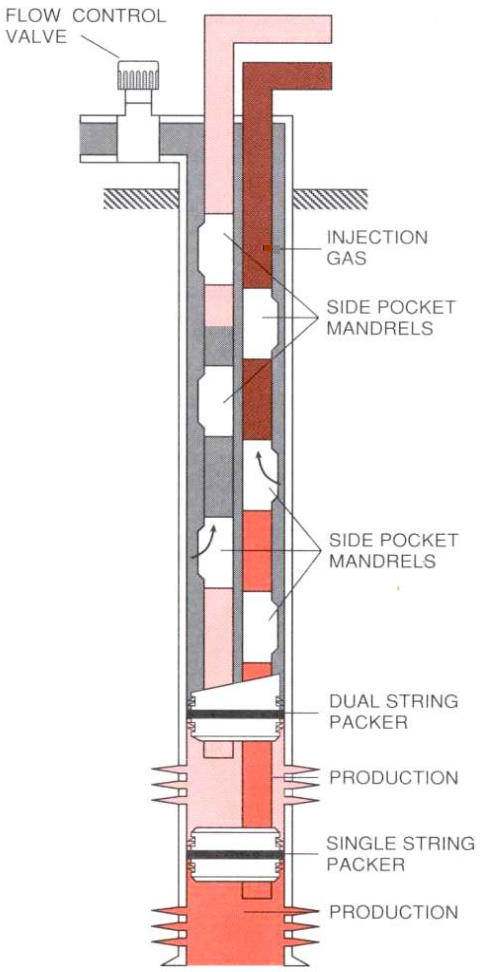

Figure 6-8 Dual gas-lift.

When simulating gas robbing, the following simulation procedure is followed. First, the system is initialized and an enough high total lifting gas rate is given so that the system can reach a dynamic steady-state that is independent on the initial condition of the system. In this simulation, a total lifting gas rate of 2.0 kg/s is tested to be enough for the purpose.

The simulation then is started based on the initial condition and the given lifting gas rate. After a short period, the system can reach a dynamic steady-state.

The total lifting gas rate is then reduced in steps. For each time, the total lifting gas rate is reduced by 0.2 kg/s within 1 minute, and then the system will operate under the new total lifting gas rate for a certain period to make sure that it has enough time to reach the new steady-state.

The simulation results are given in Figure 6-9, in which four separate sub-figures are presented. The four sub-figures give the time series of the key variables such as the total lifting gas rate, the gas injection rate to each tubing, the pressures upstream and downstream the gas-lift valves, and the surface oil production rate for each tubing. For the plot of gas injection rate, there are some numerical noises, but they are not obstructions for one to see the basic variation trend of gas injection rate. This is also the case for surface oil rate of tubing 2 between 11 and 12 hours in the plot.

As mentioned earlier, under certain boundary conditions, the simulation is started from a pre-defined initial condition and gradually reaches a dynamic steady-state that corresponds to the boundary conditions. Depending on how close the initial condition is to the final dynamic steady-state solution, it takes different time for the system to reaches the steady-state. In this simulation, the system settles down approximately after 1 hour. The sequent simulations are then based on this steady-state.

From 1 hour to 4 hours, there is no change to the system. The dual gas-lift has a total lifting gas rate of 2.0 kg/s. Because the two tubing strings are almost identical, the total lifting gas rate is then split into two strings at equal rate (1.0 kg/s for each). The pressure at the annulus bottom is about 95 bara, and the pressures inside the tubing strings are 86 bara. The surface oil rate of each tubing is about 1600 m^3/D.

At 4 hours, the total lifting gas rate is reduced from 2.0 kg/s to 1.8 kg/s. After short time transient, the system reaches a new steady-state, at which the lifting gas is also equally split into two tubing.

However, if reducing the total lifting gas rate further to 1.6 kg/s (at 8 hours), the system can not reach a steady-state with equally split gas injection. Instead, an excursive instability happens, which leads to another steady-state solution. During the excursion process, the tubing with a slight higher productivity index gradually loses all its injection gas and produce naturally at a low production rate. On the other hand, the other tubing takes all of the

lifting gas and produces at high production rate. Obviously, this new steady-state is a statically stable solution.

Since all of the lifting gas goes to tubing 1, the pressure in the annulus increases. This can be seen from the third plot in Figure 6-9. For tubing 2, the tubing pressure also increases due to loss of lifting gas and it is much higher than the pressure in annulus.

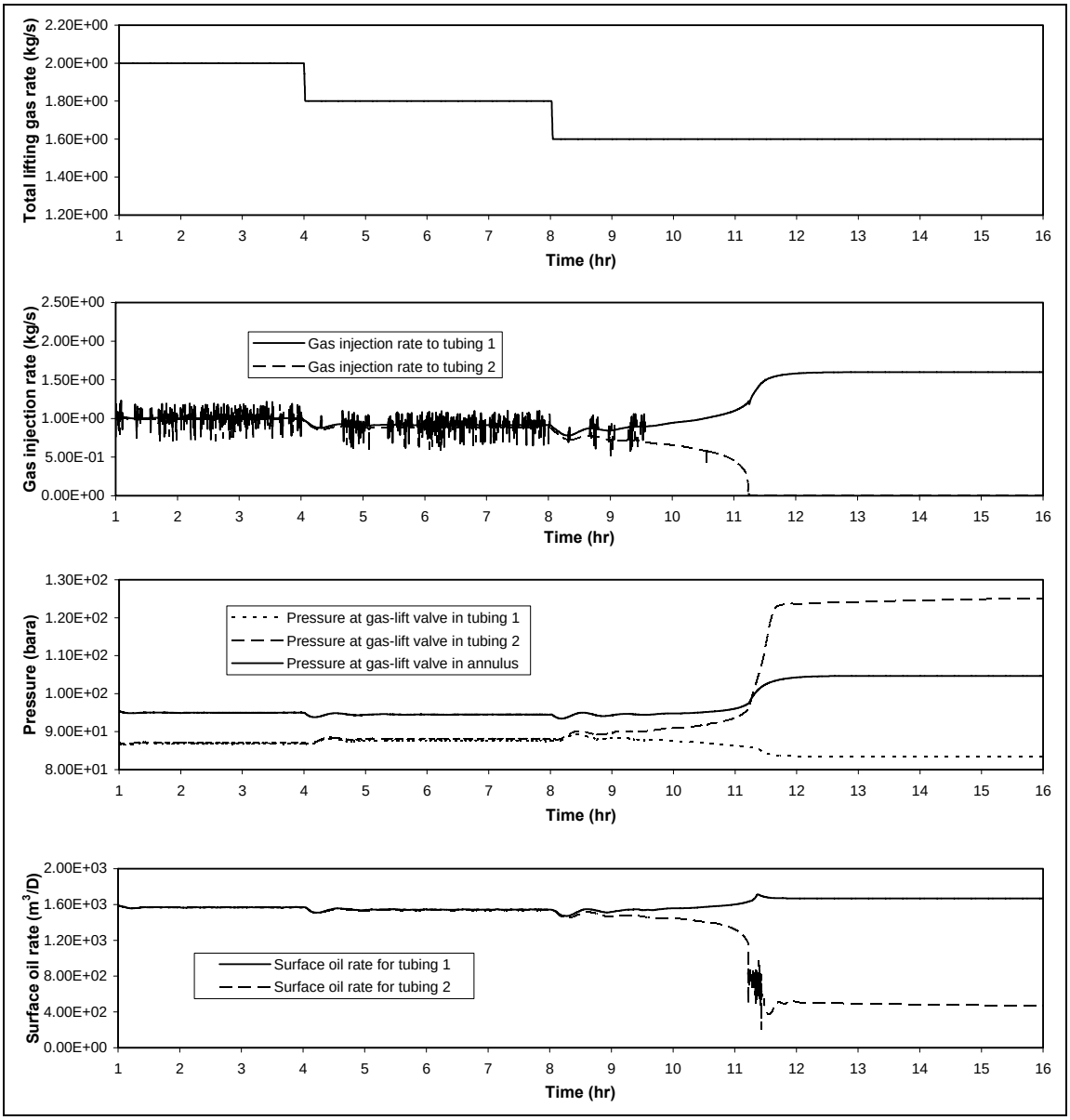

Figure 6-9 Gas robbing in dual gas-lift.

The new stable solution is just one of the many possibilities for gas robbing. It should be normal as well if one see flow oscillations due to gas robbing. Besides, some dual gas-lift wells may have unloading valves. Due to high annulus pressure and tubing pressure, unloading valves, particularly those on tubing string 2, may reopen. Lifting gas is then injected through unloading valves. The system therefore may end up with more possibilities in its production scenarios such as multipointing, alternative injection point shifting, and etc...

The reason for occurrence of gas robbing lies in two facts. First, at least the flow in one tubing string must be gravity dominant, and the tubing pressure is sensitive to lifting gas rate. Second, the other tubing can absorb additional lifting gas, and thus makes the pressure in the annulus not increase too fast and too high.

Assuming there is a negative perturbation in gas injection rate to one tubing, and then the tubing pressure will increase if the flow in the tubing is gravity dominant. The increased tubing pressure will reduce the gas injection further. Then the pressure in the annulus will increase. If the annulus pressure increase faster than in the tubing, then gas injection rate should be recovered for that tubing and the system is stable. However, if the other tubing can absorb more gas and slow down the pressure increasing in the annulus, it is possible for the first tubing to continue losing its lifting gas.

Obviously, gas robbing could happen when lifting gas rate is low since the above two facts can be more easily satisfied at lower lifting gas rate. For the simulation above, when total lifting gas rate is reduced, the tubing pressure becomes more sensitive to lifting gas rate. Tubing 2, which has a lit bit higher productivity index, should be more sensitive to the lifting gas rate change since its gas injection rate is already a lit bit lower than that of tubing 1. This can be found when total lifting gas rate is 1.8 kg/s even though the difference is tiny. When lifting gas rate reduced, the gas injection to both tubing is reduced. And the pressures in both tubing increases. Unfortunately, the pressure in tubing 2 is more sensitive to the reduction of gas injection rate and increases more than that in tubing 1, and then it starts to lose its lifting gas first.

In practice, which tubing is going to lose its lifting gas first is really a complicated issue. The observation here, like that the tubing with a higher productivity index loses its lifting gas first, can not be used as a common conclusion.

When tubing 2 starts to lose its lifting gas, the annulus pressure does not increase since tubing 1 sucks the additional lifting gas and makes the annulus

pressure relatively stable. The annulus pressure will start to increase significantly when the pressure reduction in tubing 1 can not compensate the pressure drop increase across the gas-lift valve due to increased gas flow. However, this pressure increase is too late to recover the gas injection in tubing 2 since the pressure there is already much higher than that of annulus.

6.4 Simulating density-wave oscillations

From the above simulations, it is believed that OLGA®2000 has the capability to capture the main dynamics of casing heading. This gives us the confidence of using the simulator to investigate density-wave oscillations.

In this section, a series of simulations are carried out to investigate the occurrence and characteristics of density-wave oscillations. All the simulations are initiated from steady-state solutions. Stable and unstable productions are judged from the time series of the variables. If they tend to be a straight line, then the production is said stable. Otherwise, if they develop into limit cycle, then the production is unstable.

In order to facilitate comparison with the linear stability analysis results, the same gas-lift well settings and fluids as in the analysis are used in the simulations. This means the annulus is not included in the simulations. Instead, a gas mass source is set at the bottom of the well. Only water is produced from the reservoir and lifting gas is air. The main parameter ranges are:

- Well depth: 2000~3000 m
- Tubing inner diameter: 0.1~0.15 m
- Production choke size: 0.125 m
- Separator pressure: 5~20 bara
- Reservoir temperature: 108 °C
- Reservoir pressure: 50~300 bara
- Lifting gas rate: 0~1.5 kg/s
- Mass productivity index: 2~8E-6 kg/s/Pa

6.4.1 Occurrence of density-wave instability

The occurrence of density-wave instability is investigated first. The main settings of the well parameters in this investigation are:

- Well depth: 2500 m
- Tubing inner diameter: 0.125 m
- Separator pressure: 10 bara
- Reservoir temperature: 108 °C
- Reservoir pressure: 50~300 bara

- Opening of the production choke: 100%
- Gas injection rate: 0~1.5 kg/s
- Mass productivity index: 4E-6 kg/s/Pa

A similar stability map as in linear analysis is obtained from the simulation as shown in Figure 6-10. However, more information is available from the simulations than from linear analysis. For a given reservoir pressure, particularly when it is not high enough to make the well naturally flow, three phenomena, indicated as “no production”, “unstable production”, and “stable production” in the map, can be observed when increasing gas injection rate from low to high.

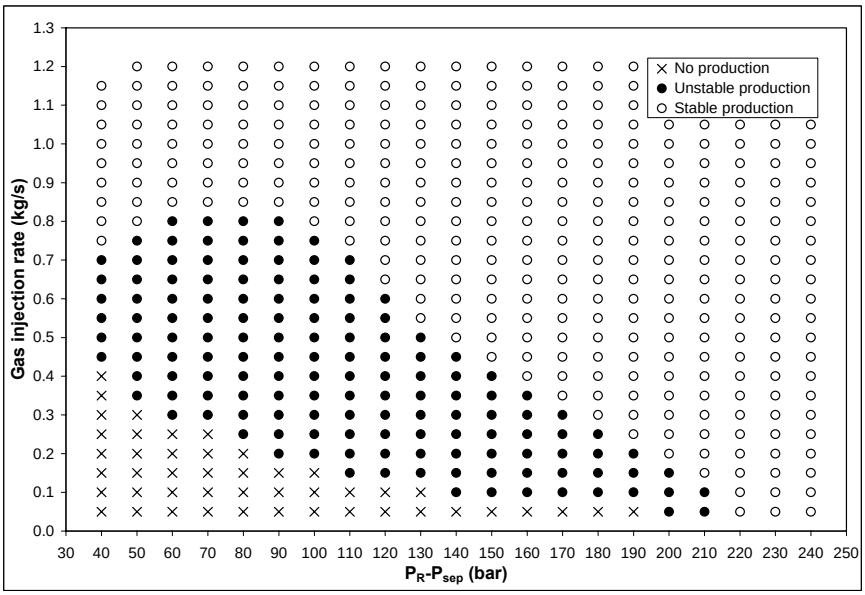

Figure 6-10 Map of density-wave instability.

When the gas rate is too low to lift the liquid, gas phase will flow through the liquid and release at the top of the well. The liquid level may be oscillating within the tubing, but no production is observed at the wellhead. This kind of phenomenon is marked by the cross sign on the stability map.

If increasing the gas rate to a certain level, a burst-like liquid production is observed. The well starts to produce unstably. Figure 6-11 gives the out-looking of the production at this situation. Long periodic time is its typical characteristic. If continue increasing the gas rate, both the frequency and the amplitude of the oscillation will increase. This is shown in Figure 6-12. The oscillation will become more harmonic-like if the gas rate is increased further

as shown in Figure 6-13. The reservoir pressure for all the cases in the Figure 6-11~6-13 is 90 bara. All the unstable cases are marked by black dots on the map.

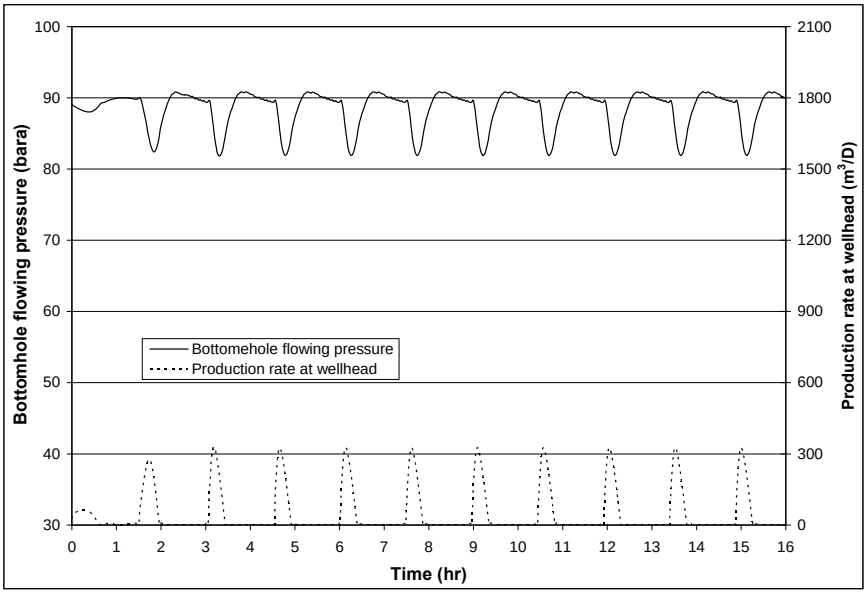

Figure 6-11 Density-wave oscillation with air injection rate of 0.25 kg/s.

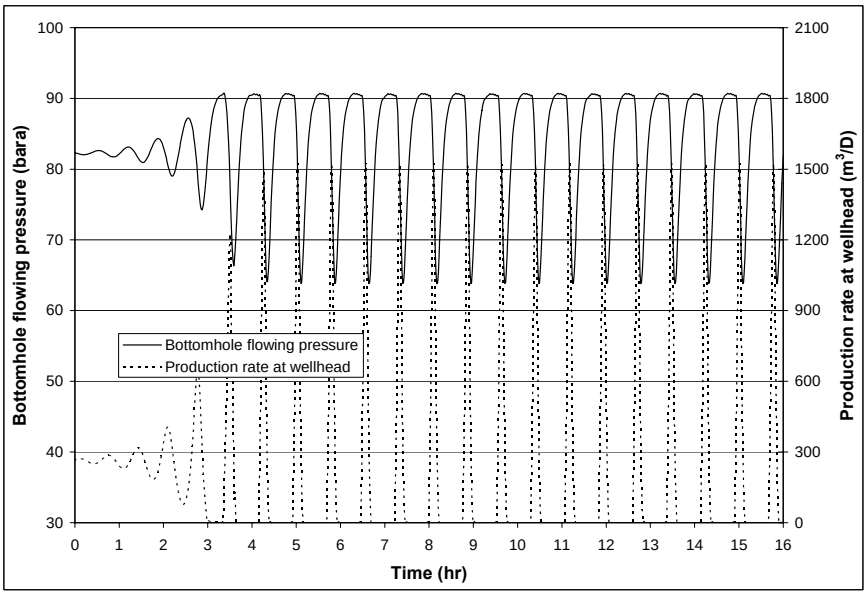

Figure 6-12 Density-wave oscillation with air injection rate of 0.6 kg/s.

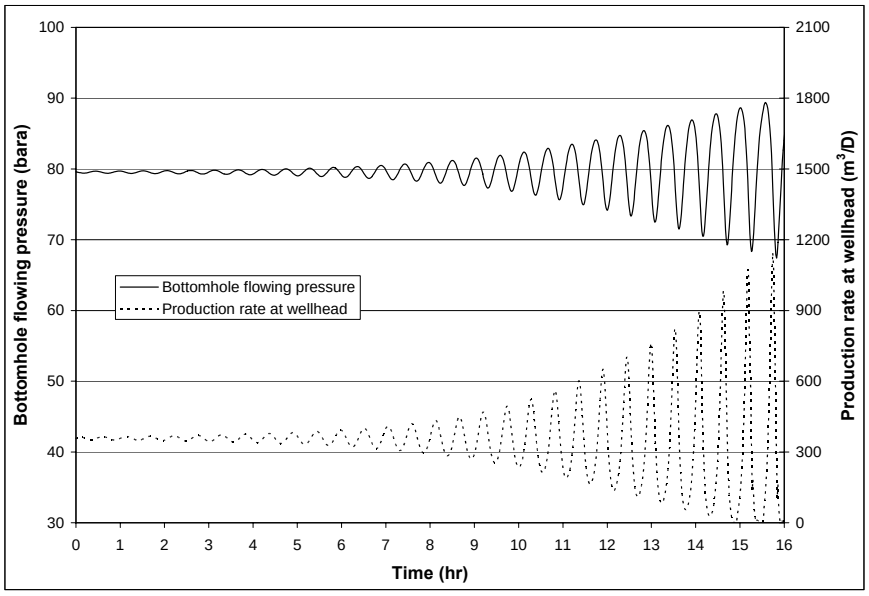

Figure 6-13 Density-wave oscillation with air injection rate of 0.8 kg/s.

The well will be stable if gas rate is high enough. The stable region is mainly located in the upper right direction on the map. All the stable cases are market with small circles.

If compare the stability maps from linear analysis and dynamic simulation, we find that the unstable regime obtained from simulation is smaller than that of linear analysis. This is mainly due to the rough two-phase flow model used in the linear analysis. The dynamic simulation results should be highlighted in terms of accuracy. But basically, the result from linear analysis is in accordance with simulation result if we emphasize the qualitative nature of the investigation.

6.4.2 Characterizing density-wave instability

Parametric study is also carried out by using OLGA®2000 simulation to characterize the density-wave instability. As did in the linear stability analysis, the study here aims at investigating the change of the stability map due to the change of different system parameters such as the productivity index, the tubing diameter, the system pressure, the well depth, and the well head choke opening.

However, unlike in the linear analysis where a neutral stability can be identified, it is difficult to find the exact boundary between stable and unstable regimes from numerical simulations. In this study, the boundary is approximately given by the upper unstable points in the stability map like in

Figure 6-10. Therefore the boundary has a maximum error of ±0.1 kg/s since this is gas rate step when parametric study is done.

Figure 6-14~18 give the results of the characterization. If comparing with the results from linear analysis, the same conclusions can be made in terms of the parametric trend.

Static choking effect on stability, which is not included in linear analysis, is also studied here from the simulation. Figure 6-18 gives the results of the simulation. Since the choke has the same diameter of tubing, the opening of the choke is in fact relative to the cross section area of tubing. If it is 100% opening, then there is no difference with that the choke is removed.

There is no clear change in the stability map if reduce the choke opening from 100% to 50%. If continue to reduce the opening to 10%, the unstable area will be slightly reduced. So, it is not very effective to use static choking to stabilize the density-wave flow oscillations. This attributes to two reasons.

First, when strong density-wave instability occurs, the flow rate is too low to get enough friction from the choking for stabilization. Second, unlike the inflow restriction, choking effect itself is not in phase with the flow variation at the bottom of the well. So, it would not be as effective as increasing the inflow restriction even though it can add more restrictions. This is in accordance with the conclusion obtained from the analysis in Chapter 4.

Based on the results here, choking should be concisely used in stabilizing density-wave oscillation since one may not see clear effect from it and take the risk of killing the well by choking too much.

Besides, both linear analysis and numerical simulations conclude that the density-wave instability seems not be able to happen when the system pressure drop is higher than the hydrostatic head assuming that tubing is filled with water. This condition is expressed by inequality 5-111.

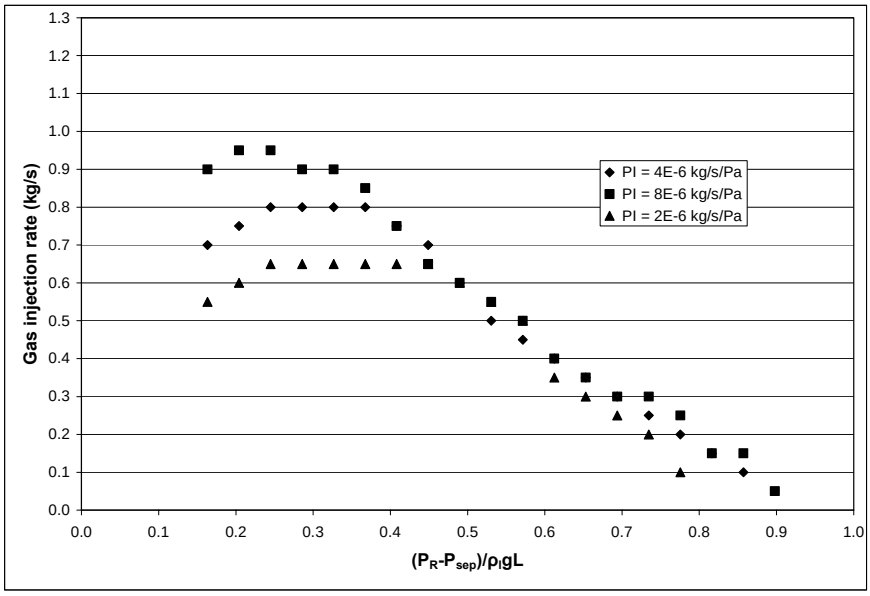

Figure 6-14 Effect of productivity index.

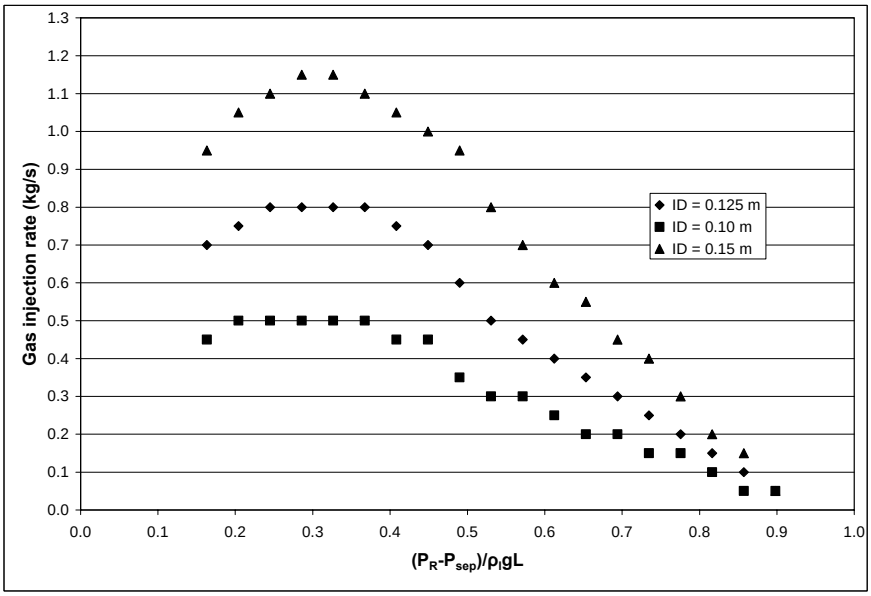

Figure 6-15 Effect of tubing diameter.

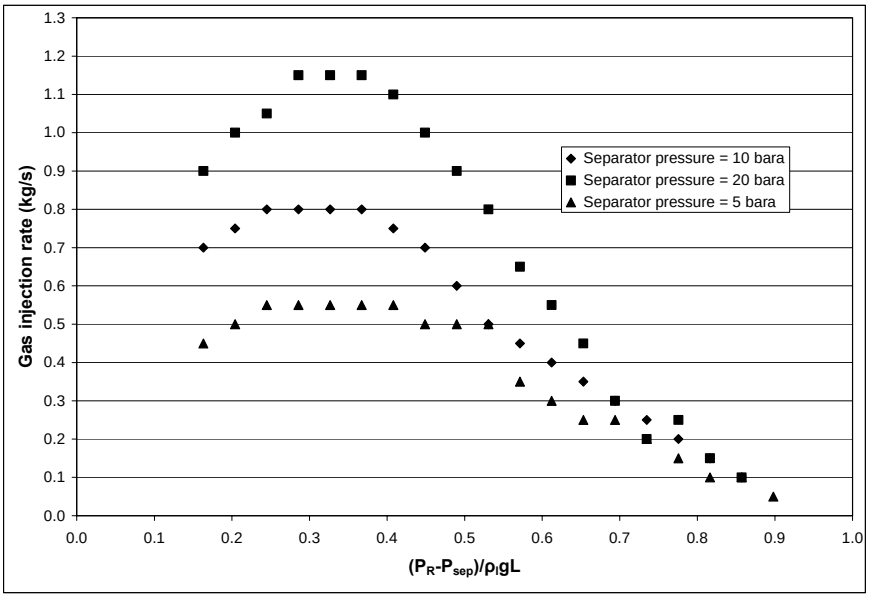

Figure 6-16 Effect of system pressure.

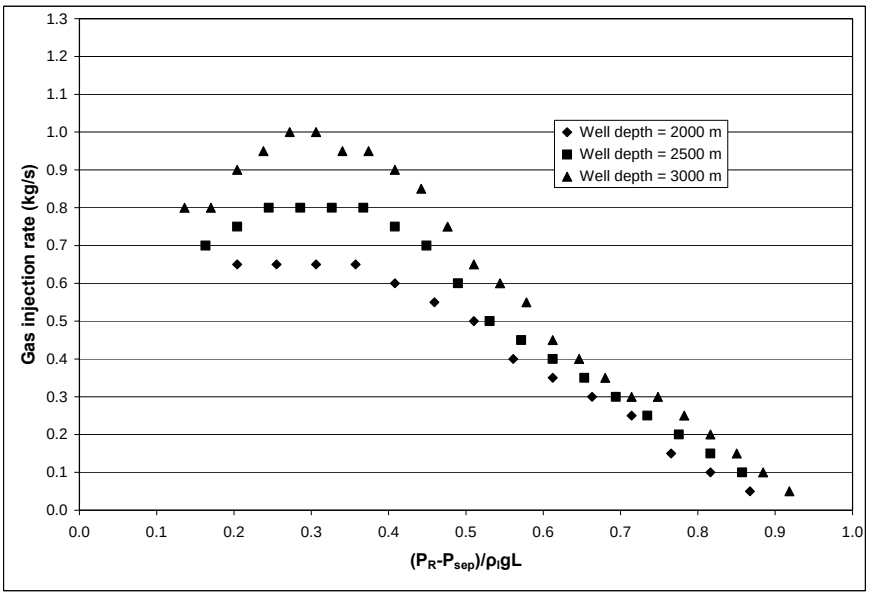

Figure 6-17 Effect of well depth.

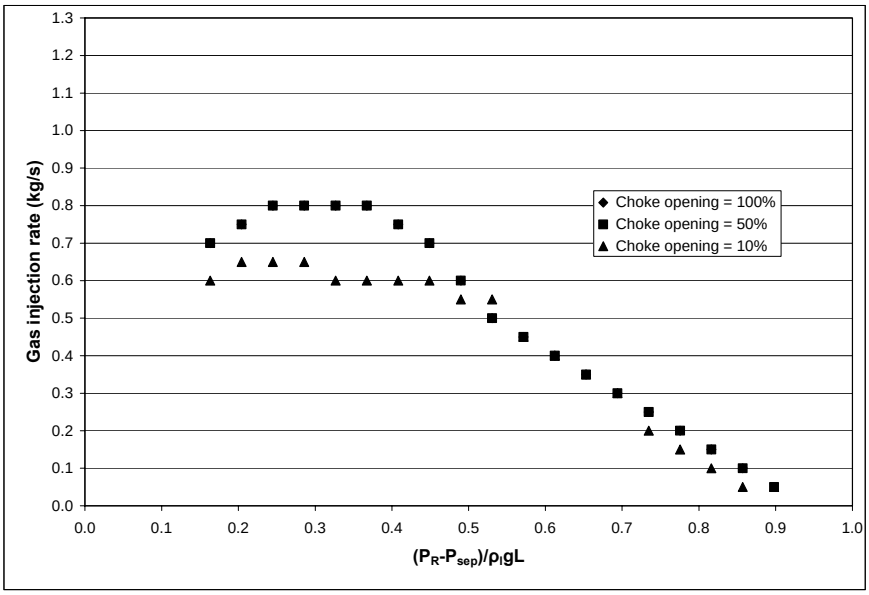

Figure 6-18 Effect of well head choking.

6.5 Production loss due to gas-lift instabilities

Besides the hazard to operation safety and smoothness, the flow and pressure fluctuation due to gas-lift instabilities can also result in production loss. Both casing heading and density-wave oscillation cause flow rate change compared with steady-state predictions.

For the casing heading, Figure 6-19 compares the daily average production rate of unstable gas-lift with the steady-state predictions. The plots are obtained from simulations based on the base case settings. The black line is the typical lift performance curve that is based on steady-state calculation. The red line is the regression curve of the dynamic simulation results. At low gas injection rate, due to casing heading, the real production rate is much lower than that predicted from steady-state calculation.

If normalize the dynamic results to the steady-state values, Figure 6-20 is obtained. It is clearer in showing the production loss due to casing heading. For example, when gas injection rate is 0.6 kg/s, the well will produce 20% lower than predicted.

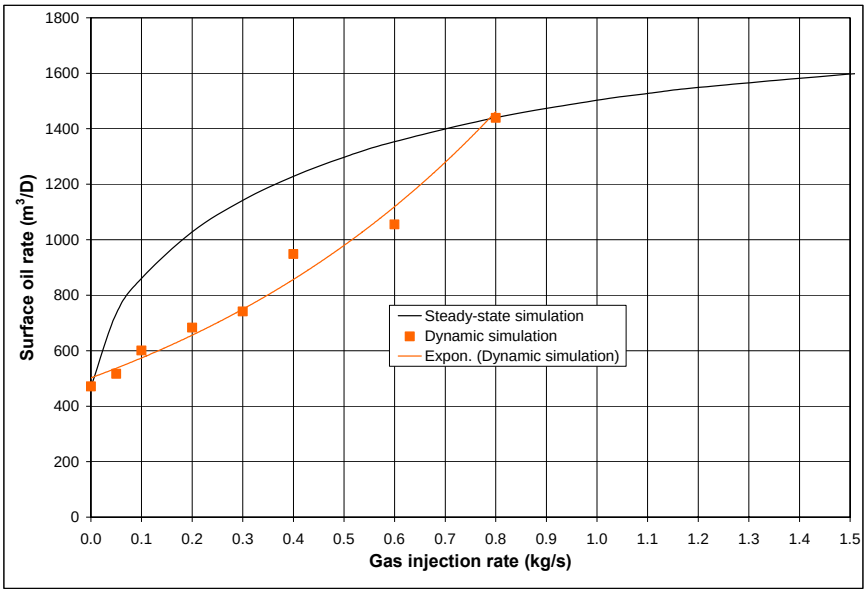

Figure 6-19 Lift performance relationship: comparison between steady-sate calculation and dynamic simulation results.

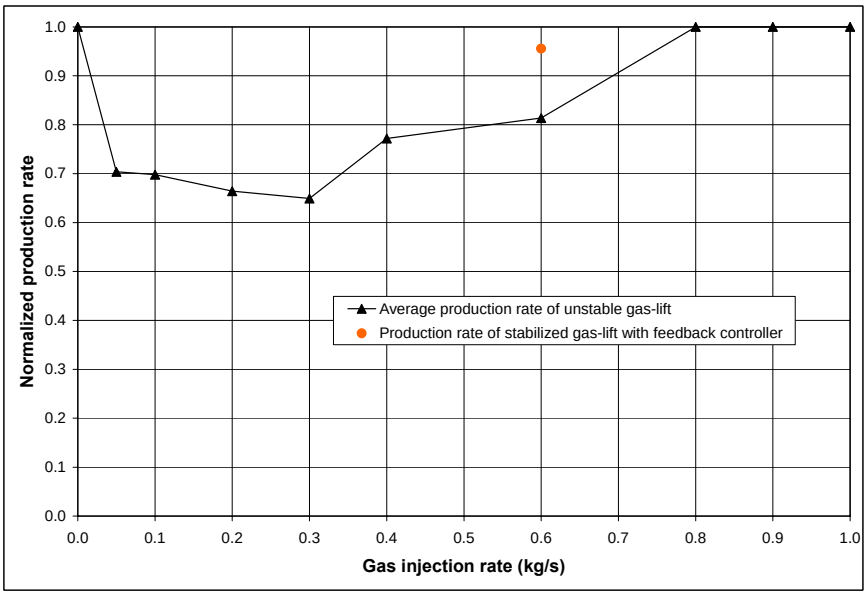

Figure 6-20 Production loss due to casing heading.

The similar can also be observed from density-wave oscillations. A series simulation is carried out along the 90 bara reservoir pressure line in the Figure 6-10 in order to make a similar comparison as did for casing heading. The results are given by Figure 6-21.

The interesting observation here is that density-wave oscillation not only can reduce the production but also can increase the production when the gas rate is very low. For example, according to the simulation result, the well can produce as twice as its steady-state prediction when the well just steps over the threshold from “no production” to “unstable production”.

However, in most situations, the range of gas rate that can increase production is not of interest in practical gas-lift operations. For the high gas rate, production loss rather than gain is often observed. According to the plot, up to 24% production reduction can occur at a certain gas injection rate.

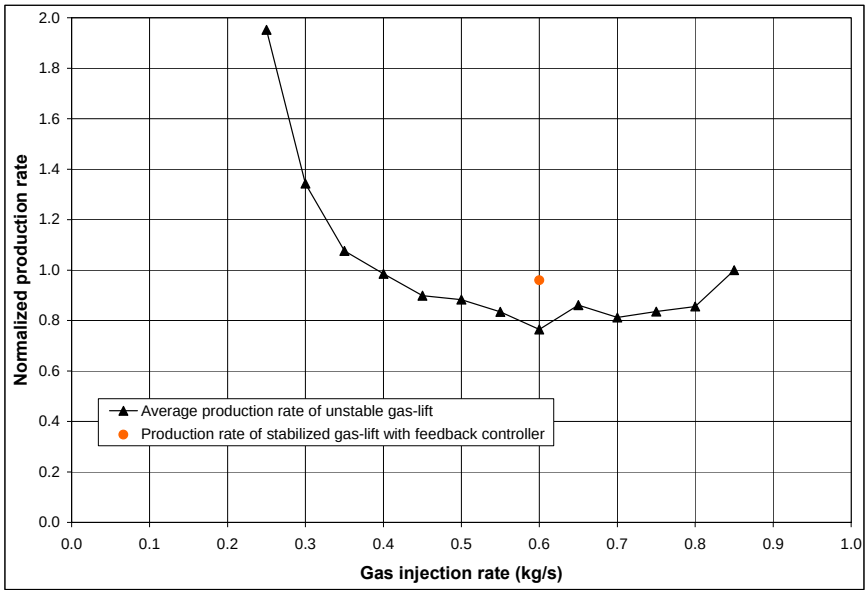

Figure 6-21 Production loss due to density-wave oscillation.

Because of the production loss, field tail production has to be prolonged in order to get the same recovery. This will tremendously increase the cost of operation. So, whenever gas-lift instability is identified, the production loss that comes along with it must also be investigated. But in practice, this is often not mentioned, particularly when the receiving facility can handle the flow fluctuations. The notion should be emphasized that production loss is the norm for oscillating wells and the instabilities have to be seriously treated even though they may not cause any operation problem sometimes.

6.6 Taming unstable gas-lift wells by active control

Effect of choking has been investigated for both casing heading and density-wave oscillation. By the simulation, it is confirmed that static choking can stabilize the well. But now the question is how much production is going to lose by static choking.

Taking the casing heading as an example, the normalized production rates from steady-state calculation and dynamic simulation are plotted against choke opening for comparison. Figure 6-22 shows the two curves. When choke is fully opened, compared with stable production, unstable production will lose 20% of production. To make the production stable, which means the dynamic simulation result is almost the same as steady-state prediction, the choke opening has to be reduced down to 20% in the example showing in Figure 6-22. The production loss is about 25%, which is 5% more than the case with fully opened choke. So, static choking stabilizes the unstable well flow at the cost of losing production.

Even though sometimes this additional production loss due to choking is not very big and some indoor experiment even shows that there could be a lit bit increase in production after the well is choked, static choking can not fill up the gap between the ideal production rate and the real production rate, which is a result of unstable well flow. So, static choking is only a method of stabilization, but not a method of optimization.

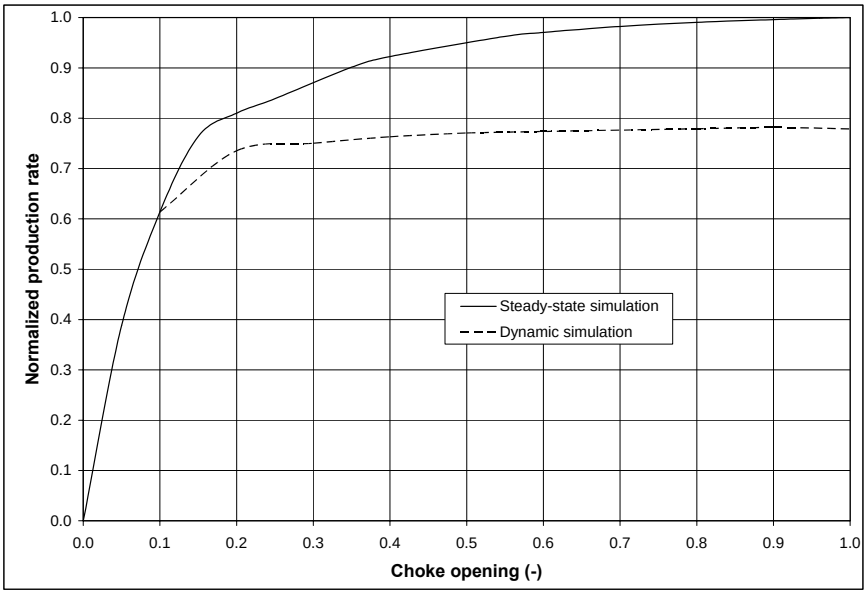

Figure 6-22 Effect of static choking on production rate.

Recently, active control has emerged as a cost-effective option for stabilizing gas-lift wells. The following simulation will demonstrate that the feedback controller not only can stabilize the well, but also reduce the production loss, which is not achievable by static choking.

A simple feedback control structure is tested in this dissertation, in which bottomhole flowing pressure is sensed to control the opening of production choke. PI controller is selected to carry out the task. The controller settings are determined by following steps.

First, the optimum setting of the bottomhole flowing pressure is determined from steady-state simulation. In fact, the setting should be a lit bit higher than the steady-state prediction. Then the integration time is selected proportion to the period time of the oscillation. A small gain value is determined so that stability can be achieved. The gain value is adjusted by trial-and-error so that the setting of bottomhole flowing pressure is as close as possible to the steady-state prediction and a quick stabilization can be realized.

Control casing heading. Figure 6-23 and 6-24 give the results of applying feedback control to the base case of casing heading shown as in Figure 6-1. The simulation is initiated by steady-state calculation, and then the limit cycle is developed. At the beginning, the choke opening is 96%. The controller is started after 8 hours from the beginning of the simulation. Figure 6-23 shows the variation of choke opening before and after controller is started. Figure 6-24 gives the change of pressure and production rate. The well is stabilized after about 3 hours after controller is started. The choke opening is about 88%.

The production rate is stabilized at the level that is very close to its steady-state prediction indicated in the figure at time 0. In fact, normalized production rate is about 95% marked by a red dot in Figure 6-20, which is much higher than that without using feedback control. The original rate is only 78%, so 17% production is saved.

If keep the choke opening determined by the controller and switch off the controller, the well will be unstable right away as shown in Figure 6-25. This demonstrates that it is the active choking rather than static choking is in functioning.

The PI controller parameters are:

- Gain K_p: 8E-6
- Integral time τ_i: 3150 s

The set point of bottomhole flowing pressure is 9850000 Pa.

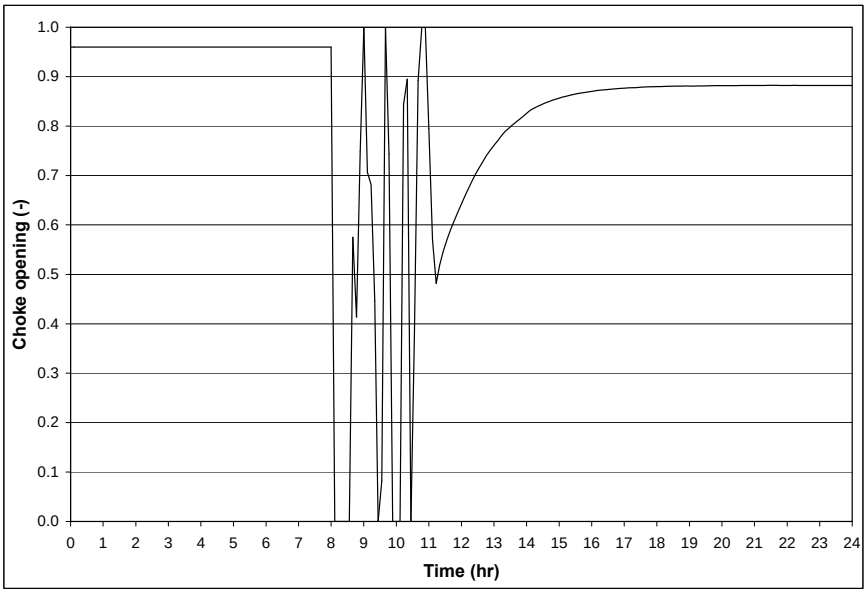

Figure 6-23 Variation of choke opening.

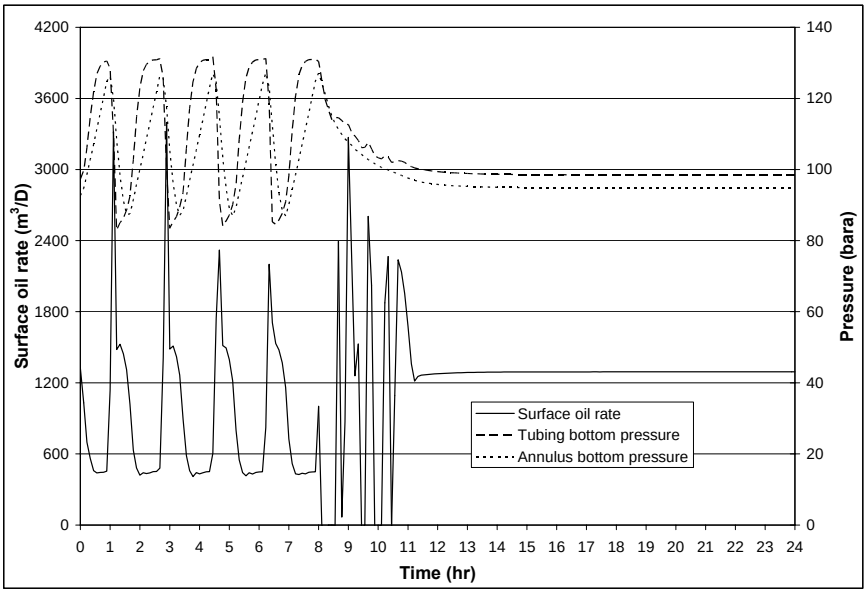

Figure 6-24 Variation of pressure and production rate before and after controller is started.

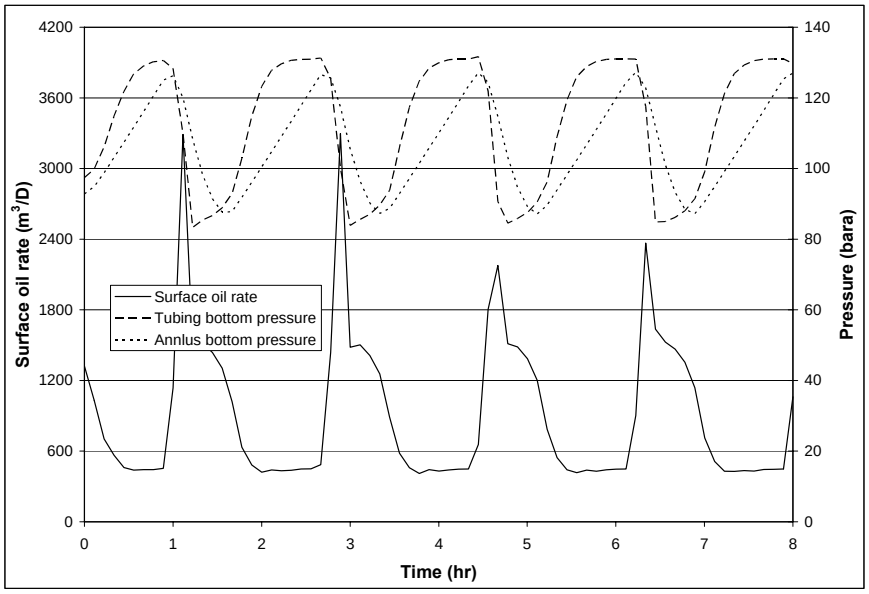

Figure 6-25 Return to limit cycle when controller is switched off.

Control density-wave oscillation. Figure 6-26 and 6-27 show the results of applying feedback control to the case given by Figure 6-12. For control purpose, the choke diameter is selected as only half of the tubing diameter. Even so, when it is fully opened, the observed oscillation is quite close to the situation in figure 12, in which no choke is installed. The reason for this has been discussed in section 6.4.2.

The controller is started after 5.5 hours from the beginning of the simulation. Figure 6-26 shows the choke opening variation. It finally approaches 40% when the well is stabilized 10 hours later after the controller is started. Figure 6-27 shows that the stabilized production rate is also quite close to steady-state prediction when choke is fully opened. In fact the normalized rate is about 96% after stabilization by feedback control. This is marked in Figure 6-21 by a red dot. Comparing with the case without using feedback control, in which the normalized rate is only 76%, 20% production is saved.

To demonstrate the function of feedback controller, keep the choke opening unchanged and switch back to manual control, the well is unstable again as shown in Figure 6-28.

The PI controller parameters are:

- Gain K_p: 1E-6
- Integral time τ_i: 2800 s

The set point of bottomhole flowing pressure is 8260000 Pa.

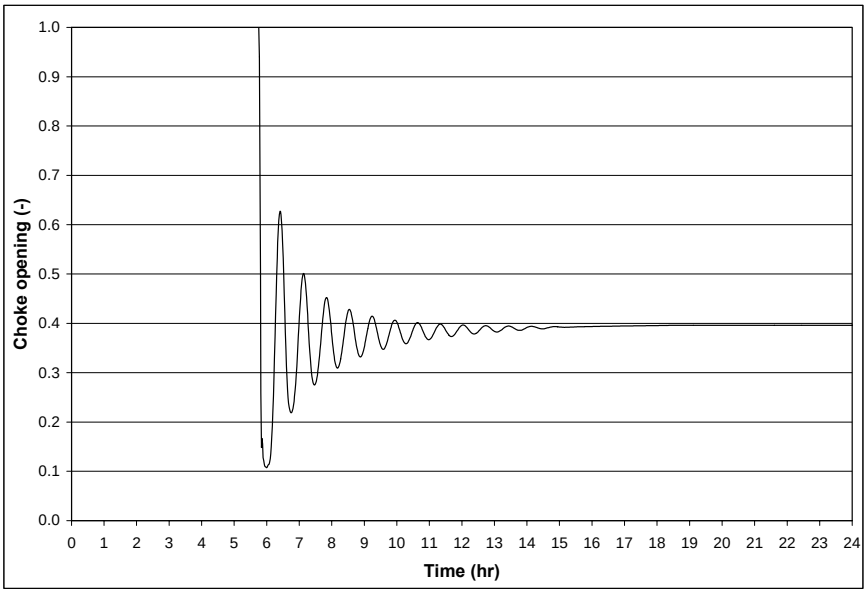

Figure 6-26 Variation of choke opening before and after controller is started.

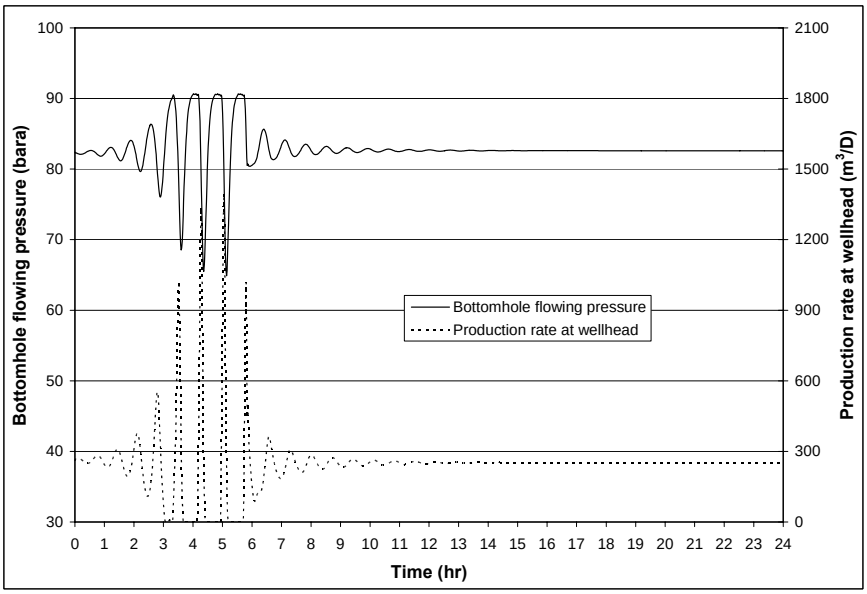

Figure 6-27 Variation of pressure and production rate before and after controller is started.

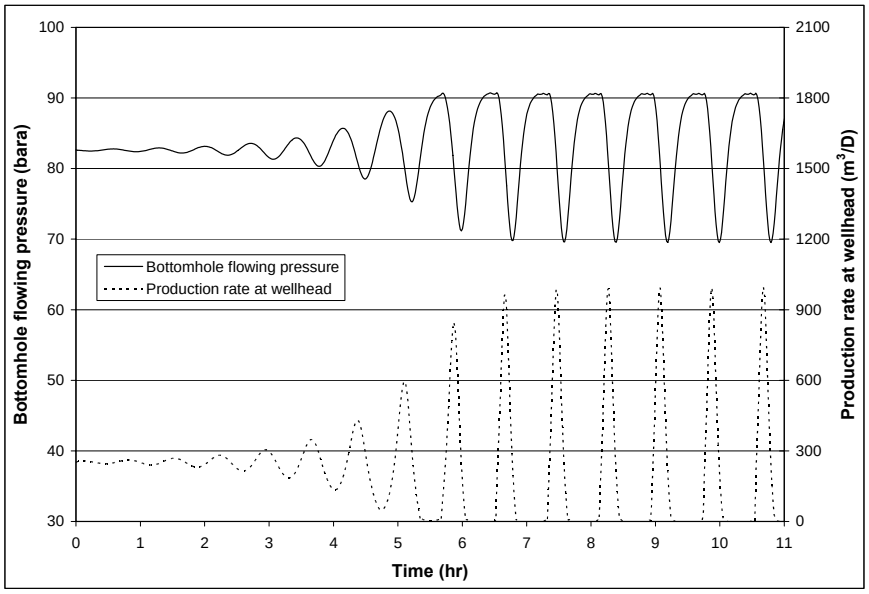

Figure 6-28 Return to limit cycle when controller is switched off.

6.7 Summary

1. Casing heading is simulated in this chapter. The results agree very well with common knowledge based on practical operation experience. Furthermore, more detailed discussion is made based on simulation results to explain how casing heading is eliminated by some approaches.

2. Gas robbing is a phenomenon based on excursive static instability. It is also demonstrated by dynamic simulation here. Gas robbing happens when flow in at least one tubing is gravity dominant, and the other tubing can absorb more lifting gas to compensate the pressure increase in the annulus.

3. Density-wave oscillation is mainly investigated in this chapter. Dynamic simulation results show that it is possible for density-wave oscillation to occur in gas-lift wells when reservoir pressure is depleted, particularly when the well loses the capability of natural flowing. The simulation results give similar stability map and parametric trend compared with the linear analysis results from last chapter. Furthermore, the simulation demonstrates the three phenomenon of applying gas lift to depleted wells, which are labelled as “no production”, “unstable production” and “stable production”.

4. Dynamic simulation also shows that static choking is an effective approach in stabilizing casing heading. It is not as effective as in stabilizing casing heading when used to smooth density-wave oscillation. This is due to that pressure drop across choke is not in phase with the flow variation at the bottom of the well.

5. Production loss is the norm of unstable production compared with steady-state predictions. Dynamic simulation demonstrates that both casing heading and density-wave oscillation can result in an inefficient use of lifting gas and a significant loss of production.

6. Static choking stabilizes the well at the cost of reduced production. This can be improved by dynamic choking, which is actuated by a feedback controller by sensing the downhole pressure. This control structure is tested for both casing heading and density-wave oscillation. Simulation results show that both two instability can be eliminated and a production rate close to steady-state prediction is obtained.

7 CONCLUSIONS AND FURTHER WORK

7.1 Conclusions

The conclusions of this dissertation are summarized as below:

1. Macroscopic instabilities can be classified into two categories based on the system response to the flow perturbations around its steady-state solutions. If the system has a positive feedback to the perturbation, then the instability is called static, on the other hand, if the system has a negative feedback to the perturbation, then it is called dynamic. The static instability in oil production system has been widely investigated. However the dynamic instability is not well addressed, particularly for the flow in oil wells.

2. Gas-lift casing heading is a static-instability based oscillation. The characteristics of casing heading have been demonstrated by both theoretical analysis and numerical simulations. General speaking, increasing gas injection, wellhead choking, well stimulation, and using smaller orifice can increase stability. Increasing separator pressure has no significant improvement to casing heading. Gas robbing in dual gas-lift is another example of static instability. Instead of oscillating, solution excursion is often observed when gas robbing occurs. The excursion process is also demonstrated by dynamic simulation.

3. Density-wave oscillation is a dynamic instability. Its basic features in an incompressible vertical system have been analytically investigated. Results show that flow restriction from reservoir to wellbore and friction losses along tubing are the main damping factors of density-wave oscillation. On the other hand, pressure drop due to hydrostatic head is the main exciting factor. The restriction of outlet choke can give either damping or exciting effect depending on the magnitude of the bottomhole inflow restrictions. If the restriction is large, outlet choking tends to give stabilizing effect, and vice versa. This explains why outlet choking destabilizes the two-phase flow in the vertical cooling channels in the nuclear reactors, where the open inlets of the channels are almost without restrictions; one the contrary it stabilizes the two-phase flow in the gas-lift wells where the inlet restriction at the bottom of the well are several orders of magnitude larger than that of cooling channels. Analysis also shows that

compressibility is a necessary condition for density-wave oscillation to occur in a vertical system whose inlet restriction is in the same order of magnitude of normal oil wells.

4. Both linear analysis and numerical simulations show that density-wave oscillation can occur in gas-lift wells, particularly those wells producing depleted reservoirs. Parametric studies from both analysis and simulations show that increasing reservoir pressure and gas injection rate increases stability, but increasing tubing diameter, PI and system pressure decreases stability. The instability may occur only when

$$\frac{P_R - P_{sep}}{\rho_l g L} < 1$$

5. Production loss is the norm of unstable gas-lift. Conventional methods can only stabilize the well by more or less sacrifice the optimum. Active control, which emerges as an alternative to conventional stabilizing method, can stabilize the well with increased production (compared with unstable production). This is also demonstrated by the simulations in this dissertation.

7.2 Further work

One of the main contributions of this dissertation is that, it shows the possibility for density-wave oscillation to occur in gas-lift wells. According to literature survey, this is the first time for the instability being documented relevant to oil wells. In this respect, the investigation in this dissertation is just a start in digging the more details of the instability background and its appearance in oil wells. Obviously, a lot of more work need to be done in order to show gas-lift personnel a more complete picture.

1. As discussed in the dissertation, density-wave oscillation is a dynamic instability that is normally impossible to foresee from node analysis. The various appearance and many possibilities related to the instability have to be investigated by dynamic simulation. For example, what might happen in a horizontal gas-lift wells where an accumulation of associated gas exists in the far end of U-shaped horizontal section? How does the gas pocket will affect the occurrence and appearance of density-wave oscillation? Many of such concrete scenarios have to be simulated in order to get a whole picture of the instability.

2. As a necessary condition for the density-wave instability to occur, the well has to lose its natural flowing capability. This has been verified by both linear analysis and numerical simulation. However the physical explanation of this condition is not clear yet. More experimental work should be done in order to testify this condition and find the right explanation

3. In this dissertation, the function of active control by simple feedback control structure has been demonstrated. However, in order to get an effective and robust control design to tame density-wave oscillation, more research work has to be done. For example, one can work on a reduced or simplified model to design the control structure and estimate the controller parameter settings. In fact, a lot of such kind research work has been done or is undergoing for the casing heading problem. It is expected that similar research effort will be given to the density-wave oscillation problem.

REFERENCES

Alhanati, F.J.S., Schmidt, Z., Doty, D.R. and Lageref, D.D.: “Continuous Gas-Lift Instability: Diagnosis, Criteria, and Solutions”, SPE 26554, presented at the 68th Annual Technical Conference and Exhibition Held in Houston, TX, 3-6 October 1993.

Alimonti, C. and Galardini, D., “The modelling of an air-lift pump for the design of its control system”, European Journal Mech. Eng., Vol 37, 3, 191-197, June 1992.

Alimonti, C., Galardini, D., Gorez, R. and Balestrino, A., “A Study of the Control of An Air-Lift Pump”, Mathematics of the Analysis and Design of Process Control, IMACS, 1992.

Apazidis, N., “Influence of Bubble Expansion and Relative Velocity on the Performance and Stability of an Airlift Pump”, Int. J. Multiphase Flow 11, 459-479, 1985.

Asheim, H.: “Analytical Solution of Dynamic Inflow Performance”, SPE 63307, presented at the 2000 SPE Annual Technical Conference and Exhibition held in Dallas, Texas, 1-4 October 2000.

Asheim, H.: “Criteria for Gas Lift Stability”, JPT (November 1988), pp1452-1456.

Asheim, H.: “Verification of Transient, Multi-Phase Flow Simulation for Gas Lift Applications”, SPE 56659, presented at the 1999 SPE Annual Technical Conference and Exhibition held in Houston, Texas, 3-6 October 1999.

Avest, D.ter and Oudeman, P.: “A Dynamic Simulator to Analyze and Remedy Gas Lift Problems”, SPE 30639, presented at the SPE Annual Technical Conference and Exhibition held in Dallas, Texas, 22-25 October 1995.

Bertuzzi, A.F., Welchon, J.K. and Poettmann, F.H.: “Description and Analysis of An Efficient Continuous-Flow Gas-Lift Installation”, presented at the Pacific Petroleum Chapter Fall Meeting in Los Angeles, Calif., Oct. 1-2, 1953.

Bendiksen, K.H., Malnes, D., Moe, R., Nuland, S.: ”The Dynamic Two-Fluid Model OLGA: Theory and Application”, SPE-PE, (May 1991) 171.

Blick, E.F. and Boone, L.: “Stabilization of Naturally Flowing Oil Wells Using Feedback Control”, SPE 15096, presented at the 56th California Regional Meeting of SPE held in Oakland, CA, 2-4 April 1986.

Blick, E.E., Enga, P.N. and Lind, P.C.: “Theoretical Stability Analysis of Flowing Oil Wells and Gas-lift Wells”, SPE Production Engineering (November 1988), pp504-514.

Blick, E.F. and Nelson, A.B.: “Root Locus Stability Analysis of Flowing Oil Well Feedback Controller”, SPE 18874, presented at the SPE Production Operation Symposium held in Oklahoma City, OK, 13-14 March 1989.

Boure, J.A., Bergles, A.E. and Tong, L.S.: “Review of Two-Phase Flow Instability”, Nuclear Engineering and Design 25 (1973) 165-192.

Buitrago, S., Rodriguez, E. and Espin, D.: “Global Optimization Techniques in Gas Allocation for Continuous Flow Gas Lift Systems”, SPE 35616, presented at the Gas Technology Conference held in Calgary, Alberta, Canada 28 April - 1 May1996.

Capucci, E.C. and Serra, K.V.: “Transient Aspect of Unloading Oil Wells Through Gas-Lift Valves”, SPE 22791, presented at the 66th SPE Annual Technical Conference and Exhibition held in Dallas, TX, 6-9 October 1991.

Caralp, L., Defaye, G. and Vidal, C.: “Dynamic behaviour of a gas-lift simulator”, Computers & Chemical Engineering, v17, Suppl, Oct, 1993, pp355-360.

Clegg, J.D.: “Discussion of Economic Approach to Oil Production and Gas Allocation in Continuous Gas Lift”, J. Pet. Tech., pp301-302 (February 1982).

de Cachard, F. and Delhaye, J.M., “Stability of Small Diameter Airlift Pumps”, Int. J. Multiphase Flow 24, 17-34, 1998.

Delhaye, J.M., Giot, M. and Riethmuller, M.L.: ”Thermohydraulics of Two-Phase Systems for Industry Design and Nuclear Engineering”, Hemisphere Publishing Corporation,

der Kinderen, W.J.G.J., Dunham, C.L. and Poulisse, H,N,J.: “Real-Time Artificial Lift Optimization”, SPE 49463, presented at the 8th Abu Dhabi International Petroleum Exhibition and Conference held in Abu Dhabi, U:A:E, 11-14 October 1998.

Dvergsnes, S.: “Modelling and Control of Gas-Lifted Oil Wells”, Diploma Thesis, Department of Engineering Cybernetics, Norwegian Univ. of Science and Technology, 1999.

Eikrem, G.O., Foss, B., Imsland, L., Hu, B. and Golan, M.: ”Stabilization of Gas Lifted Wells”, 2002 IFAC.

Everitt, T.A.: “Gas-Lift Optimization in a Large, Mature GOM Field”, SPE 28466, presented at the SPE 69th Annual Technical Conference and Exhibition held in New Orleans, LA, 25 - 28 September 1994.

Faustinelli, J., Bermudes, G. and Cuauro, A., “A Solution to Instability Problems in Continuous Gas-lift Wells Offshore Lake Maracaibo”, SPE 53959, presented at the 1999 SPE Latin American Petroleum Engineering Conference, Caracas, Venezuela 21-23 Aprill 1999.

Fitremann, J.M. And Vedrines, P.: “Non steady gas-liquid flow in pipes and gas-lifted wells”, 2nd International Conference on Multiphase Flow, London, England, 19-21 June 1985.

Gamaud, F., Casagrande, M., Fouillout, C. and Lemetayer, P.: “New Field Methods for a Maximum Lift Gas Efficiency Through Stability”, SPE 35555, presented at the European Production Operations Conference and Exhibition held in Stavanger, Norway, 16-17 April 1996.

Gilbert, W.E.: “Flowing and Gas-lift Well Perfromance”, presented at the spring meeting of the Pacific Coast District, Division of Production, American Petroleum Institute, May 1954.

Golan, M. and Whitson, C.H.: Well Performance, 2nd Edition, P T R Prentice Hall, New Jersey (1991).

Grupping, A.W., Luca, C.W.F. and Vermulen, F.D.: “Continuous Flow Gas Lift. Heading Action Analysed for Stabilization”, Oil & Gas Journal, pp47-51, July 23, 1984.

Grupping, A.W., Luca, C.W.F. and Vermulen, F.D.: “Continuous Flow Gas Lift. These Methods Can Eliminate or Control Annulus Heading”, Oil & Gas Journal, pp186-192, July 30, 1984.

Hasan, A.R. and Kabir, C.S.: “Discussion of Transient Dynamic Characteristics of the Gas-Lift Unloading Process”, SPE 57711, SPE Journal 4 (3), pp302-303, 1999

Hjalmars, S., “The Origin of Instability in Airlift Pumps”, J. Appl. Mech. 399-404, June 1973.

Hu, B.: Description of First Principle Gas Lift Model of ABB, Technical Report, Norwegian Univ. of Science and Technology, 1999.

Jansen, B., Dalsmo, M., Nøkleberg, L., Harvre, K., Kristiansen, V. and Lemetayer, P.: “Automatic Control of Unloading Lifted Wells”, SPE 56832, presented at the 1999 SPE Annual Technical Conference and Exhibition held in Houston, Texas, 3-6 October 1999.

Kakac, S. and Veziroglu, T.N.: “A Review of Two-Phase Flow Instability”, Univerisy of Miami, Coral Gables, Florida, USA.

Khalil, M.F., Elshorbagy, K.A., Kassab, S.Z. and Fahmy, R.I., “Effect of Air Injection Method on the Performance of An Air Lift Pump”, International Journal of Heat and Fluid Flow 20, 598-604, 1999.

Lemetayer, P. and Miret, P.M.: “Tool of the 90's To Optimize Gas-Lift Efficiency in the Gonelle Field, Gabon”, SPE 23089, presented at the Offshore Europe Conference held in Aberdeen, 3-6 September 1991.

Scandpower Petroleum Technology AS: OLGA2000 User Manual, 2000.

Sekoguchi, K., Matsumara, K. And Fukano, K.: “Characteristics of Flow Fluctuation in Natural Circulation Airlift Pumps”, Bull, JSME 24, 1960-1966, 1981.

Shampine, L.F., Kierzenka, J. and Reichelt, M.W.: “Solving Boundary Value Problems for Ordinary Differential Equations in Matlab with bvp4c”, The Mathworks, Inc. 26th October 2000.

Stepan, G.: “Retarded Dynamic Systems: Stability and Characteristic Function”, Longman Scientific & Technical, 1989.

Svanholm, K.: “An Analysis of Density Wave Instabilities by Means of Graphical Computations”, 2nd edition, IFE, 1989.

Tang, Y.: “Transient Dynamic Characteristics of Gas-Lift Unloading”, M.Sc. Thesis, The Univ. of Tulsa. (1998).

Tinoco, M.M.: “Validation and Improvement of Stability Criteria for Gas-Lift Wells”, M.Sc. Thesis, The Univ. of Tulsa. (1998).

Tokar, T., Schmidt, Z. and Tuckness, C.: “New Gas Lift Valve Design Stabilizes Injection Rates: Case Studies”, SPE 36597, presented at the 1996 SPE Annual Technical Conference and Exhibition held in Denver, Colorado, 6-9 October 1996.

Tore, A.J., Sapic, B., Schmidt, Z., Blais, R.N., Doty, D.R. and Brill, J.P.: “Casing heading in Flowing Oil Wells”, SPE 13801, presented at Production Operations Symposium, Oklahoma City, Oklahoma, March 10-12, 1985.

Tramba, A., Topalidou, A., Kastrinakis, E.G., Nychas, S.G., Francois, P. and Scrivener, O., “Visual Study of an Airlift Pumps Operating at low Submergence Ratios”, The Canad. J. Chem. Eng. 73, October 1995.

Xu, Z.G. and Golan, M.: “Criteria for Operation Stability of Gas Lift”, SPE 19362, unsolicited, June 9, 1989.

Zenz, F:A:, “Explore the Potential of Air-Lift Pumps and Multiphase”, Chemical Engineering Progress, 51-66, August 1993.

APPENDICES

A. Reservoir dynamical inflow properties

In this dissertation, a steady-state linear inflow performance relationship is used as the boundary at the bottom of the well, by which the dynamic properties of reservoir inflow performance are ignored. However this simplification is not always acceptable when studying transient flow in the wells.

The near wellbore flow dynamics is discussed in this appendix. The purpose of the discussion is to figure out when we can use the steady-state inflow performance relationship to approximate the dynamic inflow performance.

Nomenclature used in the discussion is listed as below

c	compressibility (1/Pa)
h	thickness of completed interval (m)
J	productivity index (m^3/s/Pa)
k	permeability (m^2)
p	pressure (Pa)
p_e	drainage boundary pressure (Pa)
p_{wf}	well bottomhole flowing pressure (Pa)
q	flow rate (m^3/s)
r	radial distance (m)
r_e	drainage radius (m)
r_w	wellbore radius (m)
t	time (s)
ϕ	porosity (-)
μ	viscosity (Pas)

The dynamic behaviour of compressible reservoirs is described by pressure diffusivity and flow equations. The radial diffusivity equation for slightly compressible reservoirs reads

$$\frac{\partial^2 p}{\partial r^2} + \frac{1}{r}\frac{\partial p}{\partial r} = \frac{c\phi\mu}{k}\frac{\partial p}{\partial t} \qquad \textbf{A-1}$$

The flow rate is proportional to the reservoir pressure gradient, as quantified by Darcy's equation

$$q = -\frac{2\pi kh}{\mu} r \frac{\partial p}{\partial r} \qquad \textbf{A-2}$$

By integration between the wellbore and the drainage boundary, we get

$$q = J(p_e - p_{wf}) \qquad \textbf{A-3}$$

where

$$J = \frac{2\pi kh}{\mu \ln(r_e / r_w)} \qquad \textbf{A-4}$$

A-3 is the linear inflow performance relationship used in this dissertation. At steady state, Equation A-2 and A-3 should give the same results. However, when well bottomhole pressure is subjected to oscillation or excursion, the two equations could give very different flow rates.

In order to quantify the difference, four examples are calculated. The basic parameters used in the examples are

- h = 10 m
- p_e = 10^7 Pa
- r_w = 0.1 m
- r_e = 25 m
- c =10^{-8} 1/Pa
- ø=0.2
- μ=0.001Pas

The calculation is done by assuming that the bottomhole pressure is subjected to a sinusoidal oscillation around its average that is 10 bar lower than the reservoir pressure. The amplitude of the oscillation is 5 bar. The reservoir is initialized to be in the same pressure (100 bara) as its drainage boundary. In this way, consequences from both oscillation and excursion are obtained.

The effects of oscillation frequency and permeability on the dynamic inflow performance are investigated by the calculation of the four examples. The bottomhole pressure signal frequency and reservoir permeability for the four examples are

Example 1: low frequency and high permeability
- f = 1/3600
- k = 0.1 Darcy

Example 2: high frequency and high permeability
- f = 1/600
- k = 0.1 Darcy

Example 3: low frequency and low permeability
- f = 1/3600
- k = 0.01 Darcy

Example 3: high frequency and low permeability
- f = 1/600
- k = 0.01 Darcy

The calculation is done by using Matlab® PDE solver. The results are shown in Figure A-1~A~4.

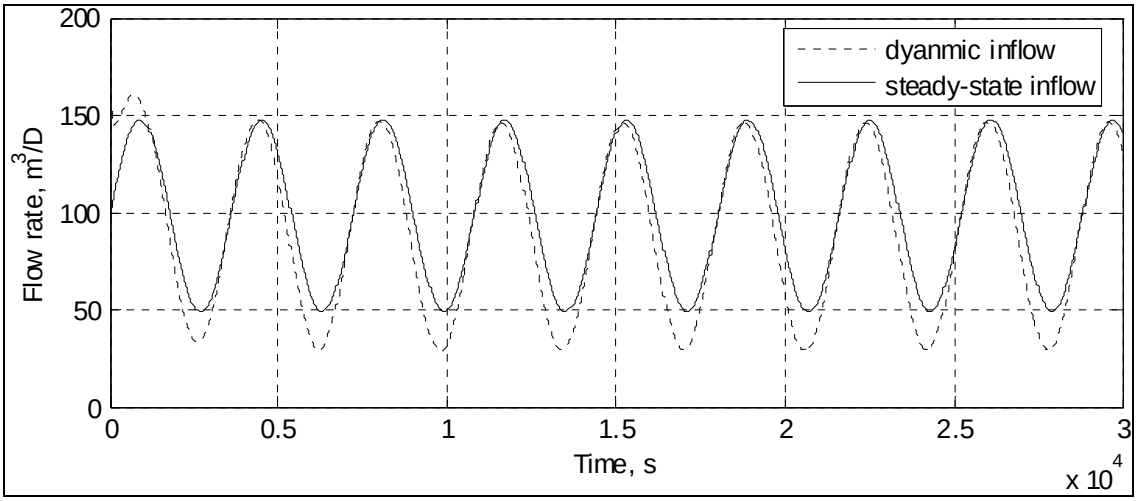

Figure A-1 Example 1: low frequency and high permeability.

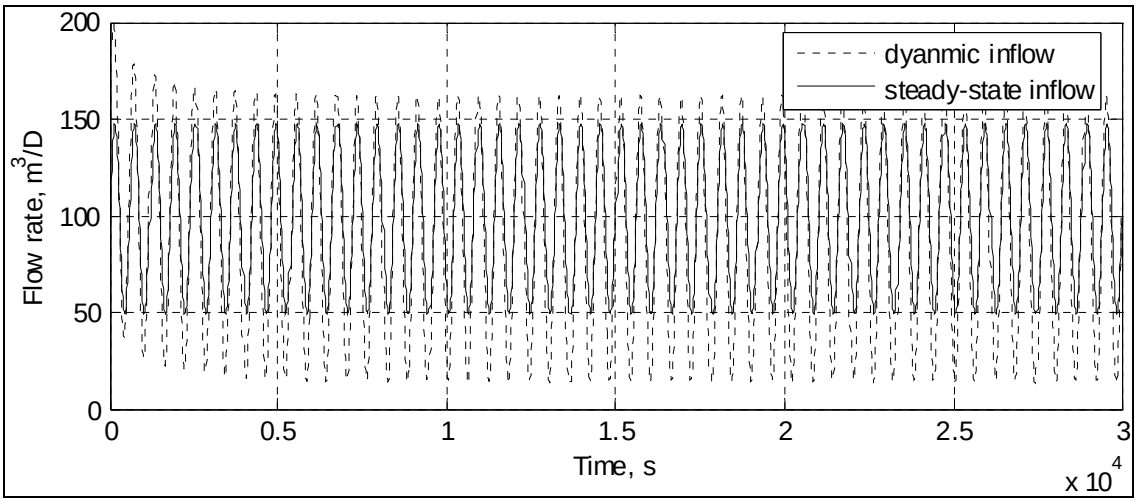

Figure A-2 Example 2: high frequency and high permeability.

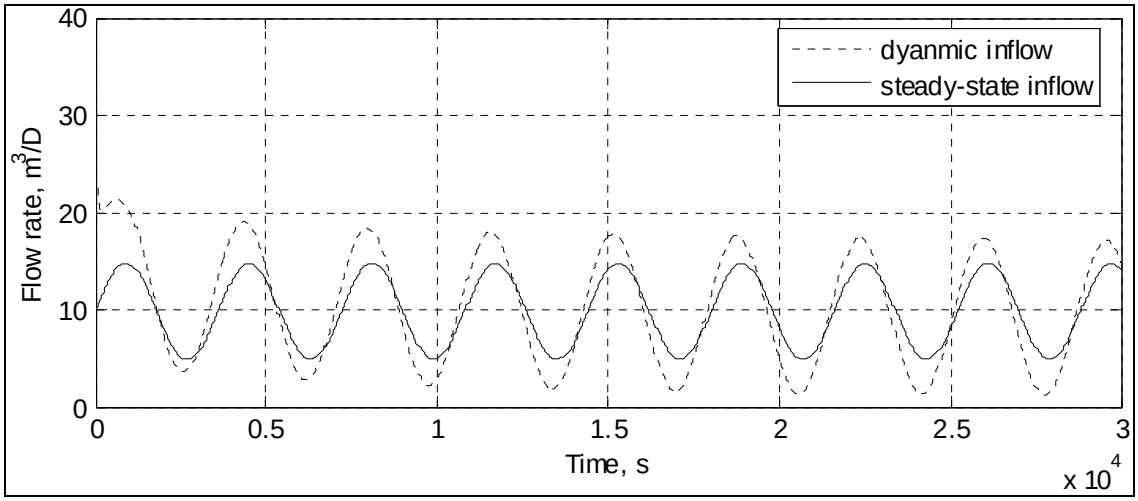

Figure A-3 Example 3: low frequency and low permeability.

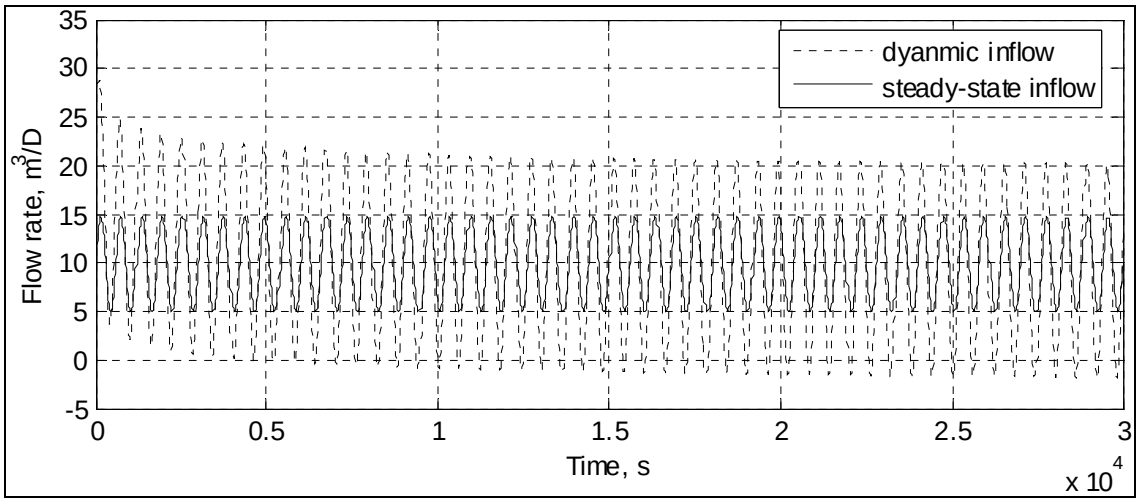

Figure A-4 Example 4: high frequency and low permeability.

Figure A-1 shows that when bottomhole pressure oscillation frequency is low and reservoir permeability is high, the dynamic inflow performance is quite close to the steady-state inflow performance. There is a small phase shift between the two curves, which indicates that excursion effect is not strong. In the meantime, the dynamic inflow seems give a lower average flowrate.

When increasing the oscillation frequency, the difference of the flow rate oscillation amplitudes between the two curves starts to increase. The dynamic inflow result gives larger amplitude. This is shown in Figure A-2.

If reduce the permeability and apply a low frequency pressure signal, very clear phase shift is observed in Figure A-3. This means the excursion delay effect becomes strong for low permeability reservoirs. In fact, it takes much longer time for the dynamic inflow oscillation to become stable from the start of simulation, in which the reservoir is initialized with a even pressure field. Besides the phase shift, the dynamic inflow for low permeability reservoir also has larger oscillation amplitude compared with the steady-sate solution.

When applying high frequency well bottomhole pressure signal to low permeability reservoir. The oscillation amplitude of dynamic inflow increases, and reverse flow from wellbore to reservoir is also observed. But the excursion delay effect becomes weak. This is shown in Figure A-4.

Based on the calculation results, it can be concluded that the steady-state inflow performance assumption is good only when pressure oscillation frequency is low and reservoir permeability is high like the case in Example 1.

When permeability is low, reservoir inflow response will be delayed. When pressure oscillation frequency is too high, the amplitude of the inflow oscillation will increase. Besides, the dynamic inflow performance seems give a lower average flow rate.

In a common sense, it should be the mobility rather than permeability to be used in the discussion. The basic conclusion here is also correct if replace permeability by mobility. The reason of using permeability here is try to make the discussion concise.

Matlab® code for Example 1

```
function dynamic_inflow
% This function compares the dynamic inflow performance and steady-state
% inflow performance.
%
% input data
rw = 0.1;      % wellbore radius
re = 25;       % drainage boundary redius
k = 1E-13;     % permeability
h = 10;        % thickness of payzone
u = 0.001;     % viscosity

% productivity index
J = 2*pi*k*h/u/log(re/rw);

m = 1;                       % m=1 indicate a cylindrical system in PDE solver
x = linspace(0.1,25,1000);  % discretize the reservoir in the radius direction
t = linspace(0,50000,6000); % simulation time span and interval for output

Pe = 10E6;                      % reservoir drainage boundary pressure
Pwf = 9e6-5e5*sin(t*pi/1800);  % well bottomhole pressure

% solve the reservoir diffusivity equation
sol = pdepe(m,@pdex1pde,@pdex1ic,@pdex1bc,x,t);
p = sol(:,:,1);                    % get the pressure field
dpdr = (p(:,1)-p(:,2))/0.0249;    % calculate the pressure gradient
Q_SI = J*(Pe-Pwf)*86400;          % Stead-state inflow
Q_DI = -2*pi*k*h*rw/u*86400*dpdr; % dynamic inflow

subplot(2,1,1)
plot(t, Pwf, 'k-')
xlabel('Time, s')
ylabel('Bottomhole pressure signal, Pa')
grid on

subplot(2,1,2)
plot(t,Q_DI,'k:',t,Q_SI,'k-')
xlabel('Time, s')
ylabel('Flow rate, m^3/D')
axis([0 50000 0 200]);
legend('dyanmic inflow','steady-state inflow');
grid on

% --------------------------------------------------------------------------
function [c,f,s] = pdex1pde(x,t,u,DuDx)
% describe the PDE
c = 20;         % the coefficient of the pressure derivative term w.r.t time
f = DuDx;
s = 0;

% --------------------------------------------------------------------------
function u0 = pdex1ic(x)
% define IC for the system
u0 = 10000000;      % reservoir is initialized at a even pressure

% --------------------------------------------------------------------------
function [pl,ql,pr,qr] = pdex1bc(xl,ul,xr,ur,t)
% define BC for the system
pl = ul-9e6+5e5*sin(t*pi/1800);
ql = 0;
pr = ur-10000000;
qr = 0;
```

B. Matlab® code for linear stability analysis

```
function gas_lift_stability
% This function carries out linear stability analysis for the simplified
% gas-lift system in Figure 3-6 and 3-7.
%
% ------------------------------------------------------------------------
% Dictionary of variables
%
% VARIABLE  DESCRIPTION(Scalar/Array)
% ------------------------------------------------------------------------
%   Aa      annulus cross-section area (S), m^2
%   ALFA    void fraction (A), -
%   At      tubing cross-section area (S), m^2
%   Da      annulus hydraulic diameter (S), m
%   Do      orifice diameter, (S), m
%   Dt      tubing inner diameter (S), m
%   DADZ    void fraction gradient along tubing (A), 1/m
%   DENSL   water density (S), kg/m^3
%   DENSM   mixtuer density (A), kg/m^3
%   DPDZa   pressure gradient along annulus(A), Pa/m
%   DPDZt   pressure gradient along tubing (A), Pa/m
%   DUDZa   gas velocity gradient along annulus (A), 1/s
%   DUDZt   mixture velocity gradient along tubing (A), 1/s
%   f       moody friction factor (S), -
%   g       acceleration of gravity force (S), m/s^2
%   L       depth of the well (S), m
%   Mg      gas injection rate (S), kg/s
%   Pa      pressure in annulus (A), Pa
%   PI      mass Productivity Index (S), (kg/s)/Pa
%   PR      reservoir pressure (S), Pa
%   Pt      pressure in tubing (A), Pa
%   Psep    separator pressure (S), Pa
%   Pu      orifice upstream pressure (S), Pa
%   Pwf     bottomhole flowing pressure (S), Pa
%   R       gas constant for air (S), J/(kg*K)
%   T       temperature (S), K
%   Uga     gas velocity in annulus (A), m/s
%   Usg     gas superficial velocity in tubing (A), m/s
%   Usl     liquid superficial velocity in tubing (S/A), m/s
%   Um      mixtuer veloctiy in tubing (A), m/s
%   za      coordinate in vertical direction for annulus (A), m
%   zt      coordinate in vertical direction for tubing (A), m
% ------------------------------------------------------------------------
clear
global At Aa Da Do Dt L PI DENSL T R g Mg f Psep PR Pwf

% Constants.
g=9.8;      % Acceleration of gravity force.
R=286.9;    % Air constant.
f=0.015;    % Friction factor.
DENSL=1000; % Liquid density.

% Input information specified by user.
Da=0.2;     % Annulus hydraulic diameter.
Dt=0.125;   % Tubing diameter.
Do=0.008;   % Orifice diameter.
L=2500;     % Well depth.
T=300;      % System temperature.
Mg=1.0;     % Gas mass injection rate.
Psep=1e6;   % Well outlet pressure.
PI=4e-6;    % Productiity Index in mass.
PR=29e6;    % Reservoir pressure.

% Calculated parameter.
At=pi*Dt^2/4.0;     % Tubing cross-section area.
Aa=pi*Da^2/4.0;     % Annulus cross-section area.
```

```
% Specify the task.
display(' ');
display('Please specify the task by typing one of the task index number:');
display(' ');
display(' 1 ---- stability check for non-critical gas injection system');
display(' 2 ---- stability check for critical gas injection system');
display(' 3 ---- neutral stability for critical gas injection system');
display(' ');
index=input('type your task index number (1,2,3) here: ','s');

switch index
    case {'1'}
        % Load initial guess from last calculation.
        load initial0
        load initial1
        load initial2

        % Find steady-state solution for tubing.
        % Usl0=0.5;
        % solinit0=bvpinit(linspace(0,L),1e6,Usl0);
        sstubing=bvp4c(@tubing,@bctubing,sstubing);
        save initial0 sstubing;
        zt=sstubing.x;
        Pt=sstubing.y;
        Pwf=Pt(1);
        Usg=Mg*R*T./Pt/At;
        Usl=PI*(PR-Pwf)/DENSL/At;
        Um=Usg+Usl;
        ALFA=Usg./Um;
        DENSM=DENSL.*(1-ALFA)+Pt./(R*T).*ALFA;
        DPDZt=sstubing.yp;
        DUDZt=-ALFA.*Um./Pt.*DPDZt;
        DADZt=-(1-ALFA).*ALFA./Pt.*DPDZt;

        % Calculate orifice upstream pressure.
        Pu=fzero(@orifice,1.2*Pwf);
        K=1.4;
        Ycr=(2.0/(K+1))^(K/(K-1));
        if Pwf/Pu<Ycr
            display('critical flow is found');
            pause;
        end

        % Find steady-state solution for annulus.
        solinit1=bvpinit(linspace(0,L),1e6,1);
        ssannulus=bvp4c(@annulus,@bcannulus,solinit1,[],Pu);
        save initial1 ssannulus
        za=ssannulus.x;
        Pa=ssannulus.y;
        Uga=Mg*R*T./Pa/Aa;
        DENSG=Pa./(R*T);
        DPDZa=ssannulus.yp;
        DUDZa=-Uga./Pa.*DPDZa;
        save case1 zt Pt Usg Usl Um ALFA DENSM DPDZt DUDZt DADZt...
             za Pa Uga DPDZa DUDZa;

        figure(1)
        subplot(2,3,1);
        plot(zt,Pt, 'k-');
        xlabel('Distance from the bottom of well, m');
        ylabel('Pressure, Pa');

        subplot(2,3,2);
        plot(zt,ALFA,'k-');
        xlabel('Distance from the bottom of well, m');
        ylabel('Void fraction, -');

        subplot(2,3,3);
        plot(zt,Um,'k-');
        xlabel('Distance from the bottom of well, m');
```

```
    ylabel('Mixture velocity, m/s');

    subplot(2,3,4);
    plot(zt,DPDZt,'k-');
    xlabel('Distance from the bottom of well, m');
    ylabel('Pressure gradient, Pa/m');

    subplot(2,3,5);
    plot(zt,DADZt,'k-');
    xlabel('Distance from the bottom of well, m');
    ylabel('Void fraction gradient, 1/m');

    subplot(2,3,6);
    plot(zt,DUDZt,'k-');
    xlabel('Distance from the bottom of well, m');
    ylabel('Mixture velocity gradient, 1/s');

    figure(2)
    subplot(2,2,1);
    plot(za,Pa,'k-');
    xlabel('Distance from the top of well, m');
    ylabel('Pressure, Pa');

    subplot(2,2,3);
    plot(za,Uga,'k-');
    xlabel('Distance from the top of well, m');
    ylabel('Gas velocity, m/s');

    subplot(2,2,2);
    plot(za,DPDZa,'k-');
    xlabel('Distance from the top of well, m');
    ylabel('Pressure gradient, Pa/m');

    subplot(2,2,4);
    plot(za,DUDZa,'k-');
    xlabel('Distance from the top of well, m');
    ylabel('Gas velocity gradient, 1/s');

    % Solve the perturbation equation to find x and y.
    Omega=[0 0];
    options=bvpset('Nmax',500);
    solinit2=bvpinit(linspace(0,L,100),[1 1 1 1 0.0 0.0 1 1 -0 -0],...
                     Omega);
    stability=bvp4c(@non_critical,@bc_non_critical,stability,...
                    options,zt,ALFA,Um,Pt,DPDZt,DUDZt,DADZt,Pwf,...
                    Pu,za,Uga,Pa,DPDZa,DUDZa);
    save initial2 stability;

    if stability.parameters(1)<=0.0
        stability.parameters
        display('The system is stable.')
        display(' ');
    else
        stability.parameters
        display('The system is unstable.')
        display(' ');
    end

case {'2'}
    % Load initial guess from previous calculation.
    load initial3
    load initial4

    % Find steady-state solution for tubing
    % Usl0=0.5;
    % solinit0=bvpinit(linspace(0,L),1e6,Usl0);
    sstubing=bvp4c(@tubing,@bctubing,sstubing);
    save initial3 sstubing;
    zt=sstubing.x;
    Pt=sstubing.y;
```

```
        Pwf=Pt(1);
        Usg=Mg*R*T./Pt/At;
        Usl=PI*(PR-Pwf)/DENSL/At;
        Um=Usg+Usl;
        ALFA=Usg./Um;
        DENSM=DENSL.*(1-ALFA)+Pt./(R*T).*ALFA;
        DPDZt=sstubing.yp;
        DUDZt=-ALFA.*Um./Pt.*DPDZt;
        DADZt=-(1-ALFA).*ALFA./Pt.*DPDZt;
        save case2 zt Pt Usg Usl Um ALFA DENSM DPDZt DUDZt DADZt;

        figure(1)
        subplot(2,3,1);
        plot(zt,Pt, 'k-');
        xlabel('Distance from the bottom of well, m');
        ylabel('Pressure, Pa');

        subplot(2,3,2);
        plot(zt,ALFA,'k-');
        xlabel('Distance from the bottom of well, m');
        ylabel('Void fraction, -');

        subplot(2,3,3);
        plot(zt,Um,'k-');
        xlabel('Distance from the bottom of well, m');
        ylabel('Mixture velocity, m/s');

        subplot(2,3,4);
        plot(zt,DPDZt,'k-');
        xlabel('Distance from the bottom of well, m');
        ylabel('Pressure gradient, Pa/m');

        subplot(2,3,5);
        plot(zt,DADZt,'k-');
        xlabel('Distance from the bottom of well, m');
        ylabel('Void fraction gradient, 1/m');

        subplot(2,3,6);
        plot(zt,DUDZt,'k-');
        xlabel('Distance from the bottom of well, m');
        ylabel('Mixture velocity gradient, 1/s');

        % Solve the perturbation equation to find x and y.
        % Omega=[0 0];
        options=bvpset('Nmax',500);
        % solinit2=bvpinit(linspace(0,L,100),[1 1 1 1 0.0 0.0],Omega);
        stability=bvp4c(@critical,@bc_critical,stability,options,zt,...
                        ALFA,Um,Pt,DPDZt,DUDZt,DADZt,Pwf);
        save initial4 stability;

        if stability.parameters(1)<=0.0
            stability.parameters
            display('The system is stable.')
            display(' ');
        else
            stability.parameters
            display('The system is unstable.')
            display(' ');
        end

    case {'3'}
        options=optimset('TolX', 0.001);
        [mg x]=fzero(@findmg,[0.1 0.2],options)

    otherwise
        display(' ');
        display('You have typed the wrong number.');
        display('Please restart the program and try again');
end
%
```

```
% ------------------------------------------------------------------------


function dpdz=tubing(z,p,usl)
% This function calculates the pressure gradient in tubing.
%
global At Dt DENSL T R g Mg f

usg=Mg*R*T/p/At;                        % calculate gas superficial velocity.
um=usl+usg;                             % calculate mixture velocity.
alfa=usg/um;                            % calculate void fraction.
densm=DENSL*(1-alfa)+p/(R*T)*alfa;      % calculate mixture density.
dpdz=1/(1-densm*um*um*alfa/p)*...
     (-densm*g-0.5*f*densm*um*um/Dt); % calculate pressure gradient.
%
% ------------------------------------------------------------------------


function res=bctubing(ya,yb,usl)
% This function sets the boundary condition for tubing flow.
%
global At PI DENSL Psep PR

res=[ya-(PR-usl*DENSL*At/PI)    % calculate the residul at the inlet.
     yb-Psep];                  % calculate the residul at the outlet.
%
% ------------------------------------------------------------------------


function err=orifice(pu)
% This function calculates the mass flowrate with given pressure difference
% acrross the orifice and compare the calculated value with given gas mass
% injection rate.
%
global Do T R Mg Pwf

pd=Pwf;
Cd=0.865;      % Discharge coefficient.
Y=pd/pu;       % Calculate the ratio of downstream and upstream pressures.
if (Y>=1.0)|(pu<100000)
    M=0;
else
    K=1.4;                      % Ratio of gas specific heats.
    Ycr=(2.0/(K+1))^(K/(K-1)); % Calculate critical pressure ratio.
    if Y<=Ycr
        Y=Ycr;
    end
    % Calculate mass flow rate.
    M=sqrt(2.0/R)*pi/4.0*pu*Do^2*Cd/sqrt(T)*sqrt(K/(K-1)*...
           (Y^(2/K)-Y^((K+1)/K)));
end
err=Mg-M;
%
% ------------------------------------------------------------------------


function dpdz=annulus(z,p,ug0,pao)
% This function calculates the pressure gradient in annulus.
%
global Aa Da T R g Mg f

ug=Mg*R*T/p/Aa;                         % Calculate gas velocity.
densg=p/(R*T);                          % Calculate gas density.
dpdz=1/(1-densg*ug*ug/p)*...
    (densg*g-0.5*f*densg*ug*ug/Da);     % Calculate pressure gradient.
%
% ------------------------------------------------------------------------


function res=bcannulus(ya,yb,ug0,pao)
```

```
% This function sets the boundary condition for annulus.
%
global Aa T R Mg

res=[ya-Mg*R*T/(Aa*ug0)     % Calculate the residul at the inlet.
     yb-pao];               % Calculate the residul at the outlet.
%
% ------------------------------------------------------------------------


function model=non_critical(zz,X,Omega,zt,alfa,um,pt,dpdzt,dudzt,...
                            dadzt,pwf,pao,za,uga,paa,dpdzaa,dudzaa)
% This function gives the solution expression of equation 5-71.
%
global Da Dt DENSL T R g f

x=Omega(1);
y=Omega(2);
p=interp1(zt,pt,zz);
u=interp1(zt,um,zz);
a=interp1(zt,alfa,zz);
dpdz=interp1(zt,dpdzt,zz);
dudz=interp1(zt,dudzt,zz);
dadz=interp1(zt,dadzt,zz);
ug=interp1(za,uga,zz);
pa=interp1(za,paa,zz);
dpdza=interp1(za,dpdzaa,zz);
dudza=interp1(za,dudzaa,zz);

b=[];
b(1)=-x*a*X(1)+y*a*X(2)+(X(3)-a*X(3)-a*X(1))*dudz-(X(1)+X(3))*u*dadz;
b(2)=-x*a*X(2)-y*a*X(1)+(X(4)-a*X(4)-a*X(2))*dudz-(X(2)+X(4))*u*dadz;
b(3)=-x*a*p*(X(5)+X(1))+y*a*p*(X(6)+X(2))-(X(1)+X(3)+X(5))*...
     (a*p*dudz+a*u*dpdz+p*u*dadz);
b(4)=-x*a*p*(X(6)+X(2))-y*a*p*(X(5)+X(1))-(X(2)+X(4)+X(6))*...
     (a*p*dudz+a*u*dpdz+p*u*dadz);
b(5)=-(a*p*u/(R*T)+(1-a)*u*DENSL)*(x*X(3)-y*X(4))-...
     (X(1)+2*X(3)+X(5))*a*p*u/(R*T)*dudz-(2*DENSL*(1-a)*X(3)-...
     a*DENSL*X(1))*u*dudz-f/(2*Dt)*(a*p*u^2/(R*T)*X(5)...
     +(a*p*u^2/(R*T)-a*DENSL*u^2)*X(1)+(a*p*u^2/(R*T)+...
     (1-a)*DENSL*u^2)*2*X(3))-(a*p/(R*T)*X(5)+...
     (a*p/(R*T)-a*DENSL)*X(1))*g-dpdz*X(5);
b(6)=-(a*p*u/(R*T)+(1-a)*u*DENSL)*(x*X(4)+y*X(3))-...
     (X(2)+2*X(4)+X(6))*a*p*u/(R*T)*dudz-(2*DENSL*(1-a)*X(4)-...
     a*DENSL*X(2))*u*dudz-f/(2*Dt)*(a*p*u^2/(R*T)*X(6)...
     +(a*p*u^2/(R*T)-a*DENSL*u^2)*X(2)+(a*p*u^2/(R*T)+...
     (1-a)*DENSL*u^2)*2*X(4))-(a*p/(R*T)*X(6)+...
     (a*p/(R*T)-a*DENSL)*X(2))*g-dpdz*X(6);
b(7)=-x*pa*X(9)+y*pa*X(10)-(X(7)+X(9))*(pa*dudza+ug*dpdza);
b(8)=-x*pa*X(10)-y*pa*X(9)-(X(8)+X(10))*(pa*dudza+ug*dpdza);
b(9)=(-pa*ug*(x*X(7)-y*X(8))-(2*X(7)+X(9))*pa*ug*dudza+pa*X(9)*g-...
     R*T*X(9)*dpdza-f/(2*Da)*pa*ug^2*(2*X(7)+X(9)))/(R*T);
b(10)=(-pa*ug*(x*X(8)+y*X(7))-(2*X(8)+X(10))*pa*ug*dudza+pa*X(10)*g-...
      R*T*X(10)*dpdza-f/(2*Da)*pa*ug^2*(2*X(8)+X(10)))/(R*T);
b=b';

c=[];
c(1,1)=a*u; c(1,3)=-(1-a)*u;
c(2,2)=a*u; c(2,4)=-(1-a)*u;
c(3,1)=a*u*p; c(3,3)=a*u*p; c(3,5)=a*u*p;
c(4,2)=a*u*p; c(4,4)=a*u*p; c(4,6)=a*u*p;
c(5,3)=a*p*u^2/(R*T)+DENSL*(1-a)*u^2; c(5,5)=p;
c(6,4)=a*p*u^2/(R*T)+DENSL*(1-a)*u^2; c(6,6)=p;
c(7,7)=pa*ug; c(7,9)=pa*ug;
c(8,8)=pa*ug; c(8,10)=pa*ug;
c(9,7)=pa*ug^2/(R*T); c(9,9)=pa;
c(10,8)=pa*ug^2/(R*T); c(10,10)=pa;

model=c\b;
%
```

```
% ------------------------------------------------------------------------


function res=bc_non_critical(ya,yb,Omega,zt,alfa,um,pt,dpdzt,dudzt,...
                             dadzt,pwf,pao,za,uga,pa,dpdza,dudza)
% This function sets the boundary conditions for equation 5-71.
%
global At Aa Do PI DENSL T R Mg PR

c1=0.1;
c2=10;
K=1.4;
Cd=0.865;
C=sqrt(2.0/(R*T))*pi/4.0*Do^2^Cd*sqrt(K/(K-1));

a0=Mg*R*T/(pwf*At)/(PI*(PR-pwf)/(DENSL*At)+Mg*R*T/(pwf*At));
ut=PI*(PR-pwf)/(DENSL*At)+Mg*R*T/(pwf*At);
ua=Mg*R*T/(pao*Aa);

K1=-Mg*R*T*DENSL*PI*(PR-2*pwf)/(PI*(PR-pwf)*pwf+Mg*R*T*DENSL)^2;
K2=R*T*DENSL*PI*(PR-pwf)*pwf/(PI*(PR-pwf)*pwf+Mg*R*T*DENSL)^2;
K3=0.5*C*pao/sqrt((pwf/pao)^(2/K)-...
   (pwf/pao)^((K+1)/K))*(2/K*pwf^(2/K-1)*pao^(-2/K)...
   -(K+1)/K*pwf^(1/K)*pao^(-(K+1)/K));
K4=C*sqrt((pwf/pao)^(2/K)-(pwf/pao)^((K+1)/K))+...
   0.5*C*pao/sqrt((pwf/pao)^(2/K)-...
   (pwf/pao)^((K+1)/K))*(-2/K*pwf^(2/K)*pao^(-2/K-1)...
   +(K+1)/K*pwf^((K+1)/K)*pao^(-(K+1)/K-1));
K5=-PI/(DENSL*At)-Mg*R*T/(pwf^2*At);
K6=R*T/(pwf*At);
K7=-Mg*R*T/(pao^2*Aa);
K8=R*T/(pao*Aa);

res=[ya(1)-(K1+K2*K3)/a0*(pwf-PR)*c1-K2*K4*pao/a0*yb(9)
     ya(2)-(K1+K2*K3)/a0*(pwf-PR)*c2-K2*K4*pao/a0*yb(10)
     ya(3)-(K5+K6*K3)/ut*(pwf-PR)*c1-K6*K4*pao/ut*yb(9)
     ya(4)-(K5+K6*K3)/ut*(pwf-PR)*c2-K6*K4*pao/ut*yb(10)
     ya(5)-(1-PR/pwf)*c1
     ya(6)-(1-PR/pwf)*c2
     yb(5)
     yb(6)
     ya(7)+ya(9)
     ya(8)+ya(10)
     yb(7)-(K7+K8*K4)*pao/ua*yb(9)-K8*K3/ua*(pwf-PR)*c1
     yb(8)-(K7+K8*K4)*pao/ua*yb(10)-K8*K3/ua*(pwf-PR)*c2];
%
% ------------------------------------------------------------------------


function model=critical(zz,X,Omega,zt,alfa,um,pt,dpdzt,dudzt,dadzt,pwf)
% This function gives the solution expression of equation 5-72.
%
global Dt DENSL T R g f

x=Omega(1);
y=Omega(2);
p=interp1(zt,pt,zz);
u=interp1(zt,um,zz);
a=interp1(zt,alfa,zz);
dpdz=interp1(zt,dpdzt,zz);
dudz=interp1(zt,dudzt,zz);
dadz=interp1(zt,dadzt,zz);

b=[];
b(1)=-x*a*X(1)+y*a*X(2)+(X(3)-a*X(3)-a*X(1))*dudz-(X(1)+X(3))*u*dadz;
b(2)=-x*a*X(2)-y*a*X(1)+(X(4)-a*X(4)-a*X(2))*dudz-(X(2)+X(4))*u*dadz;
b(3)=-x*a*p*(X(5)+X(1))+y*a*p*(X(6)+X(2))-...
     (X(1)+X(3)+X(5))*(a*p*dudz+a*u*dpdz+p*u*dadz);
b(4)=-x*a*p*(X(6)+X(2))-y*a*p*(X(5)+X(1))-...
     (X(2)+X(4)+X(6))*(a*p*dudz+a*u*dpdz+p*u*dadz);
```

```
b(5)=-(a*p*u/(R*T)+(1-a)*u*DENSL)*(x*X(3)-y*X(4))-...
     (X(1)+2*X(3)+X(5))*a*p*u/(R*T)*dudz-(2*DENSL*(1-a)*X(3)-...
     a*DENSL*X(1))*u*dudz-f/(2*Dt)*(a*p*u^2/(R*T)*X(5)...
     +(a*p*u^2/(R*T)-a*DENSL*u^2)*X(1)+(a*p*u^2/(R*T)+...
     (1-a)*DENSL*u^2)*2*X(3))-(a*p/(R*T)*X(5)+...
     (a*p/(R*T)-a*DENSL)*X(1))*g-dpdz*X(5);
b(6)=-(a*p*u/(R*T)+(1-a)*u*DENSL)*(x*X(4)+y*X(3))-...
     (X(2)+2*X(4)+X(6))*a*p*u/(R*T)*dudz-(2*DENSL*(1-a)*X(4)-...
     a*DENSL*X(2))*u*dudz-f/(2*Dt)*(a*p*u^2/(R*T)*X(6)...
     +(a*p*u^2/(R*T)-a*DENSL*u^2)*X(2)+(a*p*u^2/(R*T)+...
     (1-a)*DENSL*u^2)*2*X(4))-(a*p/(R*T)*X(6)+...
     (a*p/(R*T)-a*DENSL)*X(2))*g-dpdz*X(6);
b=b';

c=[];
c(1,1)=a*u; c(1,3)=-(1-a)*u;
c(2,2)=a*u; c(2,4)=-(1-a)*u;
c(3,1)=a*u*p; c(3,3)=a*u*p; c(3,5)=a*u*p;
c(4,2)=a*u*p; c(4,4)=a*u*p; c(4,6)=a*u*p;
c(5,3)=a*p*u^2/(R*T)+DENSL*(1-a)*u^2; c(5,5)=p;
c(6,4)=a*p*u^2/(R*T)+DENSL*(1-a)*u^2; c(6,6)=p;

model=c\b;
%
% ------------------------------------------------------------------------


function res=bc_critical(ya,yb,Omega,zt,alfa,um,pt,dpdzt,dudzt,dadzt,pwf)
% This function sets the boundary conditions for equation 5-72.
%
global At Aa PI DENSL T R Mg PR

c1=0.1;
c2=0.1;
u0=PI*(PR-pwf)/(DENSL*At)+Mg*R*T/(pwf*At);
res=[ya(1)+(PR-2*pwf)*PI*pwf/(Mg*R*T*DENSL+PI*(PR-pwf)*pwf)*(1-PR/pwf)*c1
     ya(2)+(PR-2*pwf)*PI*pwf/(Mg*R*T*DENSL+PI*(PR-pwf)*pwf)*(1-PR/pwf)*c2
     ya(3)-PI*(PR-2*pwf)/(DENSL*At*u0)*(1-PR/pwf)*c1
     ya(4)-PI*(PR-2*pwf)/(DENSL*At*u0)*(1-PR/pwf)*c2
     ya(5)-(1-PR/pwf)*c1
     ya(6)-(1-PR/pwf)*c2
     yb(5)
     yb(6)];
%
% ------------------------------------------------------------------------


function fun=findmg(mg)
% This is a calling function of case 3.
%
global At Dt L PI DENSL T R g f Psep PR
% When using continuation method, the following two commands are executed.
load initial5
load initial6

solinit=bvpinit(linspace(0,L),1e6,0.1);
stubing=bvp4c(@tubing1,@bctubing1,stubing,[],mg);
save initial5 stubing;

% Calculate the steady-state variables
zt=stubing.x;
Pt=stubing.y;
Pwf=Pt(1);
Usg=mg*R*T./Pt/At;
Usl=PI*(PR-Pwf)/DENSL/At;
Um=Usg+Usl;
ALFA=Usg./Um;
DENSM=DENSL.*(1-ALFA)+Pt./(R*T).*ALFA;
DPDZt=stubing.yp;
DUDZt=-ALFA.*Um./Pt.*DPDZt;
```

```
DADZt=-(1-ALFA).*ALFA./Pt.*DPDZt;

Omega=[0 0];
options=bvpset('Nmax',500);
solinit00=bvpinit(linspace(0,L,100),[10 10 10 10 10 10],Omega);
neutral=bvp4c(@critical1,@bc_critical1,neutral,options,zt,ALFA,Um,Pt,...
              DPDZt,DUDZt,DADZt,Pwf,mg);
save initial6 neutral;
fun=neutral.parameters(1);
%
% ------------------------------------------------------------------------


function dpdz=tubing1(z,p,usl,Mg)
% This function calculates the pressure gradient in tubing.
%
global At Dt DENSL T R g f

usg=Mg*R*T/p/At;                       % calculate gas superficial velocity.
um=usl+usg;                            % calculate mixture velocity.
alfa=usg/um;                           % calculate void fraction.
densm=DENSL*(1-alfa)+p/(R*T)*alfa;     % calculate mixture density.
dpdz=1/(1-densm*um*um*alfa/p)*...
     (-densm*g-0.5*f*densm*um*um/Dt); % calculate pressure gradient.
%
% ------------------------------------------------------------------------


function res=bctubing1(ya,yb,usl,Mg)
% This function sets the boundary condition for tubing flow.
%
global At PI DENSL Psep PR

res=[ya-(PR-usl*DENSL*At/PI)    % calculate the residul at the inlet.
     yb-Psep];                  % calculate the residul at the outlet.
%
% ------------------------------------------------------------------------


function model=critical1(zz,X,Omega,zt,alfa,um,pt,dpdzt,dudzt,dadzt,pwf,Mg)
% This function gives the solution expression of equation 5-72.
%
global Dt DENSL T R g f

x=Omega(1);
y=Omega(2);
p=interp1(zt,pt,zz);
u=interp1(zt,um,zz);
a=interp1(zt,alfa,zz);
dpdz=interp1(zt,dpdzt,zz);
dudz=interp1(zt,dudzt,zz);
dadz=interp1(zt,dadzt,zz);

b=[];
b(1)=-x*a*X(1)+y*a*X(2)+(X(3)-a*X(3)-a*X(1))*dudz-(X(1)+X(3))*u*dadz;
b(2)=-x*a*X(2)-y*a*X(1)+(X(4)-a*X(4)-a*X(2))*dudz-(X(2)+X(4))*u*dadz;
b(3)=-x*a*p*(X(5)+X(1))+y*a*p*(X(6)+X(2))-...
     (X(1)+X(3)+X(5))*(a*p*dudz+a*u*dpdz+p*u*dadz);
b(4)=-x*a*p*(X(6)+X(2))-y*a*p*(X(5)+X(1))-...
     (X(2)+X(4)+X(6))*(a*p*dudz+a*u*dpdz+p*u*dadz);
b(5)=-(a*p*u/(R*T)+(1-a)*u*DENSL)*(x*X(3)-y*X(4))-...
     (X(1)+2*X(3)+X(5))*a*p*u/(R*T)*dudz-(2*DENSL*(1-a)*X(3)-...
     a*DENSL*X(1))*u*dudz-f/(2*Dt)*(a*p*u^2/(R*T)*X(5)...
     +(a*p*u^2/(R*T)-a*DENSL*u^2)*X(1)+(a*p*u^2/(R*T)+...
     (1-a)*DENSL*u^2)*2*X(3))-(a*p/(R*T)*X(5)+...
     (a*p/(R*T)-a*DENSL)*X(1))*g-dpdz*X(5);
b(6)=-(a*p*u/(R*T)+(1-a)*u*DENSL)*(x*X(4)+y*X(3))-...
     (X(2)+2*X(4)+X(6))*a*p*u/(R*T)*dudz-(2*DENSL*(1-a)*X(4)-...
     a*DENSL*X(2))*u*dudz-f/(2*Dt)*(a*p*u^2/(R*T)*X(6)...
     +(a*p*u^2/(R*T)-a*DENSL*u^2)*X(2)+(a*p*u^2/(R*T)+...
```

```
     (1-a)*DENSL*u^2)*2*X(4))-(a*p/(R*T)*X(6)+...
     (a*p/(R*T)-a*DENSL)*X(2))*g-dpdz*X(6);
b=b';

c=[];
c(1,1)=a*u; c(1,3)=-(1-a)*u;
c(2,2)=a*u; c(2,4)=-(1-a)*u;
c(3,1)=a*u*p; c(3,3)=a*u*p; c(3,5)=a*u*p;
c(4,2)=a*u*p; c(4,4)=a*u*p; c(4,6)=a*u*p;
c(5,3)=a*p*u^2/(R*T)+DENSL*(1-a)*u^2; c(5,5)=p;
c(6,4)=a*p*u^2/(R*T)+DENSL*(1-a)*u^2; c(6,6)=p;

model=c\b;
%
% ------------------------------------------------------------------------


function res=bc_critical1(ya,yb,Omega,zt,alfa,um,pt,dpdzt,dudzt,...
                          dadzt,pwf,Mg)
% This function sets the boundary conditions for equation 5-72.
%
global At Aa PI DENSL T R PR

c1=0.1;
c2=0.1;
u0=PI*(PR-pwf)/(DENSL*At)+Mg*R*T/(pwf*At);
res=[ya(1)+(PR-2*pwf)*PI*pwf/(Mg*R*T*DENSL+PI*(PR-pwf)*pwf)*(1-PR/pwf)*c1
     ya(2)+(PR-2*pwf)*PI*pwf/(Mg*R*T*DENSL+PI*(PR-pwf)*pwf)*(1-PR/pwf)*c2
     ya(3)-PI*(PR-2*pwf)/(DENSL*At*u0)*(1-PR/pwf)*c1
     ya(4)-PI*(PR-2*pwf)/(DENSL*At*u0)*(1-PR/pwf)*c2
     ya(5)-(1-PR/pwf)*c1
     ya(6)-(1-PR/pwf)*c2
     yb(5)
     yb(6)];
%
% ------------------------------------------------------------------------
```

C. Input files for OLGA®2000 simulations

C.1 Casing heading base case

```
!*****************************************************************
! CASE Definition
!-----------------------------------------------------------------
CASE AUTHOR="Bin Hu", \
     DATE="Nov 2002 ", \
     INFO="", \
     PROJECT="Petronics", \
     TITLE="Casing heading base case"
!
!*****************************************************************
! OPTIONS Definition
!-----------------------------------------------------------------
OPTIONS COMPOSITIONAL=OFF, DEBUG=ON, PHASE=TWO, \
        POSTPROCESSOR=ON, SLUGVOID=SINTEF, \
        STEADYSTATE=ON, TEMPERATURE=WALL, \
        WAXDEPOSITION=OFF, DRILLING=OFF
!
!*****************************************************************
! FILES Definition
!-----------------------------------------------------------------
FILES PVTFILE="oilandgas.tab"
!
!*****************************************************************
! INTEGRATION Definition
!-----------------------------------------------------------------
INTEGRATION CPULIMIT=4 h, DTSTART=0.1 s, ENDTIME=10 h, MAXDT=10 s, \
            MAXTIME=0 s, MINDT=0.05 s, MINTIME=0 s, NSIMINFO=10, \
            STARTTIME=0 h
!
!*****************************************************************
! MATERIAL Definition
!-----------------------------------------------------------------
MATERIAL LABEL=STEEL, CAPACITY=500 J/kg-C, CONDUCTIVITY=50 W/m-K, \
         DENSITY=7817 kg/m3, TYPE=SOLID
MATERIAL LABEL=SOIL_1, CAPACITY=1320 J/kg-C, CONDUCTIVITY=2.3 W/m-K, \
         DENSITY=2500 kg/m3, TYPE=SOLID
MATERIAL LABEL=SOIL_2, CAPACITY=1320 J/kg-C, CONDUCTIVITY=0.2 W/m-K, \
         DENSITY=2500 kg/m3, TYPE=SOLID
MATERIAL LABEL=NEOPRENE, CAPACITY=2009 J/kg-C, \
         CONDUCTIVITY=0.163 W/m-K, DENSITY=1115 kg/m3, TYPE=SOLID
MATERIAL LABEL=ASPHALT, CAPACITY=800 J/kg-C, \
         CONDUCTIVITY=0.698 W/m-K, DENSITY=2120 kg/m3, TYPE=SOLID
MATERIAL LABEL=L_CONCRETE, CAPACITY=880 J/kg-C, \
         CONDUCTIVITY=1.2 W/m-K, DENSITY=1900 kg/m3, TYPE=SOLID
MATERIAL LABEL=H_CONCRETE, CAPACITY=880 J/kg-C, \
         CONDUCTIVITY=1.2 W/m-K, DENSITY=3050 kg/m3, TYPE=SOLID
MATERIAL LABEL=INSULATION, CAPACITY=670 J/kg-C, \
         CONDUCTIVITY=0.04 W/m-K, DENSITY=200 kg/m3, TYPE=SOLID
MATERIAL LABEL=WATER, CAPACITY=4200 J/kg-C, \
         CONDUCTIVITY=0.592 W/m-K, DENSITY=1000 kg/m3, TYPE=SOLID
MATERIAL LABEL=CARCAS, CAPACITY=460 J/kg-C, \
         CONDUCTIVITY=1000 W/m-K, DENSITY=3978 kg/m3, TYPE=SOLID
MATERIAL LABEL=RILSAN, CAPACITY=2300 J/kg-C, \
         CONDUCTIVITY=0.33 W/m-K, DENSITY=1040 kg/m3, TYPE=SOLID
MATERIAL LABEL=ZETAWIRE, CAPACITY=460 J/kg-C, \
         CONDUCTIVITY=0.93 W/m-K, DENSITY=3978 kg/m3, TYPE=SOLID
MATERIAL LABEL=TAPE, CAPACITY=1 J/kg-C, CONDUCTIVITY=1.16 W/m-K, \
         DENSITY=780 kg/m3, TYPE=SOLID
MATERIAL LABEL=POLYETEN, CAPACITY=2300 J/kg-C, \
         CONDUCTIVITY=0.41 W/m-K, DENSITY=940 kg/m3, TYPE=SOLID
MATERIAL LABEL=COFOAM, CAPACITY=1050 J/kg-C, \
         CONDUCTIVITY=0.07 W/m-K, DENSITY=540 kg/m3, TYPE=SOLID
MATERIAL LABEL=TITAN, CAPACITY=520 J/kg-C, CONDUCTIVITY=20 W/m-K, \
         DENSITY=4540 kg/m3, TYPE=SOLID
```

```
MATERIAL LABEL=POLYCHLOROPRENE, CAPACITY=1070 J/kg-C, \
         CONDUCTIVITY=0.27 W/m-K, DENSITY=1580 kg/m3, TYPE=SOLID
MATERIAL LABEL=VIKOTHERM, CAPACITY=1500 J/kg-C, \
         CONDUCTIVITY=0.13 W/m-K, DENSITY=1000 kg/m3, TYPE=SOLID
!
!*********************************************************************
! WALL Definition
!---------------------------------------------------------------------
WALL LABEL=WELL, ELECTRICHEAT=OFF, MATERIAL=( STEEL, WATER, \
     STEEL, H_CONCRETE, SOIL_1, SOIL_1, SOIL_1, SOIL_2 ), \
     POWERCONTROL=OFF, THICKNESS=( 0.0115, 0.02135,  \
     0.012, 0.03332, 0.1, 0.2, 0.6, 1.5 ) m
WALL LABEL=RISER_F6, ELECTRICHEAT=OFF, MATERIAL=( CARCAS, RILSAN, \
     ZETAWIRE, RILSAN, POLYETEN, POLYETEN, COFOAM, TAPE, RILSAN ), \
     POWERCONTROL=OFF, THICKNESS=( 0.0054,  \
     0.0055, 0.014, 0.003, 0.008, 0.006, 0.0055, 0.00075, 0.007 ) m
WALL LABEL=TITAN-1, ELECTRICHEAT=OFF, MATERIAL=( TITAN, \
     POLYCHLOROPRENE ), POWERCONTROL=OFF, THICKNESS=( 0.021, 0.008 ) m
WALL LABEL=TITAN-2, ELECTRICHEAT=OFF, MATERIAL=( TITAN, \
     POLYCHLOROPRENE, VIKOTHERM, POLYCHLOROPRENE ), \
     POWERCONTROL=OFF, THICKNESS=( 0.021, 0.008, 0.016, 0.005 ) m
WALL LABEL=STEEL-1, ELECTRICHEAT=OFF, MATERIAL=( STEEL, \
     POLYCHLOROPRENE, VIKOTHERM, POLYCHLOROPRENE ), \
     POWERCONTROL=OFF, THICKNESS=( 0.021, 0.008, 0.03, 0.005 ) m
!
!*********************************************************************
! GEOMETRY Definition
!---------------------------------------------------------------------
GEOMETRY LABEL=WELLFLOW, XSTART=0 m, YSTART=-2100 m, ZSTART=0 m
PIPE LABEL=PIPE_1, DIAMETER=0.2 m, NSEGMENTS=2, \
     ROUGHNESS=4.5e-005 m, WALL=WELL, XEND=0 m, YEND=-2000 m, ZEND=0 m
GEOMETRY LABEL=LIFTGAS, XSTART=10 m, YSTART=48 m, ZSTART=0 m
PIPE LABEL=PIPE_2, DIAMETER=0.2 m, NSEGMENTS=20, \
     ROUGHNESS=4.5e-005 m, WALL=STEEL-1, XEND=10 m, YEND=-2000 m, \
     ZEND=0 m
PIPE LABEL=PIPE_2H, DIAMETER=0.2 m, NSEGMENTS=3, \
     ROUGHNESS=4.5e-005 m, WALL=STEEL-1, XEND=0 m, YEND=-2000 m, \
     ZEND=0 m
GEOMETRY LABEL=GASLIFTED_WELL, XSTART=0 m, YSTART=-2000 m, ZSTART=0 m
PIPE LABEL=PIPE_3, DIAMETER=0.124 m, NSEGMENTS=18, \
     ROUGHNESS=3e-005 m, WALL=WELL, XEND=0 m, YEND=-100 m, ZEND=0 m
PIPE LABEL=PIPE_4, DIAMETER=0.124 m, NSEGMENTS=3, \
     ROUGHNESS=4.5e-005 m, WALL=STEEL-1, XEND=0 m, YEND=48 m, ZEND=0 m
PIPE LABEL=PIPE_5, DIAMETER=0.124 m, NSEGMENTS=3, \
     ROUGHNESS=4.5e-005 m, WALL=STEEL-1, XEND=10 m, YEND=48 m, \
     ZEND=0 m
!
!*********************************************************************
! NODE Definition
!---------------------------------------------------------------------
NODE LABEL=GAS_INLET, TYPE=TERMINAL, X=10 m, Y=48 m, Z=0 m
NODE LABEL=BOTT_WELL, TYPE=MERGE, X=0 m, Y=-2000 m, Z=0 m
NODE LABEL=WELLHEAD, TYPE=TERMINAL, X=10 m, Y=48 m, Z=0 m
NODE LABEL=RESERVOIR, TYPE=TERMINAL, X=0 m, Y=-2100 m, Z=0 m
!
!*********************************************************************
! BRANCH Definition
!---------------------------------------------------------------------
BRANCH LABEL=BRAN-1, FLOAT=ON, FLUID="1", FROM=RESERVOIR, \
       GEOMETRY=WELLFLOW, TO=BOTT_WELL
BRANCH LABEL=BRAN-2, FLOAT=ON, FLUID="1", FROM=GAS_INLET, \
       GEOMETRY=LIFTGAS, TO=BOTT_WELL
BRANCH LABEL=BRAN-3, FLOAT=ON, FLUID="1", FROM=BOTT_WELL, \
       GEOMETRY=GASLIFTED_WELL, TO=WELLHEAD
!
!*********************************************************************
! BOUNDARY Definition
!---------------------------------------------------------------------
BOUNDARY NODE=GAS_INLET, TYPE=CLOSED
BOUNDARY GASFRACTION=1 -, NODE=WELLHEAD, PRESSURE=15 bara, \
```

```
         TEMPERATURE=100 C, TYPE=PRESSURE, WATERFRACTION=0 -
BOUNDARY NODE=RESERVOIR, TYPE=CLOSED
!
!*********************************************************************
! HEATTRANSFER Definition
!---------------------------------------------------------------------
HEATTRANSFER BRANCH=BRAN-1, HAMBIENT=1000 W/m2-C, \
             HMININNERWALL=50 W/m2-C, HOUTEROPTION=HGIVEN, \
             PIPE=PIPE_1, TAMBIENT=108 C, TIMESERIES=OFF
HEATTRANSFER BRANCH=BRAN-2, HAMBIENT=1000 W/m2-C, \
             HMININNERWALL=50 W/m2-C, HOUTEROPTION=HGIVEN, \
             PIPE=PIPE_2, TAMBIENT=50 C, TIMESERIES=OFF
HEATTRANSFER BRANCH=BRAN-2, HAMBIENT=1000 W/m2-C, \
             HMININNERWALL=50 W/m2-C, HOUTEROPTION=HGIVEN, \
             PIPE=PIPE_2H, TAMBIENT=108 C, TIMESERIES=OFF
HEATTRANSFER BRANCH=BRAN-3, HAMBIENT=1000 W/m2-C, \
             HMININNERWALL=50 W/m2-C, HOUTEROPTION=HGIVEN, \
             PIPE=PIPE_3, TAMBIENT=( 108, 101, 94, 88, 81, \
             74, 67, 61, 54, 47, 40,  \
             35, 30, 23, 17, 13, 9, 5 ) C, TIMESERIES=OFF
HEATTRANSFER BRANCH=BRAN-3, HAMBIENT=1000 W/m2-C, \
             HMININNERWALL=50 W/m2-C, HOUTEROPTION=HGIVEN, \
             PIPE=PIPE_4, TAMBIENT=5 C, TIMESERIES=OFF
HEATTRANSFER BRANCH=BRAN-3, HAMBIENT=1000 W/m2-C, \
             HMININNERWALL=50 W/m2-C, HOUTEROPTION=HGIVEN, \
             PIPE=PIPE_5, TAMBIENT=5 C, TIMESERIES=OFF
!
!*********************************************************************
! CONTROLLER Definition
!---------------------------------------------------------------------
CONTROLLER LABEL=PRODCONTR, COMBINEVARIABLES=OFF, \
           EXTENDED=OFF, MAXCHANGE=0.2   , \
          SETPOINT=0.96  , STROKETIME=10 s, TIME=0 s, TYPE=MANUAL

!*********************************************************************
! SOURCE Definition
!---------------------------------------------------------------------
SOURCE LABEL=GAS_SUPPLY, BRANCH=BRAN-2, GASFRACTION=1 -, \
       MASSFLOW=0.6 kg/s, PIPE=PIPE_2, PRESSURE=12000000 Pa, \
       SECTION=1, TEMPERATURE=60 C, TIME=0 s, WATERFRACTION=0 -
!
!*********************************************************************
! WELL Definition
!---------------------------------------------------------------------
WELL LABEL=WELL-1, AINJ=0 , APROD=0  , BINJ=2.47e-006  , \
     BPROD=2.47e-006  , BRANCH=BRAN-1,  \
     GASFRACTION=-1 -, INJOPTION=LINEAR, ISOTHERMAL=YES, \
     LOCATION=BOTTOM, PIPE=PIPE_1, PHASE=OIL, PRODOPTION=LINEAR, \
     RESPRESSURE=150 bara, RESTEMPERATURE=108 C, SECTION=1,  \
     TIME=0 s, WATERFRACTION=0 -
!
!*********************************************************************
! VALVE Definition
!---------------------------------------------------------------------
VALVE LABEL=PRODCHOKE, BRANCH=BRAN-3, CD=0.84  , \
      CONTROLLER=PRODCONTR, CRITFLOWMODEL=FROZEN,  \
      DIAMETER=0.07 m, PIPE=PIPE_5, SECTIONBOUNDARY=2
VALVE LABEL=GASLIFT_VALVE, BRANCH=BRAN-2, CD=0.84  , \
      CRITFLOWMODEL=FROZEN, DIAMETER=0.0125 m,  \
      OPENING=1  , PIPE=PIPE_2H, SECTIONBOUNDARY=2, TIME=0 s
!
!*********************************************************************
! CHECKVALVE Definition
!---------------------------------------------------------------------
CHECKVALVE LABEL=CHECK-1, BRANCH=BRAN-2, DIRECTION=POSITIVE, \
           PIPE=PIPE_2H, SECTIONBOUNDARY=3
!
!*********************************************************************
! OUTPUT Definition
!---------------------------------------------------------------------
```

```
OUTPUT COLUMNS=6, DELETEPREVIOUS=OFF, DTOUT=100 s
OUTPUT BRANCH=BRAN-1, COLUMNS=4, DELETEPREVIOUS=OFF, \
       VARIABLE=( UL, UG, GT, GLT,  \
       GLTHL, GG, AL, PT BARA, TM, VOL, ID, HOL, ROG, ROL )
OUTPUT BRANCH=BRAN-2, COLUMNS=4, DELETEPREVIOUS=OFF, \
       VARIABLE=( UL, UG, GT, GLT,  \
       GLTHL, GG, AL, PT BARA, TM, VOL, ID, HOL, ROG, ROL )
OUTPUT BRANCH=BRAN-3, COLUMNS=4, DELETEPREVIOUS=OFF, \
       VARIABLE=( UL, UG, GT, GLT,  \
       GLTHL, GG, AL, PT BARA, TM, VOL, ID, HOL, ROG, ROL )
!
!*********************************************************************
! TREND Definition
!*********************************************************************
TREND BRANCH=BRAN-3, DELETEPREVIOUS=OFF, DTPLOT=60 s, PIPE=PIPE_5, \
      SECTION=1, TIME=0 s, VARIABLE=( QLT, QG, GG, GLT )
TREND BRANCH=BRAN-1, DELETEPREVIOUS=OFF, PIPE=PIPE_1, SECTION=1, \
      TIME=0 s, VARIABLE=PT
TREND BRANCH=BRAN-2, DELETEPREVIOUS=OFF, PIPE=PIPE_2H, SECTION=1, \
      TIME=0 s, VARIABLE=PT
TREND BRANCH=BRAN-2, PIPE=PIPE_2H, SECTION=3, VARIABLE=GG
TREND BRANCH=BRAN-3, DELETEPREVIOUS=OFF, DTPLOT=10 s, \
      TIME=0 s, VARIABLE=LIQC
TREND BRANCH=BRAN-2, DELETEPREVIOUS=OFF, PIPE=PIPE_2H, \
      SECTION=2, TIME=0 s, VARIABLE=PT
TREND BRANCH=BRAN-2, DELETEPREVIOUS=OFF, PIPE=PIPE_2H, \
      SECTION=3, TIME=0 s, VARIABLE=PT
!
!*********************************************************************
! PROFILE Definition
!---------------------------------------------------------------------
PROFILE BRANCH=BRAN-1, DELETEPREVIOUS=OFF, DTPLOT=60 s, \
        VARIABLE=( HOL, PT )
PROFILE BRANCH=BRAN-3, DELETEPREVIOUS=OFF, DTPLOT=60 s, \
        VARIABLE=( HOL, PT )
!
ENDCASE
```

C.2 Gas robbing in dual gas-lift

```
!*********************************************************************
! CASE Definition
!---------------------------------------------------------------------
CASE AUTHOR="Bin Hu", \
     DATE="Dec 20 2000 ", \
     INFO="ABB hyperthetical model ", \
     PROJECT="LSL project", \
     TITLE="Network dynamics"
!
!*********************************************************************
! OPTIONS Definition
!---------------------------------------------------------------------
OPTIONS COMPOSITIONAL=OFF, DEBUG=OFF, PHASE=TWO, POSTPROCESSOR=ON, \
        SLUGVOID=SINTEF, STEADYSTATE=OFF, TEMPERATURE=WALL, \
        WAXDEPOSITION=OFF
!
!*********************************************************************
! FILES Definition
!---------------------------------------------------------------------
FILES PVTFILE="oilandgas.tab"
!
!*********************************************************************
! INTEGRATION Definition
!---------------------------------------------------------------------
INTEGRATION CPULIMIT=20 h, DTSTART=0.1 s, ENDTIME=16 h, \
            MAXDT=0.1 s, MAXTIME=0 s, MINDT=0.1 s, MINTIME=0 s, \
            NSIMINFO=10, STARTTIME=0 h
!
!*********************************************************************
```

```
! MATERIAL Definition
!-----------------------------------------------------------------------
MATERIAL LABEL=STEEL, CAPACITY=500 J/kg-C, CONDUCTIVITY=50 W/m-K, \
         DENSITY=7817 kg/m3, TYPE=SOLID
MATERIAL LABEL=SOIL_1, CAPACITY=1320 J/kg-C, CONDUCTIVITY=2.3 W/m-K, \
         DENSITY=2500 kg/m3, TYPE=SOLID
MATERIAL LABEL=SOIL_2, CAPACITY=1320 J/kg-C, CONDUCTIVITY=0.2 W/m-K, \
         DENSITY=2500 kg/m3, TYPE=SOLID
MATERIAL LABEL=NEOPRENE, CAPACITY=2009 J/kg-C, \
         CONDUCTIVITY=0.163 W/m-K, DENSITY=1115 kg/m3, TYPE=SOLID
MATERIAL LABEL=ASPHALT, CAPACITY=800 J/kg-C, \
         CONDUCTIVITY=0.698 W/m-K, DENSITY=2120 kg/m3, TYPE=SOLID
MATERIAL LABEL=L_CONCRETE, CAPACITY=880 J/kg-C, \
         CONDUCTIVITY=1.2 W/m-K, DENSITY=1900 kg/m3, TYPE=SOLID
MATERIAL LABEL=H_CONCRETE, CAPACITY=880 J/kg-C, \
         CONDUCTIVITY=1.2 W/m-K, DENSITY=3050 kg/m3, TYPE=SOLID
MATERIAL LABEL=INSULATION, CAPACITY=670 J/kg-C, \
         CONDUCTIVITY=0.04 W/m-K, DENSITY=200 kg/m3, TYPE=SOLID
MATERIAL LABEL=WATER, CAPACITY=4200 J/kg-C, \
         CONDUCTIVITY=0.592 W/m-K, DENSITY=1000 kg/m3, TYPE=SOLID
MATERIAL LABEL=CARCAS, CAPACITY=460 J/kg-C, \
         CONDUCTIVITY=1000 W/m-K, DENSITY=3978 kg/m3, TYPE=SOLID
MATERIAL LABEL=RILSAN, CAPACITY=2300 J/kg-C, \
         CONDUCTIVITY=0.33 W/m-K, DENSITY=1040 kg/m3, TYPE=SOLID
MATERIAL LABEL=ZETAWIRE, CAPACITY=460 J/kg-C, \
         CONDUCTIVITY=0.93 W/m-K, DENSITY=3978 kg/m3, TYPE=SOLID
MATERIAL LABEL=TAPE, CAPACITY=1 J/kg-C, CONDUCTIVITY=1.16 W/m-K, \
         DENSITY=780 kg/m3, TYPE=SOLID
MATERIAL LABEL=POLYETEN, CAPACITY=2300 J/kg-C, \
         CONDUCTIVITY=0.41 W/m-K, DENSITY=940 kg/m3, TYPE=SOLID
MATERIAL LABEL=COFOAM, CAPACITY=1050 J/kg-C, \
         CONDUCTIVITY=0.07 W/m-K, DENSITY=540 kg/m3, TYPE=SOLID
MATERIAL LABEL=TITAN, CAPACITY=520 J/kg-C, CONDUCTIVITY=20 W/m-K, \
         DENSITY=4540 kg/m3, TYPE=SOLID
MATERIAL LABEL=POLYCHLOROPRENE, CAPACITY=1070 J/kg-C, \
         CONDUCTIVITY=0.27 W/m-K, DENSITY=1580 kg/m3, TYPE=SOLID
MATERIAL LABEL=VIKOTHERM, CAPACITY=1500 J/kg-C, \
         CONDUCTIVITY=0.13 W/m-K, DENSITY=1000 kg/m3, TYPE=SOLID
!
!***********************************************************************
! WALL Definition
!-----------------------------------------------------------------------
WALL LABEL=WELL, ELECTRICHEAT=OFF, MATERIAL=( STEEL, WATER, \
     STEEL, H_CONCRETE, SOIL_1, SOIL_1, SOIL_1, SOIL_2 ), \
     POWERCONTROL=OFF, THICKNESS=( 0.0115, 0.02135,  \
     0.012, 0.03332, 0.1, 0.2, 0.6, 1.5 ) m
WALL LABEL=RISER_F6, ELECTRICHEAT=OFF, MATERIAL=( CARCAS, RILSAN, \
     ZETAWIRE, RILSAN, POLYETEN, POLYETEN, COFOAM, TAPE, RILSAN ), \
     POWERCONTROL=OFF, THICKNESS=( 0.0054,  \
     0.0055, 0.014, 0.003, 0.008, 0.006, 0.0055, 0.00075, 0.007 ) m
WALL LABEL=TITAN-1, ELECTRICHEAT=OFF, MATERIAL=( TITAN, \
     POLYCHLOROPRENE ), POWERCONTROL=OFF,  \
     THICKNESS=( 0.021, 0.008 ) m
WALL LABEL=TITAN-2, ELECTRICHEAT=OFF, MATERIAL=( TITAN, \
     POLYCHLOROPRENE, VIKOTHERM, POLYCHLOROPRENE ), \
     POWERCONTROL=OFF, THICKNESS=( 0.021, 0.008, 0.016, 0.005 ) m
WALL LABEL=STEEL-1, ELECTRICHEAT=OFF, MATERIAL=( STEEL, \
     POLYCHLOROPRENE, VIKOTHERM, POLYCHLOROPRENE ),
     POWERCONTROL=OFF, THICKNESS=( 0.021, 0.008, 0.03, 0.005 ) m
!
!***********************************************************************
! GEOMETRY Definition
!-----------------------------------------------------------------------
GEOMETRY LABEL=WELLFLOW, XSTART=0 m, YSTART=-2100 m, ZSTART=0 m
PIPE LABEL=PIPE_1, DIAMETER=0.2 m, NSEGMENTS=3, \
     ROUGHNESS=4.5e-005 m, WALL=WELL, XEND=0 m, YEND=-2000 m, ZEND=0 m
GEOMETRY LABEL=LIFTGAS, XSTART=0 m, YSTART=-2000 m, ZSTART=0 m
PIPE LABEL=PIPE_2, NSEGMENTS=50, \
     ROUGHNESS=4.5e-005 m, WALL=STEEL-1, XEND=0 m, YEND=48 m, ZEND=0 m
PIPE LABEL=PIPE_3, NSEGMENTS=2, ROUGHNESS=4.5e-005 m, \
```

```
     WALL=STEEL-1, XEND=10 m, YEND=48 m, ZEND=0 m
GEOMETRY LABEL=GASLIFTED_WELL, XSTART=10 m, YSTART=48 m, ZSTART=0 m
PIPE LABEL=PIPE_1, DIAMETER=0.124 m, NSEGMENTS=2, \
     ROUGHNESS=3e-005 m, WALL=WELL, XEND=0 m, YEND=48 m, ZEND=0 m
PIPE LABEL=PIPE_2, DIAMETER=0.124 m, NSEGMENTS=5, \
     ROUGHNESS=4.5e-005 m, WALL=STEEL-1, \
     XEND=0 m, YEND=-100 m, ZEND=0 m
PIPE LABEL=PIPE_3, DIAMETER=0.124 m, NSEGMENTS=50, \
     ROUGHNESS=4.5e-005 m, WALL=STEEL-1, \
     XEND=0 m, YEND=-2000 m, ZEND=0 m
GEOMETRY LABEL=INJECTION, XSTART=0 m, YSTART=-2000 m, ZSTART=0 m
PIPE LABEL=PIPE_1, DIAMETER=0.1 m, NSEGMENTS=3, \
     ROUGHNESS=4.5e-005 m, WALL=STEEL-1, \
     XEND=5 m, YEND=-2000 m, ZEND=0 m
!
!*********************************************************************
! NODE Definition
!---------------------------------------------------------------------
NODE LABEL=GAS_INLET, TYPE=MERGE, X=15 m, Y=48 m, Z=0 m
NODE LABEL=BOTT_WELL, TYPE=MERGE, X=0 m, Y=-2000 m, Z=0 m
NODE LABEL=WELLHEAD, TYPE=TERMINAL, X=10 m, Y=48 m, Z=0 m
NODE LABEL=RESERVOIR, TYPE=TERMINAL, X=0 m, Y=-2100 m, Z=0 m
NODE LABEL=BOTT_WELL-1, TYPE=MERGE, X=10 m, Y=-2000 m, Z=0 m
NODE LABEL=WELLHEAD-1, TYPE=TERMINAL, X=20 m, Y=48 m, Z=0 m
NODE LABEL=RESERVOIR-1, TYPE=TERMINAL, X=10 m, Y=-2100 m, Z=0 m
NODE LABEL=INJECTION, TYPE=TERMINAL, X=15 m, Y=50 m, Z=0 m
!
!*********************************************************************
! BRANCH Definition
!---------------------------------------------------------------------
BRANCH LABEL=BRAN-1, FLOAT=ON, FLUID="1", FROM=RESERVOIR, \
       GEOMETRY=WELLFLOW, TO=BOTT_WELL
BRANCH LABEL=BRAN-2, FLOAT=ON, FLUID="1", FROM=BOTT_WELL, \
       GEOMETRY=INJECTION, TO=GAS_INLET
BRANCH LABEL=BRAN-3, FLOAT=ON, FLUID="1", FROM=WELLHEAD, \
       GEOMETRY=GASLIFTED_WELL, TO=BOTT_WELL
BRANCH LABEL=BRAN-4, FLOAT=ON, FLUID="1", FROM=RESERVOIR-1, \
       GEOMETRY=WELLFLOW, TO=BOTT_WELL-1
BRANCH LABEL=BRAN-5, FLOAT=ON, FLUID="1", FROM=BOTT_WELL-1, \
       GEOMETRY=INJECTION, TO=GAS_INLET
BRANCH LABEL=BRAN-6, FLOAT=ON, FLUID="1", FROM=WELLHEAD-1, \
       GEOMETRY=GASLIFTED_WELL, TO=BOTT_WELL-1
BRANCH LABEL=BRAN-7, FLOAT=ON, FLUID="1", FROM=GAS_INLET, \
       GEOMETRY=LIFTGAS, TO=INJECTION
!
!*********************************************************************
! BOUNDARY Definition
!---------------------------------------------------------------------
BOUNDARY NODE=INJECTION, TYPE=CLOSED
BOUNDARY GASFRACTION=1 -, NODE=WELLHEAD, PRESSURE=15 bara, \
         TEMPERATURE=5 C, TYPE=PRESSURE, WATERFRACTION=0 -
BOUNDARY NODE=RESERVOIR, TYPE=CLOSED
BOUNDARY GASFRACTION=1 -, NODE=WELLHEAD-1, PRESSURE=15 bara, \
         TEMPERATURE=5 C, TIME=0 s, TYPE=PRESSURE, WATERFRACTION=0 -
BOUNDARY NODE=RESERVOIR-1, TYPE=CLOSED
!
!*********************************************************************
! INITIALCONDITIONS Definition
!---------------------------------------------------------------------
INITIALCONDITIONS BRANCH=BRAN-1, INPRESSURE=150 bara, \
                  INTEMPERATURE=60 C, INTERPOLATION=VERTICAL,  \
                  INVOIDFRACTION=1  , INWATERCUT=0 -, \
                  OUTPRESSURE=150 bara, OUTTEMPERATURE=60 C,  \
                  OUTVOIDFRACTION=1  , OUTWATERCUT=0 -
INITIALCONDITIONS BRANCH=BRAN-2, INPRESSURE=150 bara, \
                  INTEMPERATURE=60 C, INTERPOLATION=VERTICAL,  \
                  INVOIDFRACTION=1  , INWATERCUT=0 -, \
                  OUTPRESSURE=150 bara, OUTTEMPERATURE=60 C,  \
                  OUTVOIDFRACTION=1  , OUTWATERCUT=0 -
INITIALCONDITIONS BRANCH=BRAN-3, INPRESSURE=150 bara, \
```

```
                  INTEMPERATURE=60 C, INTERPOLATION=VERTICAL,  \
                  INVOIDFRACTION=1  , INWATERCUT=0 -, \
                  OUTPRESSURE=150 bara, OUTTEMPERATURE=60 C,  \
                  OUTVOIDFRACTION=1  , OUTWATERCUT=0 -
INITIALCONDITIONS BRANCH=BRAN-4, INPRESSURE=150 bara, \
                  INTEMPERATURE=60 C, INTERPOLATION=VERTICAL,  \
                  INVOIDFRACTION=1  , INWATERCUT=0 -, \
                  OUTPRESSURE=150 bara, OUTTEMPERATURE=60 C,  \
                  OUTVOIDFRACTION=1  , OUTWATERCUT=0 -
INITIALCONDITIONS BRANCH=BRAN-5, INPRESSURE=150 bara, \
                  INTEMPERATURE=60 C, INTERPOLATION=VERTICAL,  \
                  INVOIDFRACTION=1  , INWATERCUT=0 -, \
                  OUTPRESSURE=150 bara, OUTTEMPERATURE=60 C,  \
                  OUTVOIDFRACTION=1  , OUTWATERCUT=0 -
INITIALCONDITIONS BRANCH=BRAN-6, INPRESSURE=150 bara, \
                  INTEMPERATURE=60 C, INTERPOLATION=VERTICAL,  \
                  INVOIDFRACTION=1  , INWATERCUT=0 -, \
                  OUTPRESSURE=150 bara, OUTTEMPERATURE=60 C,  \
                  OUTVOIDFRACTION=1  , OUTWATERCUT=0 -
INITIALCONDITIONS BRANCH=BRAN-7, INPRESSURE=150 bara, \
                  INTEMPERATURE=60 C, INTERPOLATION=VERTICAL,  \
                  INVOIDFRACTION=1  , INWATERCUT=0 -, \
                  OUTPRESSURE=150 bara, OUTTEMPERATURE=60 C,  \
                  OUTVOIDFRACTION=1  , OUTWATERCUT=0 -
!
!*****************************************************************
! HEATTRANSFER Definition
!-----------------------------------------------------------------
HEATTRANSFER BRANCH=BRAN-1, HAMBIENT=1000 W/m2-C, \
             HMININNERWALL=50 W/m2-C, HOUTEROPTION=HGIVEN,  \
             TAMBIENT=108 C
HEATTRANSFER BRANCH=BRAN-2, HAMBIENT=1000 W/m2-C, \
             HMININNERWALL=50 W/m2-C, HOUTEROPTION=HGIVEN,  \
             TAMBIENT=108 C
HEATTRANSFER BRANCH=BRAN-3, HAMBIENT=1000 W/m2-C, \
             HMININNERWALL=50 W/m2-C, HOUTEROPTION=HGIVEN,  \
             INTAMBIENT=5 C, INTERPOLATION=VERTICAL, \
             OUTTAMBIENT=108 C, PIPE=PIPE_3
HEATTRANSFER BRANCH=BRAN-3, HAMBIENT=1000 W/m2-C, \
             HMININNERWALL=50 W/m2-C, HOUTEROPTION=HGIVEN,  \
             PIPE=PIPE_2, TAMBIENT=5 C
HEATTRANSFER BRANCH=BRAN-3, HAMBIENT=1000 W/m2-C, \
             HMININNERWALL=50 W/m2-C, HOUTEROPTION=HGIVEN,  \
             PIPE=PIPE_1, TAMBIENT=5 C
HEATTRANSFER BRANCH=BRAN-4, HAMBIENT=1000 W/m2-C, \
             HMININNERWALL=50 W/m2-C, HOUTEROPTION=HGIVEN,  \
             TAMBIENT=108 C
HEATTRANSFER BRANCH=BRAN-5, HAMBIENT=1000 W/m2-C, \
             HMININNERWALL=50 W/m2-C, HOUTEROPTION=HGIVEN,  \
             TAMBIENT=108 C
HEATTRANSFER BRANCH=BRAN-6, HAMBIENT=1000 W/m2-C, \
             HMININNERWALL=50 W/m2-C, HOUTEROPTION=HGIVEN,  \
             INTAMBIENT=5 C, INTERPOLATION=VERTICAL, \
             OUTTAMBIENT=108 C, PIPE=PIPE_3
HEATTRANSFER BRANCH=BRAN-6, HAMBIENT=1000 W/m2-C, \
             HMININNERWALL=50 W/m2-C, HOUTEROPTION=HGIVEN,  \
             PIPE=PIPE_2, TAMBIENT=5 C
HEATTRANSFER BRANCH=BRAN-6, HAMBIENT=1000 W/m2-C, \
             HMININNERWALL=50 W/m2-C, HOUTEROPTION=HGIVEN,  \
             PIPE=PIPE_1, TAMBIENT=5 C
HEATTRANSFER BRANCH=BRAN-7, HAMBIENT=1000 W/m2-C, \
             HMININNERWALL=50 W/m2-C, HOUTEROPTION=HGIVEN,  \
             INTAMBIENT=108 C, INTERPOLATION=VERTICAL, \
             OUTTAMBIENT=5 C
!
!*****************************************************************
! SOURCE Definition
!-----------------------------------------------------------------
SOURCE LABEL=GAS_SUPPLY, BRANCH=BRAN-7, GASFRACTION=( 6:1 ) -, \
       MASSFLOW=( 2, 2, 1.8, 1.8, 1.6, 1.6 ) kg/s, PIPE=PIPE_3, \
```

```
       SECTION=2, TEMPERATURE=6:60 C, \
       TIME=( 0, 4, 4.02, 8.02, 8.04, 16.04 ) h, \
       WATERFRACTION=( 6:0 ) -
!
!*********************************************************************
! WELL Definition
!---------------------------------------------------------------------
WELL LABEL=WELL-1, AINJ=0  , APROD=0  , BINJ=2.7e-006  , \
     BPROD=2.7e-006  , BRANCH=BRAN-1, GASFRACTION=-1 -, \
     INJOPTION=LINEAR, ISOTHERMAL=YES, \
     LOCATION=BOTTOM, PIPE=PIPE_1,  \
     PRODOPTION=LINEAR, RESPRESSURE=150 bara, \
     RESTEMPERATURE=108 C, SECTION=1, TIME=0 s
WELL LABEL=WELL-2, AINJ=0  , APROD=0  , BINJ=2.71e-006  , \
     BPROD=2.71e-006  , BRANCH=BRAN-4, GASFRACTION=-1 -, \
     INJOPTION=LINEAR, ISOTHERMAL=YES, \
     LOCATION=BOTTOM, PIPE=PIPE_1,  \
     PRODOPTION=LINEAR, RESPRESSURE=150 bara, \
     RESTEMPERATURE=108 C, SECTION=1, TIME=0 s
!
!*********************************************************************
! VALVE Definition
!---------------------------------------------------------------------
VALVE LABEL=PRODCHOKE, BRANCH=BRAN-3, CD=0.84  , \
      CRITFLOWMODEL=FROZEN, DIAMETER=0.07 m,  \
      OPENING=1  , PIPE=PIPE_1, SECTIONBOUNDARY=1, TIME=0 s
VALVE LABEL=GASLIFT_VALVE, BRANCH=BRAN-2, CD=0.84  , \
      CRITFLOWMODEL=FROZEN, DIAMETER=0.0125 m,  \
      OPENING=1  , PIPE=PIPE_1, SECTIONBOUNDARY=2, TIME=0 s
VALVE LABEL=PRODCHOKE-1, BRANCH=BRAN-6, CD=0.84  , \
      CRITFLOWMODEL=FROZEN, DIAMETER=0.07 m,  \
      OPENING=1  , PIPE=PIPE_1, SECTIONBOUNDARY=1, TIME=0 s
VALVE LABEL=GASLIFT_VALVE-1, BRANCH=BRAN-5, CD=0.84  , \
      CRITFLOWMODEL=FROZEN, DIAMETER=0.0125 m,  \
      OPENING=1  , PIPE=PIPE_1, SECTIONBOUNDARY=2, TIME=0 s
!
!*********************************************************************
! CHECKVALVE Definition
!---------------------------------------------------------------------
CHECKVALVE LABEL=CHECK-1, BRANCH=BRAN-2, \
           DIRECTION=NEGATIVE, PIPE=PIPE_1, SECTIONBOUNDARY=2
CHECKVALVE LABEL=CHECK-2, BRANCH=BRAN-5, \
           DIRECTION=NEGATIVE, PIPE=PIPE_1, SECTIONBOUNDARY=2
!
!*********************************************************************
! OUTPUT Definition
!---------------------------------------------------------------------
OUTPUT COLUMNS=4, DELETEPREVIOUS=OFF, DTOUT=1 h
OUTPUT COLUMNS=4, DELETEPREVIOUS=OFF, VARIABLE=( UL, UG, GT, GLT, \
       GLTHL, GG, AL, PT BARA, TM, VOL, ID, HOL, ROG, ROL )
OUTPUT BRANCH=BRAN-1, COLUMNS=4, DELETEPREVIOUS=OFF, \
       VARIABLE=( UL, UG, GT, GLT,  \
       GLTHL, GG, AL, PT BARA, TM, VOL, ID, HOL, ROG, ROL )
OUTPUT BRANCH=BRAN-2, COLUMNS=4, DELETEPREVIOUS=OFF, \
       VARIABLE=( UL, UG, GT, GLT,  \
       GLTHL, GG, AL, PT BARA, TM, VOL, ID, HOL, ROG, ROL )
OUTPUT BRANCH=BRAN-3, COLUMNS=4, DELETEPREVIOUS=OFF, \
       VARIABLE=( UL, UG, GT, GLT,  \
       GLTHL, GG, AL, PT BARA, TM, VOL, ID, HOL, ROG, ROL )
OUTPUT BRANCH=BRAN-4, COLUMNS=4, DELETEPREVIOUS=OFF, \
       VARIABLE=( UL, UG, GT, GLT,  \
       GLTHL, GG, AL, PT BARA, TM, VOL, ID, HOL, ROG, ROL )
OUTPUT BRANCH=BRAN-5, COLUMNS=4, DELETEPREVIOUS=OFF, \
       VARIABLE=( UL, UG, GT, GLT,  \
       GLTHL, GG, AL, PT BARA, TM, VOL, ID, HOL, ROG, ROL )
OUTPUT BRANCH=BRAN-6, COLUMNS=4, DELETEPREVIOUS=OFF, \
       VARIABLE=( UL, UG, GT, GLT,  \
       GLTHL, GG, AL, PT BARA, TM, VOL, ID, HOL, ROG, ROL )
OUTPUT BRANCH=BRAN-7, COLUMNS=4, DELETEPREVIOUS=OFF, DTOUT=1 h, \
       VARIABLE=( UL, UG, GT, GLT, glthl, GG, AL, PT BARA, \
```

```
       TM, VOL, ID, HOL, ROG, ROL )
!
!*****************************************************************
! TREND Definition
!-----------------------------------------------------------------
TREND BRANCH=BRAN-3, DELETEPREVIOUS=OFF, DTPLOT=5 s, \
      PIPE=PIPE_1, SECTION=1, TIME=0 s, VARIABLE=QL
TREND BRANCH=BRAN-6, DELETEPREVIOUS=OFF, \
      PIPE=PIPE_1, SECTION=1, TIME=0 s, VARIABLE=QL
TREND VARIABLE=GTSOUR
TREND BRANCH=BRAN-2, PIPE=PIPE_1, SECTION=3, VARIABLE=GG
TREND BRANCH=BRAN-5, PIPE=PIPE_1, SECTION=3, VARIABLE=GG
TREND BRANCH=BRAN-3, PIPE=PIPE_3, SECTION=50, VARIABLE=PT
TREND BRANCH=BRAN-6, PIPE=PIPE_3, SECTION=50, VARIABLE=PT
TREND BRANCH=BRAN-2, PIPE=PIPE_1, SECTION=2, VARIABLE=PT
TREND BRANCH=BRAN-5, PIPE=PIPE_1, SECTION=2, VARIABLE=PT
!
!*****************************************************************
! PROFILE Definition
!-----------------------------------------------------------------
PROFILE BRANCH=BRAN-1, DELETEPREVIOUS=OFF, DTPLOT=3600 s, \
        VARIABLE=( HOL, TM, PT BARA, GLT, GLTHL, GT, GG, AL )
PROFILE BRANCH=BRAN-2, DELETEPREVIOUS=OFF, DTPLOT=3600 s, \
        VARIABLE=( HOL, TM, PT BARA, GLT, GLTHL, GT, GG, AL )
PROFILE BRANCH=BRAN-3, DELETEPREVIOUS=OFF, DTPLOT=3600 s, \
        VARIABLE=( HOL, TM, PT BARA, GLT, GLTHL, GT, GG, AL )
PROFILE BRANCH=BRAN-4, DELETEPREVIOUS=OFF, DTPLOT=3600 s, \
        VARIABLE=( HOL, TM, PT BARA, GLT, GLTHL, GT, GG, AL )
PROFILE BRANCH=BRAN-5, DELETEPREVIOUS=OFF, DTPLOT=3600 s, \
        VARIABLE=( HOL, TM, PT BARA, GLT, GLTHL, GT, GG, AL )
PROFILE BRANCH=BRAN-6, DELETEPREVIOUS=OFF, DTPLOT=3600 s, \
        VARIABLE=( HOL, TM, PT BARA, GLT, GLTHL, GT, GG, AL )
PROFILE BRANCH=BRAN-7, DELETEPREVIOUS=OFF, DTPLOT=3600 s, \
        VARIABLE=( HOL, TM, PT BARA, GLT, GLTHL, GT, GG, AL )
!
ENDCASE
```

C.3 Density-wave oscillation base case

```
!*****************************************************************
! CASE Definition
!-----------------------------------------------------------------
CASE AUTHOR="Bin Hu", \
     DATE="May 9th", \
     INFO="L2500PI4e-6Psep10baraUc100%", \
     PROJECT="Thesis and Petronics", \
     TITLE="Gas-lift density wave instability"
!
!*****************************************************************
! OPTIONS Definition
!-----------------------------------------------------------------
OPTIONS COMPOSITIONAL=OFF, DEBUG=OFF, PHASE=TWO, \
        POSTPROCESSOR=OFF, SLUGVOID=SINTEF,  \
        STEADYSTATE=ON, TEMPERATURE=OFF, \
        WAXDEPOSITION=OFF,DRILLING=OFF
!
!*****************************************************************
! FILES Definition
!-----------------------------------------------------------------
FILES PVTFILE="waterandair.tab"
!
!*****************************************************************
! INTEGRATION Definition
!-----------------------------------------------------------------
INTEGRATION CPULIMIT=1 h, DTSTART=0.001 s, ENDTIME=10 h, \
            MAXDT=20 s, MAXTIME=0 s, MINDT=0.001 s, \
            MINTIME=0 s, NSIMINFO=10, STARTTIME=0 s
!
```

```
!*********************************************************************
! GEOMETRY Definition
!---------------------------------------------------------------------
GEOMETRY LABEL=GEOMETRY-1, XSTART=0 m, YSTART=0 m, ZSTART=0 m
PIPE LABEL=PIPE-1, DIAMETER=0.125 m, NSEGMENTS=3, \
     ROUGHNESS=4.5e-005 m, XEND=0 m, YEND=6 m, ZEND=0 m
PIPE LABEL=PIPE-2, DIAMETER=0.125 m, NSEGMENTS=25, \
     ROUGHNESS=4.5e-005 m, XEND=0 m, YEND=2500 m, ZEND=0 m
PIPE LABEL=PIPE-3, DIAMETER=0.125 m, NSEGMENTS=2, \
     ROUGHNESS=4.5e-005 m, XEND=1 m, YEND=2500 m, ZEND=0 m
!
!*********************************************************************
! NODE Definition
!---------------------------------------------------------------------
NODE LABEL=NODE-1, TYPE=TERMINAL, X=0 m, Y=0 m, Z=0 m
NODE LABEL=NODE-2, TYPE=TERMINAL, X=1 m, Y=2500 m, Z=0 m

!*********************************************************************
! BRANCH Definition
!---------------------------------------------------------------------
BRANCH LABEL=BRANCH-1, FLOAT=ON, FLUID="1", FROM=NODE-1, \
       GEOMETRY=GEOMETRY-1, TO=NODE-2
!
!*********************************************************************
! BOUNDARY Definition
!---------------------------------------------------------------------
BOUNDARY GASFRACTION=1 -, NODE=NODE-2, PRESSURE=10 bara, \
         TEMPERATURE=30 C, TIME=0 s, TYPE=PRESSURE, WATERFRACTION=0 -
BOUNDARY NODE=NODE-1, TYPE=CLOSED
!
!*********************************************************************
! SOURCE Definition
!---------------------------------------------------------------------
SOURCE LABEL=SOURCE-1, BRANCH=BRANCH-1, GASFRACTION=1 -, \
       MASSFLOW=0.6 kg/s, PIPE=PIPE-1,  \
       SECTION=2, TEMPERATURE=30 C, TIME=0 s, WATERFRACTION=0 -
!
!*********************************************************************
! WELL Definition
!---------------------------------------------------------------------
WELL LABEL=WELL-1, AINJ=0  , APROD=0  , BINJ=4e-006  , \
     BPROD=4e-006  , BRANCH=BRANCH-1,  \
     GASFRACTION=0 -, INJOPTION=LINEAR, ISOTHERMAL=YES, \
     LOCATION=BOTTOM, PIPE=PIPE-1,  \
     PHASE=OIL, PRODOPTION=LINEAR, RESPRESSURE=100 bara, \
     RESTEMPERATURE=30 C, SECTION=1,  \
     TIME=0 s, WATERFRACTION=0 -
!
!*********************************************************************
!      VALVE Definition
!---------------------------------------------------------------------
VALVE LABEL=VALVE-1, BRANCH=BRANCH-1, CD=0.84  , \
      CRITFLOWMODEL=FROZEN, DIAMETER=0.125 m,  \
      OPENING=1  , PIPE=PIPE-3, SECTIONBOUNDARY=3, TIME=0 s
!
!*********************************************************************
!      OUTPUT Definition
!---------------------------------------------------------------------
OUTPUT BRANCH=BRANCH-1, COLUMNS=4, DELETEPREVIOUS=OFF, \
       DTOUT=24 h, PIPE=PIPE-1
!
!*********************************************************************
! TREND Definition
!---------------------------------------------------------------------
TREND BRANCH=BRANCH-1, DELETEPREVIOUS=OFF, DTPLOT=60 s, \
      PIPE=PIPE-1, SECTION=1, TIME=0 s, VARIABLE=PT
TREND BRANCH=BRANCH-1, DELETEPREVIOUS=OFF, DTPLOT=60 s, \
      PIPE=PIPE-1, SECTION=3, TIME=0 s, \
      VARIABLE=( GG, QG, GLTHL, QLTHL, GT, QT, PT )
TREND BRANCH=BRANCH-1, DELETEPREVIOUS=OFF, DTPLOT=60 s, \
```

```
      PIPE=PIPE-2, SECTION=10, TIME=0 s, \
      VARIABLE=( GG, QG, GLTHL, QLTHL, GT, QT, PT )
TREND BRANCH=BRANCH-1, DELETEPREVIOUS=OFF, DTPLOT=60 s, \
      PIPE=PIPE-2, SECTION=20, TIME=0 s, \
      VARIABLE=( GG, QG, GLTHL, QLTHL, GT, QT, PT )
TREND BRANCH=BRANCH-1, DELETEPREVIOUS=OFF, DTPLOT=60 s, \
      PIPE=PIPE-3, SECTION=2, TIME=0 s, \
      VARIABLE=( GG, QG, GLTHL, QLTHL, GT, QT, PT )
TREND BRANCH=BRANCH-1, DELETEPREVIOUS=OFF, DTPLOT=60 s, \
      TIME=0 s, VARIABLE=( GASC, OILC, OILOUT )
!
!*********************************************************************
!      PROFILE Definition
!---------------------------------------------------------------------
PROFILE BRANCH=BRANCH-1, DELETEPREVIOUS=OFF, DTPLOT=10 m, \
        VARIABLE=( HOL, PT, QLT, QG, GLT, GG )
!
ENDCASE
```

D. Key words and format of OLGA PVT table

In addition to the file giving the simulation case description like in Appendix C, OLGA requires a data file that contains the fluid physical properties as a function of temperature and pressure. The two data files used in the simulations are included in the enclosed disc. This appendix is not a general description of OLGA PVT table structure. It is only valid to those two files, which contain two two-phase tables that are equidistant in pressure and temperature. The following explains how to read the data files.

To explain the data structure, the following variables are defined:

FLUIDF (-)	Fluid identifier enclosed in apostrophes.
NTABP (-)	Number of pressure points in the table
NTABT (-)	Number of temperature points in the table
DP (N/m^2)	Pressure step in the table
DT (°C)	Temperature step in the table
PP(I) (N/m^2)	Pressure values in the table, I=1,NTABP
TT(J) (°C)	Temperature values in the table, J = 1, NTABT
PBB(J) (N/m^2)	Bubble point pressures, J = 1, NTABT
PDEW(J) (N/m^2)	Dew point pressures, J = 1, NTABT
TABTEX(L) (-)	Text string to identify the different properties

For all variables below, J = 1, NTABT and I = 1, NTABP.

ROGTB(J,I) (kg/m^3)	Gas densities
ROOTB(J,I) (kg/m^3)	Oil densities
DRGPTB(J,I) (s^2/m^2)	Partial derivatives of gas densities w.r.t pressure
DROPTB(J,I) (s^2/m^2)	Partial derivatives of oil densities w.r.t pressure
DRGTTB(J,I) (kg/m^3C)	Partial derivatives of gas densities w.r.t temperature
DROTTB(J,I) (kg/m^3C)	Partial derivatives of oil densities w.r.t temperature
RSGTB(J,I) (kg/kg)	Gas mass fraction in gas and oil mixture.
VSGTB(J,I) (Ns/m^2)	Dynamic viscosities for gas
VSOTB(J,I) (Ns/m^2)	Dynamic viscosities for oil
CPGTB(J,I) (J/kgC)	Gas heat capacities at constant pressure
CPOTB(J,I) (J/kgC)	Oil heat capacities at constant pressure
HGTB(J,I) (J/kg)	Gas enthalpies
HOTB(J,I) (J/kg)	Oil enthalpies
TKGTB(J,I) (W/mC)	Gas thermal conductivities
TKOTB(J,I) (W/mC)	Oil thermal conductivities
SIGOGT(J,I) (N/m)	Surface tension between gas and oil
SGTB(J,I) (J/kgC)	Gas specific entropy
SOTB(J,I) (J/kgC)	Oil specific entropy

The data file reads as below:

FLUIDF
NTABP NTABT

DP DT
PP(1) TT(1)
PBB(1)……PBB(NTABT)
PDEW(1)……PDEW(NTABT)

TABTEX(1)
ROGTB(1,1)……ROGTB(NTABT,1)
.
.
ROGTB(1,NTABP)……ROGTB(NTABT,NTABP)

TABTEX(2)
ROOTB(1,1)……ROOTB(NTABT,1)
.
.
ROOTB(1,NTABP)……ROOTB(NTABT,NTABP)

TABTEX(3)
DRGPTB(1,1)……DRGPTB(NTABT,1)
.
.
DRGPTB(1,NTABP)……DRGPTB(NTABT,NTABP)

TABTEX(4)
DROPTB(1,1)……DROPTB(NTABT,1)
.
.
DROPTB(1,NTABP)……DROPTB(NTABT,NTABP)

TABTEX(5)
DRGTTB(1,1)……DRGTTB(NTABT,1)
.
.
DRGTTB(1,NTABP)……DRGTTB(NTABT,NTABP)

TABTEX(6)
DROTTB(1,1)……DROTTB(NTABT,1)
.
.
DROTTB(1,NTABP)……DROTTB(NTABT,NTABP)

TABTEX(7)
RSGTB(1,1)……RSGTB(NTABT,1)
.
.
RSGTB(1,NTABP)……RSGTB(NTABT,NTABP)

TABTEX(8)
VSGTB(1,1)……VSGTB(NTABT,1)

.
.
VSGTB(1,NTABP)……VSGTB(NTABT,NTABP)

TABTEX(9)
VSOTB(1,1)……VSOTB(NTABT,1)
.
.
VSOTB(1,NTABP)……VSOTB(NTABT,NTABP)

TABTEX(10)
CPGTB(1,1)……CPGTB(NTABT,1)
.
.
CPGTB(1,NTABP)……CPGTB(NTABT,NTABP)

TABTEX(11)
CPOTB(1,1)……CPOTB(NTABT,1)
.
.
CPOTB(1,NTABP)……CPOTB(NTABT,NTABP)

TABTEX(12)
HGTB(1,1)……HGTB(NTABT,1)
.
.
HGTB(1,NTABP)……HGTB(NTABT,NTABP)

TABTEX(13)
HOTB(1,1)……HOTB(NTABT,1)
.
.
HOTB(1,NTABP)……HOTB(NTABT,NTABP)

TABTEX(14)
TKGTB(1,1)……TKGTB(NTABT,1)
.
.
TKGTB(1,NTABP)……TKGTB(NTABT,NTABP)

TABTEX(15)
TKOTB(1,1)……TKOTB(NTABT,1)
.
.
TKOTB(1,NTABP)……TKOTB(NTABT,NTABP)

TABTEX(16)
SIGOGT(1,1)……SIGOGT(NTABT,1)
.

.
SIGOGT(1,NTABP)……SIGOGT(NTABT,NTABP)

TABTEX(17)
SGTB(1,1)……SGTB(NTABT,1)
.
.
SGTB(1,NTABP)……SGTB(NTABT,NTABP)

TABTEX(18)
SOTB(1,1) ……SOTB(NTABT,1)
.
.
SOTB(1,NTABP)……SOTB(NTABT,NTABP)